10-29-2008

Development of lead-free thick film resistor

Xudong Chen
Florida International University

DOI: 10.25148/etd.FI14060179

FLORIDA INTERNATIONAL UNIVERSITY

Miami, Florida

DEVELOPMENT OF A LEAD-FREE THICK FILM RESISTOR

A thesis submitted in partial fulfillment of the

requirements for the degree of

MASTER OF SCIENCE

in

MATERIALS SCIENCE AND ENGINEERING

by

Xudong Chen

2008

To: Interim Dean Amir Mirmiran
College of Engineering and Computing

This thesis, written by Xudong Chen, and entitled Development of a Lead-Free Thick Film Resistor, having been approved in respect to style and intellectual content, is referred to you for judgment.

We have read this thesis and recommend that it be approved.

Kuang-His Wu

Jiuhua Chen

Grover L. Larkins

W. Kinzy Jones, Major Professor

Date of Defense: October 29, 2008

The thesis of Xudong Chen is approved.

Interim Dean Amir Mirmiran
College of Engineering and Computing

Dean George Walker
University Graduate School

Florida International University, 2008

DEDICATION

I dedicate this thesis to my family.

ACKNOWLEDGMENTS

This project is supported by Heraeus Inc. and most of the work was done in Advanced Materials Engineering Research Institute (AMERI) at FIU.

I would like to thank my major professor, Dr. W. Kinzy Jones, for his great guidance, support and encouragement. Also, I wish to thank the members of my committee, Dr. Larkins, Dr. Chen and Dr. Wu for their guidance.

I would also like to thank Mr. Randy Klein, Dr. Yanqing Liu, Ms. Jian Wang, and Dr. Wenzhong Wu for their contributions to this work. And I would extend my gratefulness to Mr. Neal Ricks for his help in every aspect in the lab.

Finally, I would like to thank my colleagues and good friends, Dr. Yao Chen, Mr. Yong Gao, and Mr. Xiaohua Li for numerous times they helped me out with my work.

ABSTRACT OF THE THESIS

DEVELOPMENT OF A LEAD-FREE THICK FILM RESISTOR

by

Xudong Chen

Florida International University, 2008

Miami, Florida

Professor W. Kinzy Jones, Major Professor

Thick film resistors (TFRs) are widely used in hybrid microelectronics. Currently most of the resistor paste products contain lead, which is potentially a major problem to the environment resulting from electronics disposal. The purpose of this study is to develop a lead-free thick film resistor that is compatible to the typical industry thick film processing and has comparable electrical properties as the lead bearing counterpart. The research started from and focused on evaluation and selection of suitable lead-free glass material, which is one of the most important ingredients in a thick film resistor. The fired resistors were characterized in terms of microstructure and material interaction and the electrical properties were tested. The sheet resistance of TFRs prepared using the selected glasses spanned from 400 ohms per square (Ω/□) to 0.4 mega-ohms per square (MΩ/□). The temperature coefficient of resistance (TCR) fell in a range of ±350ppm/°C.

TABLE OF CONTENTS

LIST OF TABLES

TABLE PAGE

LIST OF FIGURES

FIGURE PAGE

CHAPTER 1

INTRODUCTION

1.1 General

When the development of electronics stepped into the third era [1], the integrated circuit era, there was a great deal of interest during the late 1950s to search for a new approach to miniaturization which could lead to low-cost, reliable, small electronic systems of high complexity [2]. Many design functions of light weight and compact electronic circuits, especially microelectronic circuits, such as flexibility in component use, high voltage requirements and powder dissipation that are beyond the range of monolithic technology and thin film technology have been greatly fulfilled by thick film technology [3]. A thick film circuit is normally considered to be one which comprises layers of special ink (also referred as paste) deposited onto an insulating substrate. With the addition of integrated circuits or films formed by other technologies, the concept of hybrid circuit is realized [4, 5]. Being widely used in electronics for over 40 years, thick film technology is now very mature and almost universally used for hybrid and microwave circuits [1-7].

Thick film technology began decades ago as a proprietary art and people believe that it is still best classified as a proprietary art although the worldwide market for thick film microcircuits is tens of billions per year [6]. Typically, it consists of screen printing, drying and firing conductor, resistor or dielectric inks. Most thick film inks contain, at a

minimum, three basic ingredients: a functional material that provides the electrical function of the fired thick film; an organic binder, also referred as polymer vehicle, provides proper viscosity control and thixotropic property to the ink allowing printability; an inorganic binder such as a glass frit that binds the functional material particles together and to the substrate. Screen printing is the most commonly used technique to deposit thick film ink on the substrate into desired pattern [1-7]. Direct-write dispensing gives another solution to deposit thick film ink without using a screen mask [8]. However, the throughput of this technique in term of thick film application still can not compare to screen printing for the time being. The deposited film is then dried and fired to remove the organic binder and melt the inorganic binder. The firing process is very fast and usually takes less than an hour for heating, isothermal and cooling. Most of the material interactions take place during this stage, which result in very complex and non-equilibrium material systems. The physical properties of prepared thick films are intimately related to their microstructure, which is determined by the property and composition of each ingredient as well as processing conditions.

Thick film resistors (TFRs) are widely used in hybrid microelectronic circuits. They are composite materials in which the selected conductive phase is embedded in a continuous glass matrix. By changing the volume ratio of the conductive phase to glass phase, a range of resistance can be obtained. The most commonly used conductive phase includes ruthenium oxide and ruthenates because of their high conductivity and stability

to air firing at high temperature [4, 6]. Glass frits with low softening point and high resistivity provides an insulator matrix and the attachment of the film onto the substrate after firing. In addition, other additives sometimes are also added to modify the film properties. Typically, conductive particles in nano-scale, glass frits in a few micrometers and polymer vehicle are mixed thoroughly to obtain a printable ink with desired rheology. Screen printing is used to deposit the resistor film with desired thickness and geometry onto the substrate with pre-fired conductor. A wide range of sheet resistance value, low temperature coefficient of resistance (TCR), small drift of resistance, relatively low noise, capability of withstanding various voltage and current loads, good ability for trimming and etc. are the appreciated properties of a thick film resistor. Considered to be the most interesting but intriguing class of thick film materials [2-5], thick film resistors have received a lot of research attention in the past decades. However, the detailed technical information of TFRs mainly resides in the thick film ink manufacturers. The conduction mechanism is still under debate because of the complicated material interactions between the conductive phase, glass and substrate during the firing process [3-4, 9-12].

At present there are many commercially available thick film resistor inks on the market. However, most of the products contain lead, mainly in form of lead oxide (PbO) existing in the glass. As part of environmental initiatives, EU RoHS (European Union Restriction of Hazardous Substance) lead free program has been developed in 2002. Also, the directive on Waste Electronic and Electrical Equipment (WEEE) placed responsibility

on manufacturers to minimize the use of hazardous materials in 2005. The current global trend is to restrict or possibly eliminate the toxic elements such as lead from electronic components and products. It is significant to develop lead-free material systems for TFRs soon to reduce the negative environmental effects resulting from disposal of electronics. Many manufacturers have already started to develop lead-free material systems to replace the lead bearing counterparts. However, only partially success has been reported [13-19].

1.2 Objective and Scope

The overall objective of this work is to identify suitable lead-free glass candidates in order to develop a lead-free ruthenium oxide (RuO_2) based thick film resistor material system, which is able to cover a wide range of sheet resistance with relatively low TCR. The resistor material system to be developed should be compatible with the typical industry firing process (50°C/min ramp to 850°C, dwell for 10 minutes at this peak temperature).

It was felt that the only way to reach an understanding of thick film resistors is to first perform experiments with the basic ingredient materials and to limit the variety of experimental samples to those that were as conceptually simple and easy to define as possible. In addition, a better understanding the of conduction mechanism in thick film resistors is always desired before scientifically sound programs can be initiated to either develop new materials or improve existing systems. However, this part is always under debating and there is no consistent theoretical model even for lead-bearing TFRs. Current

research on lead-free TFR formulations indicates that the reaction of the investigated lead-free glass formulations behave unlike their leaded counterparts for RuO_2-based resistors [13-16]. Therefore, to develop a good lead-free TFR material system requires extensive experimental work due to the lack of pre-existing research. The overall objective will be fulfilled by carefully evaluating and choosing suitable lead-free glass material.

The primary source of lead in currently available thick film resistor ink products is the glass, which is mainly lead silicate or lead borosilicate glass containing 40%~65% PbO. Besides, some TFRs use lead ruthenate ($Pb_2Ru_2O_7$) as the conductive phase. The intuitive solution is to replace the lead bearing component by lead-free material. Generally, for TFRs application, the desired glass should have proper softening point, proper viscosity or surface tension at peak temperature, good wetting to conductive phase and alumina substrate, and proper coefficient of thermal expansion (CTE) to match the substrate material. The desired glass also should remain vitreous after firing and provide a low TCR. Lead-free glass evaluation and selection were the primary work of this project. A pool of electronic grade lead-free glass frits were obtained from different manufacturers and a series of analytical techniques were used to evaluate each glass frit in order to select suitable ones that satisfy the desired property requirements.

Thick film resistor inks were prepared using the selected glass frits and RuO_2 for electrical properties testing. In addition, the microstructure of fired films as well as

interactions between the ingredient materials and substrate were studied. Being considered as the first phase of the development research work on lead-free TFRs, the primary thrust of this study was to identify the suitable glass with proper properties and important processing variables, which could pave a way for further investigation to finalize a success lead-free thick film resistor film system.

CHAPTER 2

LITERATURE REIVEW

2.1 Materials

The switch from conventional circuit construction techniques to a thick film hybrid process entails for a drastic change in outlook concerning the materials used. Unlike a printed circuit board (PCB) that requires little material knowledge, in thick film circuit techniques the circuit assembler has become a producer of components who must be concerned with the effect of the processes on the properties of the circuit elements. Any successful thick film operation must be based on a materials awareness, which includes the understanding of the nature of each ingredient used and their possible chemical and physical interactions during the different steps of the thick film process.

As mentioned earlier, most thick film materials exist in form of inks. Typically, they contain a functional material, an inorganic binder and an organic vehicle for printing viscosity control. For resistors, the functional materials are highly conducting metal or metal oxide. The inorganic binder is usually a glass frit to provide adhesion to the substrate but quite often influence the film electrical properties, and the organic vehicle is a mixture of high molecular weight polymer dissolved in a solvent. The formulated inks are deposited on a substrate, which is also a significant participant in some of the chemical reactions [1].

The main reason that thick film resistor have become technologically important is that the sheet resistance can be varied over several orders of magnitude by changing the relative amounts of glass and conducting particles [2-6]. The sheet resistance can change from 10 ohms per square (Ω/□) to 10 mega-ohms per square (MΩ/□) solely by altering the weight or volume fraction of conductive particles from about 2% to 40%, as shown schematically in Figure 2.1.

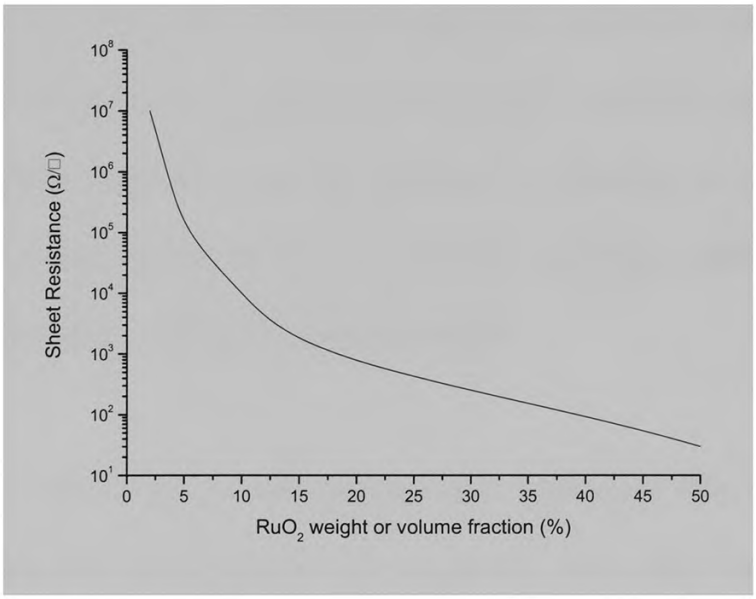

Figure 2.1 A schematic view of sheet resistance verses RuO_2 fraction [4]

2.1.1 Conductive Phase

Due to the thick film processing and application requirement, the qualified conductive phase should possess a reasonable resistivity and be both physically and chemically stable at high temperature in air. The earliest conductive phase used for thick film resistive systems was palladium or silver metal particles [4]. However, they were found

to form metal solid solution during the firing process, which limited the resistivity range. The high TCR of resistors based on these metals was an additional shortcoming. Significant improvements were obtained when ruthenium oxide was identified and used in TFRs due to its metal-like conductivity and relative good stability when fired at high temperature in air [3-6]. Iridium oxide (IrO_2) was also reported [7-10] to be used as conductive ingredients. Besides, ruthenium based ruthenates and perovskites [16-18] were claimed to be more thermal stable with comparable conductivity to ruthenium oxide. Among all of the conductive materials mentioned above, ruthenium oxide was most commonly used by thick film resistor ink manufacturers. Generally, the particle size of RuO_2 is several hundred nanometers or less in order to obtain a relatively uniform inorganic mixture and a continuous conduction network.

2.1.2 Glass

Glasses are very important materials in electronics applications. They serve in more varied roles than the ceramic materials. Historically they were used in tube envelopes, capacitor dielectrics, and sometimes substrates due to their reproducible electrical properties, ease of fabrication into complex shapes, and low cost. They are valued for their superior properties including insulating properties, surface smoothness, controllable thermal deformability and the ability to serve as an inorganic binder.

Glasses are non-crystalline solids existing in frits or fine particles. They have random structure of a liquid which gets solidified as the melted glass is cooled. The feature which

permits glasses to remain amorphous rather than crystallizing is the very high viscosity of the melted material. Since glasses are not definite crystals but closer to chemical mixtures, they may have an infinite range of compositions. In spite of this, almost all glasses are based on four glass-forming oxides: SiO_2, B_2O_3, P_2O_5 and occasionally GeO_2. The first three ingredients are often intermixed by different ratios. In addition to these basic oxides, a number of softener or fluxes (the oxides of alkali metals Li, Na, K, Rb, Cs and Pb) and extenders (the oxides of alkaline earth metals Mg, Ca, Sr, and Ba) are usually added. Another common group of nonfunctional additives are colorants (the oxides of Co, Mn, Fe, and Cr).

Glass frits are added to most thick film inks and there are certain general properties that they should possess. Typically, they should have high electrical resistivity and thermal shock resistance, environmental inertness, as well as low dielectric loss. In addition, several other physical properties such as softening point, thermal expansion, surface tension and reactivity toward both substrate and other inorganic constituents in the inks are always of great interests. These properties should have proper values for different given applications. Because of the applications in electrical circuits, thick film glasses must have a very low alkali content, which makes the majority of the glass literature of little use for guidance in selecting compositions [4-6]. Moreover, thick film glasses are desired to remain vitreous after firing. Devitrification of fired glass usually affects the electrical properties of thick films due to the existence of grain boundary.

Thick film glasses are typically borosilicate with intermediates and modifiers such as Al_2O_3, Bi_2O_3, PbO, CdO, ZnO, BaO, and CaO. The lead bearing glass is by far the most common; with a typical composition 63wt%PbO-25wt%B_2O_3-12wt%SiO_2 due to its low softening point [1-7]. This glass satisfies most of the general requirement stated previously. Although there are some arguments that the lead bearing glasses are susceptible to partial reduction under certain firing conditions [6], the advantages including close match of coefficient of thermal expansion to alumina substrate, proper viscosity and surface tension for firing around 850°C and good durability make it superior than other compositions.

2.1.3 Polymer Vehicle

Polymer vehicle, also referred as a screening agent, is a mixture of a solvent and a polymeric material with high molecular weight. Generally, the solvent provides viscosity control during screen printing. A low-vapor-pressure solvent is required so that the viscosity does not change with the time as a result of solvent evaporation while the ink is spread out on the screen. But it also should be easily volatized during the initial drying process at 125~150°C for 10 to 20 minutes. The most commonly used solvent is terpineol. The polymeric material provides thixotropic properties to the thick film ink, allowing it to flow through the screen mesh under pressure of squeegee but to cease flowing on removal of the squeegee. It should be easily oxidized and burned out during the early stages of firing. Ethyl cellulose is the most popular material used.

The solvent is mixed with the polymeric material in a proper ratio to get a homogeneous solution. Other organic constituents that act as surfactants and thixotropes are also commonly added. Many of these organic systems used in commercial thick film inks are developed by the paint related industry and are proprietary formulations.

2.1.4 Substrate

The substrate is also classified as a raw material in this section because of the fact that in most cases it participates in the interactions with the ink ingredients during the processing of the thick film inks. Typically, the substrate should serve many functions and the most important ones are:

1. Support the circuit and provide a means for mounting.
2. Protect the circuit from mechanical damage and from the working environment.
3. Heat dissipation.
4. Provide electrical isolation.

According to these basic requirements, there are some general properties that thick film substrates should possess, such as high mechanical strength, electrical resistivity, dielectrical strength, thermal shock resistance and thermal conductivity, relatively low dielectric constant and dielectric loss. In addition, chemistry reactivity, surface characteristics, thermal expansion, dimensional stability and refractoriness are also the properties of most interest depending on the particular application. Besides, the cost of the substrate should be reasonable.

Alumina (96 to 99.8% Al_2O_3) is the most commonly used material for substrates. The majority of commercial thick film inks were developed to give optimum properties when fired on alumina substrate. Most of the fundamental research studies on thick films have been conducted using alumina substrates as well. Alumina (96%) substrates are historically used for most of the thick film resistor applications. The most common additives are magnesia (MgO) and silica (SiO_2). Magnesia inhibits grain growth of alumina grains through segregation at the alumina boundaries whose movement is then prevented. Silica is useful since the interactions between Al_2O_3 and SiO_2 gives rise to a new inter-grain phase which binds the whole system.

2.2 Thick Film Fabrication Process

2.2.1 Ink Making

The basic purpose of the thick film ink is to produce a fired composite that controls the electrical property of the printed film geometry. In resistors, modulated conduction over a range of resistances is anticipated. Ink making is essentially a two-step process. Firstly, the conductive particles and glass frits are grinded by wet or dry ball milling to obtain a desired particles size, which is usually indicated by the fineness of grind (FOG). Perfect blending of the inorganic constituents is difficult to be achieved and maintained because the conductive particles and the glass frits usually have different densities. A long milling time could give a relatively uniform inorganic mixture. The second step is a thorough mixing of the inorganic mixtures and the organic vehicle to produce a

homogeneous ink with proper viscosity. This step is usually conduced on a 3-roll mill. Figure 2.2 shows how the three-roll mill works. Two adjustable rolls are designed to mill the slurry and receive the paste respectively. The shear force between the milling roll and the fixed roll can be adjusted to obtain a uniform dispersion of inorganic particles in the polymer vehicle.

2.2.2 Screen Printing

Given the requirement that the thick film inks must have a high viscosity, screen printing is the most commonly used method to deposit them in the desired pattern. The process of stenciling or screen printing patterns is an ancient one. The Egyptians used this technique thousands of years ago to decorate pottery and the walls of building and tombs. The principle concept is using a mask with open and closed areas defining the pattern, which is brought into contact with the surface to be decorated. A fluid ink is forced through the opening in the mask using a rag, fingers or a piece of wood. When the mask is removed, the ink pattern remains. This is basically the same process used today for production of thick film circuits.

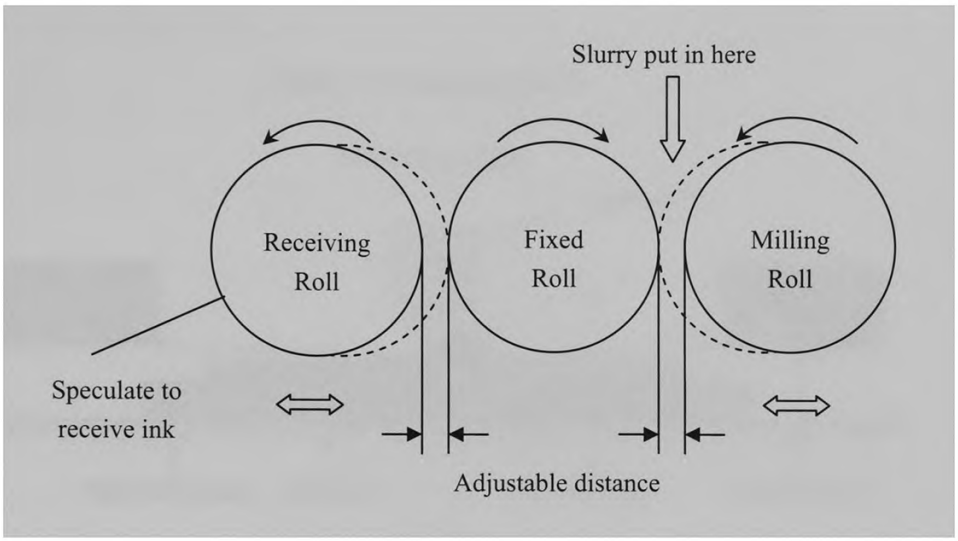

Figure 2.2 A schematic view of a 3-roll mill

The screen, which is the mask, defines the pattern of the printed film and also meters the amount of the ink which is deposited. The most common type of screen comprises a frame, normally cast aluminum, onto which a finely woven mesh is stretched and coated with a light-sensitive emulsion. The most commonly used mesh material is stainless steel. The diameter and the size of the opening can be varied depending on the process requirements. In general, the larger the opening the more material deposited on the substrate. The opening size is usually given in terms of a standard mesh number. It is possible to obtain the screen mesh aligned in several orientations, the most common three mesh angles are 22.5, 45 and 90°.

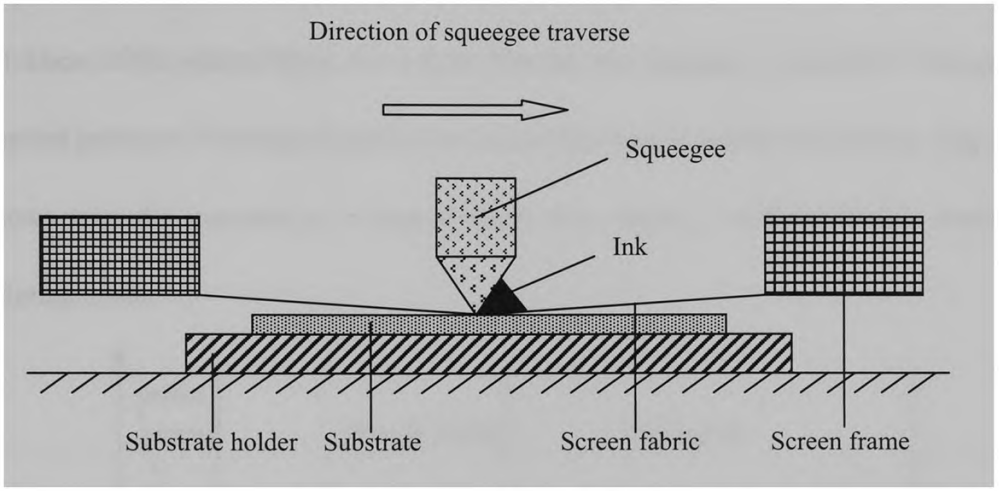

Figure 2.3 The basic screen printing process

Figure 2.3 shows the constituent parts of a typical screen printer. The substrate is held in position by either a vacuum chuck or a special jig, which is usually termed the substrate holder. There is a small gap between the paralleled screen and substrate surface that gives rise to the term of off-contact printing process. Enough amount of ink is applied to the upper surface of the screen fabric and a flexible rubber squeegee is traversed across the screen. The mesh fabric is pressed into contact with substrate surface and the ink is forced through the opening areas of the screen mesh. Directly behind the squeegee the screen peels away from the substrate and leaves a deposit of ink as the desired pattern on the substrate surface with a certain thickness.

The viscosity of inks is the most important property that affects the geometry and thickness of the printed films. For a thick film ink the viscosity is required to change with applied pressure. The classification for fluid of this type is termed thxiotropic. Figure 2.4 shows how the viscosity of a typical thick film varies at different stages during the printing cycle.

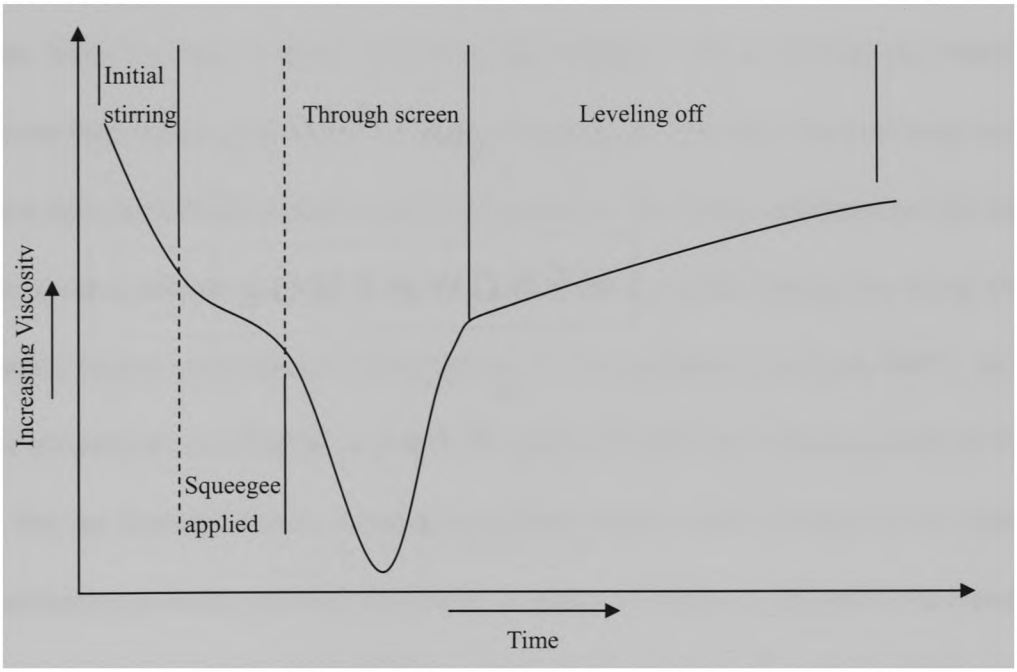

Figure 2.4 The viscosity of a ink varies at different stages of the printing cycle

2.2.3 Drying and Firing

The film is allowed to stand in air for a few minutes after printing in order for the ink to level off and settle. Then the film is placed into a conventional box oven or a moving belt infra-red furnace drying at a temperature between 120~150°C for 10 to 15 minutes. The objective of this process is to remove the organic solvent, make the printed film

adherent to the substrate and develop a "green" (unfired) strength relatively immune to smudging. The polymeric material is still present in the ink at this stage. After drying the substrate may either be overprinted with another thick film layer or they will proceed to the firing stage.

The high temperature firing cycle is designed to remove the remaining organic binders from the film, to bond the ink to the substrate and to develop the desired microstructure, which gives rise to the electrical properties. The final electrical properties of some inks, particularly resistors, are very sensitive to the firing conditions and for this reason accurate control over the processing parameters is needed. During the firing, the polymeric organic component is burned out in air at temperature lower than 500°C. At a higher temperature, usually 550° to 700°C, the glass transition and softening points of the glass frits are attained. Ideally, a continuous glassy matrix starts to be formed in which the conductive particles remains imbedded. A proper viscosity is obtained at the peak firing temperature (usually around 850°C), while allows a relatively uniform distribution of the conductive particles in the matrix. Then a cooling stage allows the glass to solidify. Most thick film furnaces are moving belt furnaces providing a fast ramp (usually 50°C per minute), which is typically used for both heating and cooling rather than a lower rate to possibly reduce or prevent some undesired interactions between the resistor ingredients and the substrate. Figure 2.5 shows a typical firing profile for thick film inks.

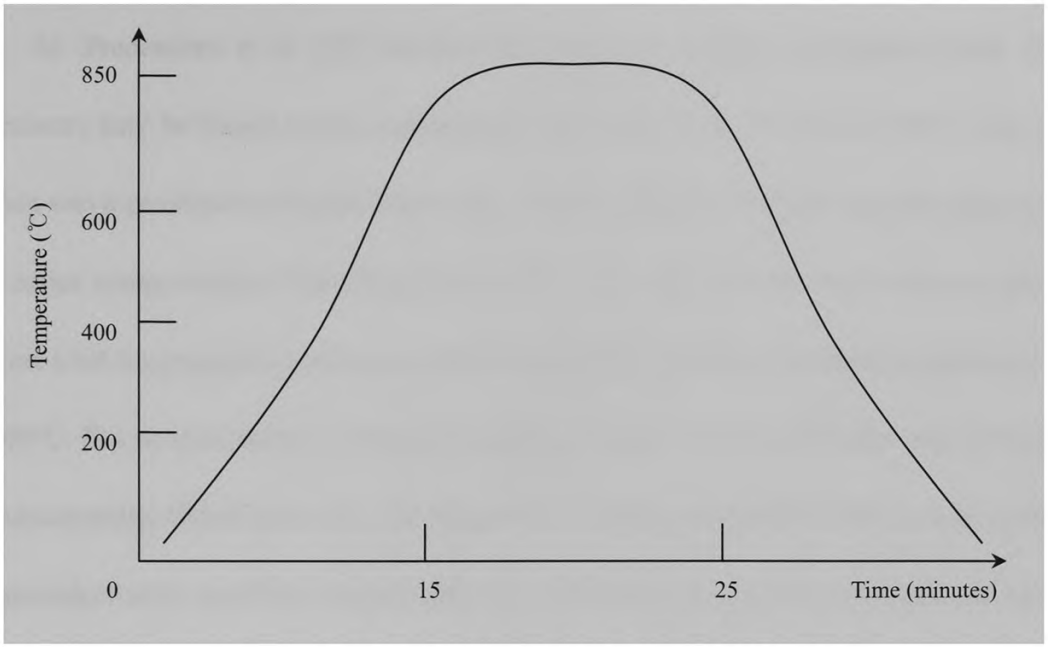

Figure 2.5 A typical firing profile for thick film inks

2.3 Research on Lead-Free Thick Film Resistors

2.3.1 Technical Literature

Urged by the global environmental initiatives, lead-free resistor systems have been researched for over 10 years. Some efforts have been made to identify suitable lead-free glass frits and new conductive phase to replace the lead-bearing glasses and lead ruthenates in order to obtain a lead-free thick film resistor formulation, which is able to cover a wide resistance range with low a TCR value. Due to the proprietary nature of thick films, most of the knowledge of TFRs resides in the manufacturers and unpublished. The open literature is somewhat restrictive on interactions and conduction mechanism and the reports of lead-free TFRs are even limited, which make the development of such a lead-free TFR system difficult.

M. Prudenziati et al. [15] claimed that the early studies on lead-free thick film resistors may be traced in the experimental work done by R. W. Vest in 1979 when Dr. Vest was a professor at Purdue University. It was mentioned that the lead-free glass with a major composition of $CaO\text{-}BaO\text{-}B_2O_3\text{-}SiO_2\text{-}Al_2O_3$ and RuO_2 as the conductive phase were tried for preparation of resistors with acceptable stability at operating temperature of 500°C. But no information of material interactions and electrical properties was disclosed. Subsequently, Chiou and Vest [13] suggested that high temperature materials for hybrid microelectronics could be realized with lead-free pastes having high transition and strain points.

A model system of TFR has been studied by B. Morten et al. [14] using the proposed CaBaBAlSi lead-free glass and RuO_2. It was found that the microstructure development of the resistor films followed the same pattern as the common layers made with lead-containing glass at a relatively high temperature (from 600 to 1000°C). However, in the work of M. Prudenziati [15], seven lead-free glass frits including the CaBaBAlSi glass were selected to prepare for RuO_2-based TFRs. The study evidenced a myriad of complex phenomena, including devitrification, relevant bleeding of the glass on the alumina substrate, anomalous distribution of conductive grains in the glass matrix and phase separation. A very short resistance range (within a few KΩ/□) was obtained by varying the volume fraction of RuO_2 from 1.7 to 10%. There was an abrupt change of resistance from around 1 KΩ/□ to larger than 100 MΩ/□, which is usually considered as

an insulator. The author concluded that the higher conductivity of the prepared resistors may be due to a large solubility of Ru in silicate glasses with large amount of B_2O_3, an unusual distribution of RuO_2 grains in the glassy matrix and different interactions between RuO_2 and glasses.

M. G. Busana et al. [16] used a bismuthate glass and successfully avoided the negative effects such as devitrification, bleeding of glass on the alumina substrate, anomalous distribution of conductive grains in the glassy matrix and phase separation observed in other systems [15]. The primary composition of the glass used is SiO_2-Bi_2O_3-Al_2O_3-ZnO with a minor amount of MgO, CuO and CaO. Some TCR drivers, typically oxides such as TiO_2, Nb_2O_5 and Mn_2O_3 and inert fillers such as SiO_2 and $ZrSiO_4$ were blended with the glass frits to modify the TCR and reduce resistor expansion, respectively. The obtained sheet resistance spanned two decades from ~10 to ~1000Ω/□ by changing the RuO_2 weight fraction from 14 to 52% and the TCR remained in ±300ppm/°C. Although the resistance range is short, the resistors exhibited good reproducibility and the work showed a promising progress on the development of RuO_2-based lead-free TFRs.

J. Setina et al. [24] prepared RuO_2-based lead-free TFRs using phosphate glasses with a primary composition of ZnO (MgO)-P_2O_5-SiO_2-V_2O_5. The author reported that phosphate glasses have suitable thermal and chemical properties for the formation of high quality coating on alumina with a high electrical resistivity, sufficient chemical durability

and viscosity-temperature relationship suitable for thick film inks. A complete saturation of RuO_2 film with the glass phase without chemical interactions between glass, RuO_2 and the alumina substrate was found at firing temperature 850°C. Gold was used as the conductor electrodes and the sheet resistance spanned from kilo-ohms to giga-ohms per square with a RuO_2 weight fraction from 7.7 to 30%. No TCR testing was carried out in this work.

The work on RuO_2-based lead-free TFRs was not just limited to the reports mentioned above. Many of them remained unpublished and existed as proprietary technical reports to the ink manufacturers. The open literature gave only some partially successful results and almost all of them tried glasses with similar composition. Moreover, the research work based on pyrochlore bismuth ruthenate ($Bi_2Ru_2O_7$) was also carried out but not as extensive as the RuO_2-based formulations. Leaching of Bi_2O_3 from $Bi_2Ru_2O_7$ was reported by B. Morten [14], which led to a short resistance range with high positive TCR. For the same reason, there were few reports published regarding this topic.

Due to the limitations met in RuO_2 and pyrochlore ruthenate based lead-free TFR systems, a lot of efforts have been done to identify other suitable conductive phase as well as lead-free glasses. Recently, perovskite ruthenate such as $CaRuO_3$ was the subject of considerable research attention as a comparable conductive phase due to their relatively stability at high temperature in air. R. Klein and K. Jones [25] evaluated the TFR formulations using $CaRuO_3$ that are compatible with LTCC co-firing. S. Rane et al.

[26] prepared TFRs containing $CaRuO_3$ and the CaBaBAlSi glass [14, 15]. There were some negative affects such as devitrification, formation of voids, leaching of RuO_2 at a temperature higher than the conventional 850°C firing temperature. But a range of sheet resistance from 6 to 75KΩ/□ was obtained at a low temperature (750°C). The hot and cold TCR was -145 and -150ppm/°C respectively achieved for a resistor with 25% $CaRuO_3$ by volume. Generally, the result was superior to the previous lead-free TFR systems in terms of the resistance range. There were still several limitations and problems which limit its performance including porous structure, unstable electrical properties and non-compatible firing process with typical industry thick film processing. Another report [17] from the same researchers tried another glass composition (SiO_2-CaO-BaO-SrO-K_2O-B_2O_3) on $CaRuO_3$ for preparation of TFRs on both alumina and LTCC substrates. The firing process used in this work was a two-step process including a firing profile of 750°C peak temperature for 8 minutes and a re-firing at 850°C for 8 minutes in order to limit the formation of voids and achieve a better morphology of the resistors. A 25 vol. % $CaRuO_3$ resistor formulation gave 5KΩ/□ sheet resistance with 225ppm/°C hot TCR for resistors fired on alumina substrate. A further study [18] showed that 800°C for 10 minutes firing is an optimized profile to get better surface morphology and stability of electrical properties of the prepared TFRs for the same formulations. By varying the volume fraction of $CaRuO_3$ from 10 to 25%, a sheet resistance covered three decades from 60Ω/□ to 1.1KΩ/□ and there was an sharp increase

to larger than 50MΩ/□ for the 10% formulation. Without adding any additives to adjust the TCR, the resistors exhibited a relatively low TCR value (in the range of 180 to 580ppm/°C). A more recent research [19] was conduced to study the effect of firing condition and temperature to this CaBaBAlSi glass and $CaRuO_3$ lead-free thick film resistor formulation. The 800°C firing profile was showed again to be an optimized temperature for the prepared formulation. The resistors fired in conventional thick film firing furnace were found to be denser and morphologically more uniform than the resistors fired in normal tube furnace. For the same resistor composition, a substantially higher resistance value with a lower TCR was obtained for the resistors fired in a thick film belt furnace than the ones fired in tube furnace.

2.3.2 Patent Literature

Most of the patents involving thick-film resistor inks have been directed toward developing economical, reproducible, stable materials which can be fired in air. The thick film resistor paste patents generally describe the conductive phase composition and many aspects of the patents deal with the effects of small additions of materials (of the order of 1%) on the electrical properties of the finished resistor. A survey of patents related to lead-free thick film resistor compositions was made for the period within the recent two decades.

U.S. Patent #5,491,118 [27] assigned to DuPont claimed a thick film paste composition suitable for forming resistor or thermistor patterns on a substrate. The

conductive phase is ruthenium-based containing RuO_2 and related pyrochlore ruthenates. The glass, which is cadmium and lead free, essentially consists of Bi_2O_3-B_2O_3-SiO_2-CuO-ZnO-CoO-Fe_2O_3 by different mole fraction. The prepared samples cover only a short sheet resistance range that not exceeds a few kilo-ohms per square and the TCR is relatively high.

U. S. Patent #6,171,987 B1 [28] assigned to Ben-Gurion University of the Negev claimed a lead-free glass composition that comprises mainly B_2O_3-SiO_2-Bi_2O_3-Al_2O_3 with minor ZnO-CuO-CaO-MgO modifiers for thick film formulations. The thick film resistor prepared by M. G. Busana et al. [16] using one of the glass composition from this patent was claimed to overcome the negative effects encountered in the previous studies [14, 15]. However the electrical property of the prepared TFR was not satisfied.

2.3.3 Product Literature

Lead-free thick film resistor is an area of the market where many manufacturers are working but little success has been achieved or sustained till now. DuPont has announced the LF19x series of lead-free resistors recently but they are still in the stage of development for completion and there is no commercially available product now.

2.4 Problem Statements and Challenges

In summary, the previous work on the development of a lead-free TFR system can be classified into two categories in terms of ingredient substitution. On the one hand, lead-free glasses were tried on the traditional ruthenium oxide based conductive materials.

Only several partial successes have been obtained and the developed systems do not have a relatively stable electrical property. The range of the sheet resistance was short and limited under a few kilo-ohms per square. On the other hand, some efforts have been made to identify new conductive materials that are relatively stable during thick film processing. A wider sheet resistance range was obtained by a few researchers, however, at a lower temperature than the conventional industry thick film firing profile. Both of the works have evidenced the different behavior of lead-free glasses from the lead bearing glasses and some other negative phenomena, which emphasize the critical choice of glass composition for a suitable resistor structure. In addition, the proprietary nature of thick films enhances the difficulty to develop a lead-free thick film resistor formulation that is comparable to the traditional leaded ones in term of electrical properties. The following are the summarized challenges of this work:

- The interactions between the conductive phase, glass and the substrate are very complicated and it is difficult to derive them by only studying the final composition and microstructure of TFRs.
- Most thick film resistor knowledge resides in manufacturers and is protected by trade secrets and unpublished. Research in open literature has always been somewhat restrictive on reactions and conduction mechanism within thick film resistors. The effort in lead-free resistor systems is even more limited.

- Though several partially successful attempts on lead-free thick film resistor formulations have been reported, it is still a big challenge in covering a wide range of sheet resistance with a low TCR value in these systems. .

CHAPTER 3

METHODOLOGY AND EXPERIMENT

3.1 Material Preparation and Characterization

3.1.1 Conductive Phase

In this work, the most commonly used conductive phase, ruthenium oxide (RuO_2), was obtained directly from the vender and ready to use. Table 3-1 shows the general properties of RuO_2. The morphology and particle size of RuO_2 powder were characterized using a JEOL JSE-6330F field emission scanning electron microscope (SEM), which is equipped with an energy dispersive X-ray analyzer (EDS) for chemical analysis. A FEI CM200ST transmission electron microscope (TEM) was also used to charactreize the conductive particles. X-ray diffraction was used to verify the composition of RuO_2 powders on a Siemens diffractometer (D5000) using CuK_α radiation.

Table 3-1 General Properties of RuO_2

Specific Gravity	Electrical Resistivity	Average Particle Size	Melting Point
6.97 g/cm^3	$4.0\times10^{-5}\Omega\cdot$cm	~20nm	1200°C

3.1.2 Glass Frit

Thirty-three commercially available electronic grade lead-free glass frits from different manufacturers are provided by Heraeus Inc., a thick film ink manufacturer. The basic information of all glasses is attached in the glass catalog (See Appendix 1). Several

basic physical properties including major composition, coefficient of thermal expansion, specific gravity, softening point and average particle size are provided in the product description. Starting from these basic properties, the down selection of glass was carried out phase by phase according to the general criteria set for thick film resistor application. This part is explained in details in Section 3.2.

3.1.3 Substrate and Polymer Vehicle

The substrate material is the most commonly used 96% alumina. They are obtained from CeramTec North America (Laurens, South Carolina). The dimension is a 2 by 2 inch with 25 mils thickness. Table 3-2 lists several general properties of the 96% alumina substrates.

The polymer vehicle for ink making is provided by Heraeus Inc. and ready to use. The major ingredients are ethylcellulous and terpineol, the typically mixing ratio is 1:9 by weight.

Table 3-2 Properties of 96% alumina substrate

Density (g/cm^3)	3.8
Young's Modulus ($dyn/cm^2 \times 10^{10}$)	310
Thermal Expansion ($10^{-7}/°C$)	69
Dielectric Strength (V/μm)	13.1
Volume Resistivity (Ω·cm)	10^{15}
Dielectric Constant K at 25°C, 1Mhz	10.0

3.2 Lead-Free Glass Evaluation and Selection

Glass frit plays a critical role as one of the essential ingredients in thick film inks, especially in thick film resistor formulations. It usually occupies 40~98% of the thick film resistor formulation by weight or volume as the primary component and has been considered to contribute significantly to the electrical conduction of TFRs. Glass frit also provides a medium where various types of chemical reactions can occur during the firing process. These reactions greatly contribute to the developed microstructure and hence, to the electrical properties of TFRs. Therefore, it is critical to select a suitable glass material. However, the specific ingredient information of TFRs is always considered as proprietary, especially in term of glass frits.

The down selection work to determine a suitable glass frit from a pool of candidates for resistor formulation is divided into two phases. The first one is pre-selection based on the desired basic physical properties. A series of methods and techniques were used to narrow down the number of candidates in a simple but effective way.

Typically, the glass should possess a proper coefficient of thermal expansion (CTE) to match the CTE of the substrate in order to prevent potential thermal stress that usually results in cracks or inferior interface bonding after fire processing. Good wetting to the substrate is another property to ensure good adhesion to the substrate. A suitable softening point is required for the glass to melt and have proper viscosity so that a desired microstructure of the thick film can be obtained. The major composition may vary

somewhat in fraction but typically consists of the oxides of essential elements such as B_2O_3 and SiO_2. Other oxides have various functions such as providing the mechanical strength, lowering the softening point, adjusting the CTE, provide the desired reactions and etc. In this work there is no specific requirement for the glass composition except those containing large fraction of ZnO, which is considered as one of the most reactive ingredients and the major cause of devitrification after firing. Moreover, the electrical properties also depend on the film geometry; therefore the glass should maintain its shape after firing. This requires the glass to be dense and compact after firing.

To summaries, the following properties are set as the criteria for the pre-selection of glass:

- ✓ Composition: Free of PbO, with no large content of ZnO.
- ✓ Softening point (T_s): Between 400°C and 700°C.
- ✓ CTE: Match the CTE of alumina substrate (65-75×10^{-7}/°C), preferably less.
- ✓ Good wetting to the alumina substrate.
- ✓ Dense and compact after firing.
- ✓ No significant expansion and shrinkage.
- ✓ Remain vitreous or no major crystallized phase after firing.

Among all these property requirements mentioned above, only the CTE information and softening point can be obtained directly from the product description. The major composition provided is not in detail and still needed to be verified. In addition, there are

no enough literature references to provide guidance. Therefore, it is still difficult to down-select the glass candidates under these conditions. A simple but effective method was used here to help the selection process. A small amount of glass powders was pressed into a pill and placed on top of an alumina substrate. A programmable Lindburg Blue high temperature box furnace was used for firing both the glass pills and thick film resistors. The same firing profile was carried out to the glass pills, which is from room temperature to 850°C with a 50°C per minute ramp and hold for 10 minutes at the peak temperature. The glass after firing can be directly evaluated visually in several aspects including the wetting and bonding condition to alumina substrate, the surface smoothness, cracks and voids, shape and geometry. After screening out all the glass pills, a portion of candidates were removed from the list based on this experiment.

The rest of the fired bulk glass pills were tested by X-ray diffraction. Due to the large thickness of the fired glass pills, the scanned surface area can be considered to be pure fired glass without the interface of the alumina substrate. The ones that devitrify after firing were removed. Moreover, the thermal behaviors in terms of softening point and devetrification of the glasses can be observed by testing the glass powders using a TA Instruments SDT Q600, which combines differential scanning calorimetry (DSC) and thermogravimetry analysis (TGA) and can give both data simultaneously.

Due to the complicated interactions between the conductive particles, glass frits and the substrate during firing process, the selection of suitable glass can not be finished

without making them into resistor inks for further characterization and testing, which is the second phase. After the pre-selection, the remained glass candidates were characterized and then proportionally mixed with RuO_2 and a polymer vehicle to formulate thick film inks for further characterization and testing.

3.3 Thick Film Processing

For thick film resistors, the ink property and firing condition are also very important to the final electrical properties of films. The thick film processing in this work follows the same steps and parameters of the typical industry thick film processing. It consists of inorganic powder preparation, ink making, screen printing, drying and firing.

3.3.1 Ink Making

Particle size is one of the key factors that affect the thick film paste property and the final electrical properties of resistors. And the uniformity of inorganic mixtures directly determines the uniformity of the inks as well. To better control the following process, the first step is to mix the conductive powder and glass frits to obtain a uniform inorganic mixture and desired particle size. Weighted glass frit and RuO_2 were mixed in de-ionized (DI) water and the mixed slurry was ball milled with half-inch cylindrical alumina medium (US Stoneware, East Palestine, OH) in a 300ml alumina jar (US Stoneware, East Palestine, OH) with an inside diameter of 2.75 inches. Typically, ball mills are operated at a speed less than (usually 55%-75%) the "critical speed", which is expressed in rpm by the formula:

$$N_c = \frac{54.19}{\sqrt{r}}$$

where r is the inside radius of the mill in feet. For both grinding and mixing purposes, a speed of 50 rpm was used and the milling time is at least 18 hours. After milling, the inorganic mixture was washed out by DI water into a glass dish, which was then placed into a high temperature oven for drying. A three-hour drying at 300°C was used to completely remove the water. This was followed by another dry mill for at least an hour, after which the inorganic powders were collected for another mixing step with the polymer vehicle.

The polymer vehicle is also provided by Heraeus Inc. and ready to use. Weighted inorganic powders and organic vehicle were mixed in a glass container till thoroughly wet slurry was obtained. A three-roll mill was used to get a uniform paste with desired viscosity. Fineness of grind (FOG) test was done to measure the inorganic particle size and their distribution in the polymer binder. The volume ratio of organic vehicle to inorganic mixture is kept at 3:7 till milling is completed. Typically, a small pressure is used to wet out the particles first and then increased step by step to a maximum of around 400-500lbs for both mixing and milling till desired dispersion of inorganic particles is obtained. Then the pressure is lowered to around 100-150lbs and deficient vehicle is added till desired viscosity is obtained. Due to the difference of density between RuO_2 and glass, a thorough stirring before using is needed although the paste is thixotropic.

3.3.2 Screen Printing

In this work, the screen printing process was conducted on a MPM TF-100 micro-printing system (MPS International Corporation, Los Angeles, California). The 5 inch by 5 inch, 325 mesh stainless steel screens from MicroScreen L.L.C. (South Bend, Indiana) were used. Two groups of patterns were generated by AutoCAD. One is 10 by 10 cm square for X-ray diffraction sample. Another is a pair of resistor and conductor patterns for electrical property testing purpose, as shown schematically in Figure 3.1. There are six groups of resistor, that is, different lengths from 1sq to 10sq as labeled by numbers in the graph. The used silver conductor paste (C4740S) was from Heraeus Inc. and a conductor layer was printed and fired first. The second layer of the resistor pattern is then aligned and printed onto the substrate.

3.3.3 Drying and Firing

After printing, the samples are usually left on a flat surface in air at room temperature for around 10 minutes for self adjusting and leveling. Then the substrate with thick films on it is dried at 150°C for 10-15 minutes to remove the solvents. A Blue M single-wall oven was used for the drying process. As mentioned in last chapter, a typical industry firing process for TFR is 850°C for 10 minutes with a 50°C per minute heating and cooling ramp. The whole firing process is usually conduced in a belt furnace and takes less than 60 minutes. In this work, the programmable Lindburg high temperature box furnace and the same firing profile were used to fire the samples.

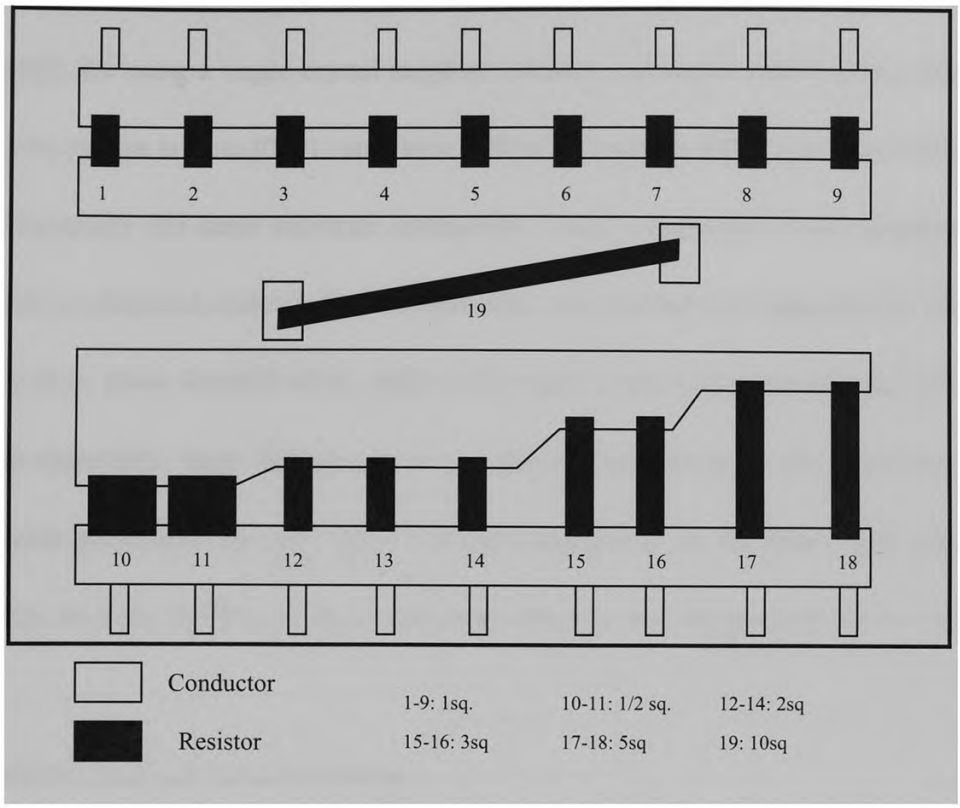

Figure 3.1 A schematic view of resistor pattern on the alumina substrate

3.4 Ink Characterization

The surface of the fired resistor films was observed by a Buehler Versamet3 optical microscope. The microstructure was further studied by SEM. To better understand the distribution of conductive particles and glass phase, the cross section that is parallel to the film surface was obtained by carefully grinding and polishing. Also, the vertical cross section samples of resistor film were prepared as well. X-ray diffraction is considered to be the best method to evaluate materials interactions. However, polycrystalline alumina has a large number of diffraction lines, with a number of peaks that are identical to the

major lines of RuO_2, making analysis of RuO_2 on polycrystalline alumina almost impossible. By using a single crystal sapphire substrate cut on the (0001) plane, the only diffraction pattern is from (0001) and there will be no multiple diffraction lines while still providing nearly the same substrate interaction. Energy dispersive X-ray spectroscopy was used for chemical analysis. Some interactions are reported to be desirable [3, 29], but some lead to glass devitrification, which will cause undesirable consequence [19, 30] such as extremely, large differences in the thermal expansion of the crystalline and amorphous phase that can give rise to fissures and cracks in the films, reducing their durability or even destroying their structural integrity and destructing the conductive path.

3.5 Resistor Electrical Property Testing

All the resistors are prepared according the pattern shown in Figure 3.1 and tested using two-probe method on a HP 34401A multimeter. Typically, the resistance value is measured at temperature of -55°, 25° and 125°C , and the measured values (R_{-55}, R_{25}, and R_{125} respectively) are used to calculate the hot and cold temperature coefficient of resistance (HTCR and CTCR, respectively), using the ordinary equations [4, 31]:

$$\text{HTCR(ppm/°C)}=\frac{R_{125}\text{-}R_{25}}{R_{25}(125-25)}\times 10^6$$

$$\text{CTCR(ppm/°C)}=\frac{R_{25}\text{-}R_{-55}}{R_{-55}(-55-25)}\times 10^6$$

In this work, the resistance was measured at 25 and 125°C and HTCR was calculated.

CHAPTER 4

RESULTS AND DISCUSSION

4.1 Characterization of Ingredient Materials

4.1.1 Lead Free Glass Evaluation and Selection

Photographs of all the fired glass pills on alumina substrate are attached, together with the basic glass property information in Appendix 1. Every glass candidate was evaluated according to the property criteria set for the pre-selection. Although the thickness of a typical TFR is around 15 to 25 micrometers, the shape and morphology of the fired glass pill in macro scale is indicative of the glass behavior during firing in the application scale. The following glasses are excluded from the list in Appendix 1 due to various reasons described briefly as following, which make them unacceptable.

- Glass LC1102 is not compact and dense. In addition, it has significant cracks, which is unacceptable for adhesion to the alumina substrate and resistor performance.
- Glass LC1246 has a relatively low softening point and significant phase separation was evidenced after firing. Moreover, it does not wet the substrate well.
- Glass LC1247, LC1248, LC1264 and LC1367 have proper softening point, good CTE match to the substrate. However, the fired glass pills are porous, which will create major voids and porous structure in thick films.

- Glass LC1260 has a higher softening point than 850°C and does not melt during firing as shown in the attached photograph. This makes it not compatible with the typical firing profile for thick film processing.
- Glass LC1269 and LC1362 exhibited a minimal wetting to the substrate and the fired bulk glasses are also porous.
- Glass LC1276, LC1391, and LC1434 are not compact and dense after firing.
- Glass LC1288, LC1361, LC1366, and LC1432 have cracks after firing and the glass pill have major voids.
- Glass LC1364, LC1365, LC1394, LC1433, LC1440 and LC1435 exhibited excessive wetting to the substrate. This might result in bleeding and large geometry change of printed films. Glass LC1435 exhibited cracking due to the CTE mismatch to the substrate.
- Glass LC1430 has significant shrinkage after firing, which will be a potential problem to maintain the geometry of printed pattern.
- Glass LC1452 is dense and compact, however, it has a higher CTE than the alumina substrate and the glass pill has significant cracks due to either CTE mismatch to the substrate or devitrification.
- Glass LC1588 and RF110 exhibited excessive wetting. The fired glasses spread almost the entire substrate. In addition, air bubbles were found in the fired glasses.

After the above selection process, seven glass candidates were left for further evaluation. They are LC1101, LC1281, LC1309, LC1366, LC1380, LC1428, and LC1429. Subsequently, a quick scan to the fired bulk pills of these glasses was conducted by X-ray diffraction using Cu K_α radiation (λ=1.544Å) on a Siemens D5000 diffractometer. The X-ray spectra were collected from the angular region of 10-90° in the 2θ-step scanning mode. The conditions used were: filament current 40mA, 40kV and step size of 0.01°. Figures 4.1 to 4.7 show the X-ray patterns. Since the X-ray beam can only penetrate tens of microns at most, the scanned area of the fired glass bulk can be considered as pure glass. It can be seen that after firing, glass LC1101, LC1282, LC1366, LC1428, and LC1429 all have multiple major peaks which indicate devitrification. The broad peaks at around 16° and 23° in glass LC1281, LC1366, LC1428 and LC1429 are crystallized silica in nano-scale. Glass LC1309 and LC1380 still remain vitreous.

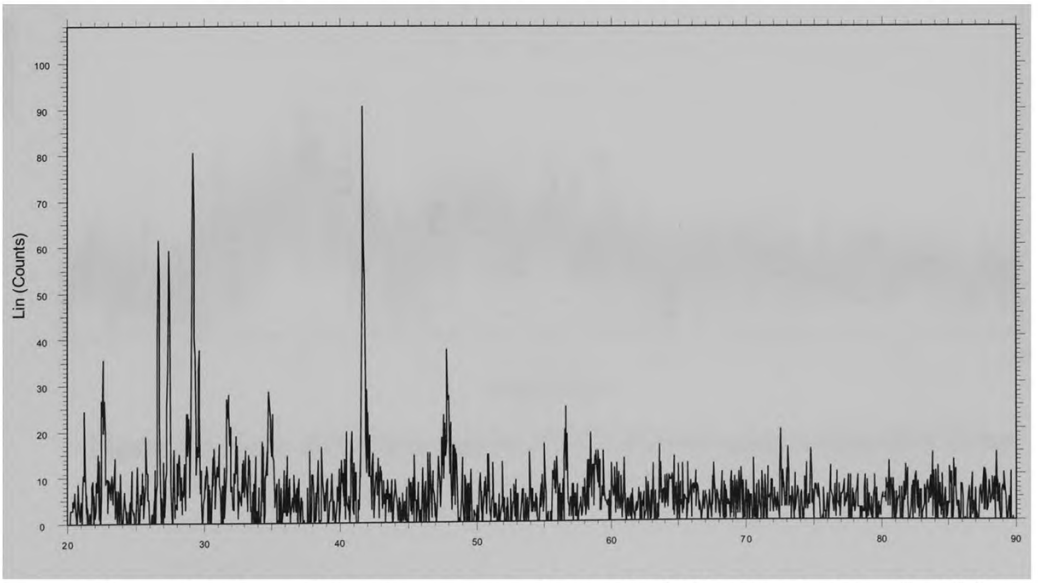

Figure 4.1 X-ray diffraction pattern of LC1101 bulk glass sample after firing

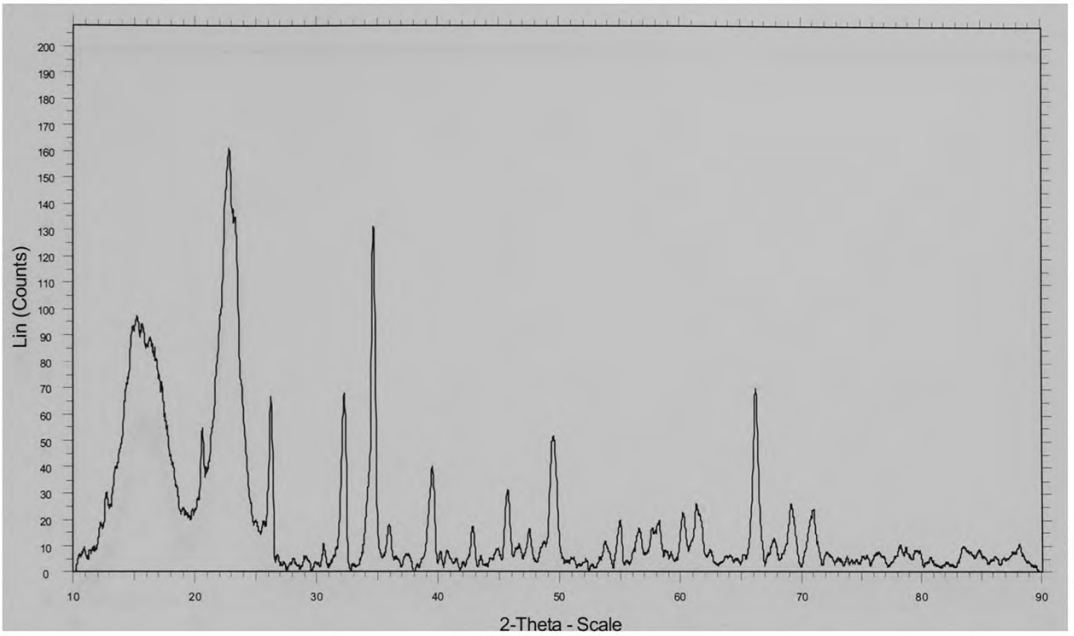

Figure 4.2 X-ray diffraction pattern of LC1281 bulk glass sample after firing

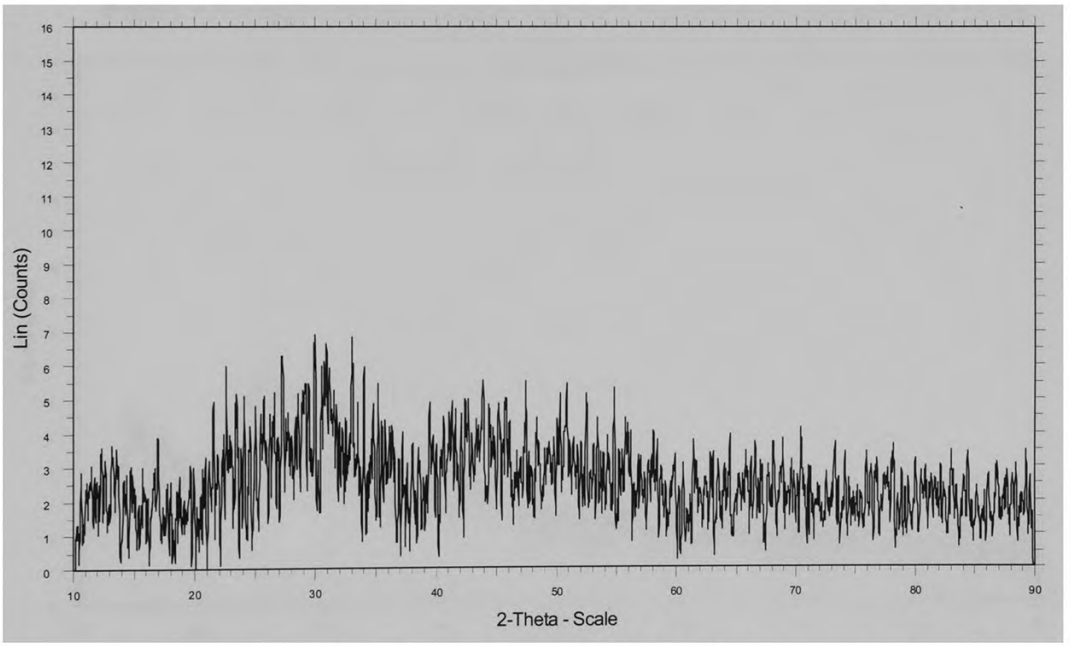

Figure 4.3 X-ray diffraction pattern of LC1309 bulk glass sample after firing

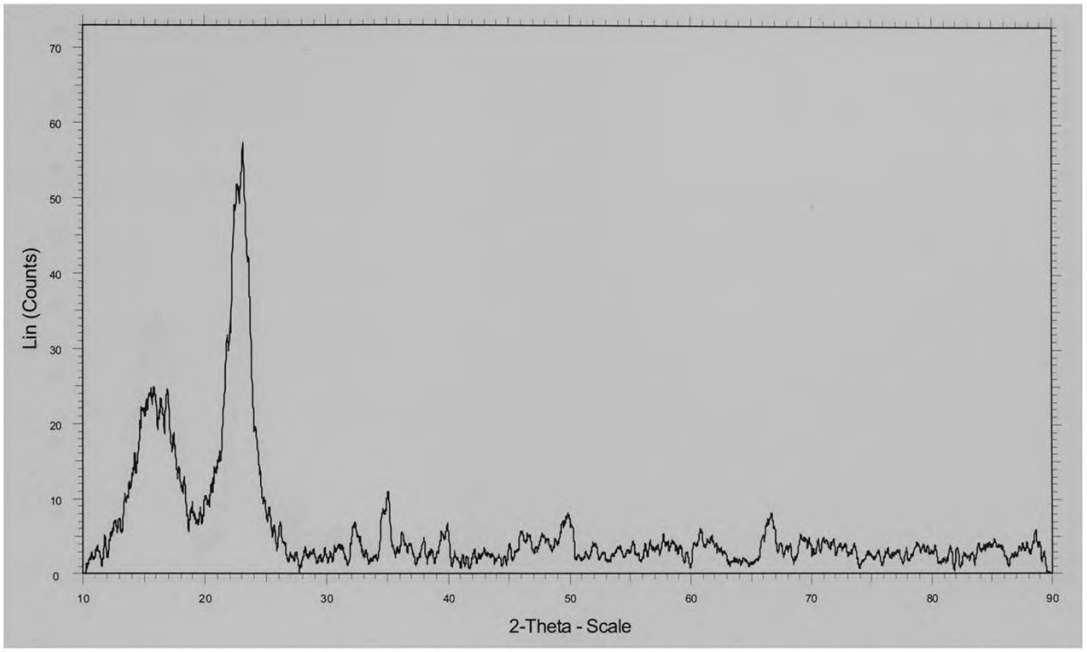

Figure 4.4 X-ray diffraction pattern of LC1366 bulk glass sample after firing

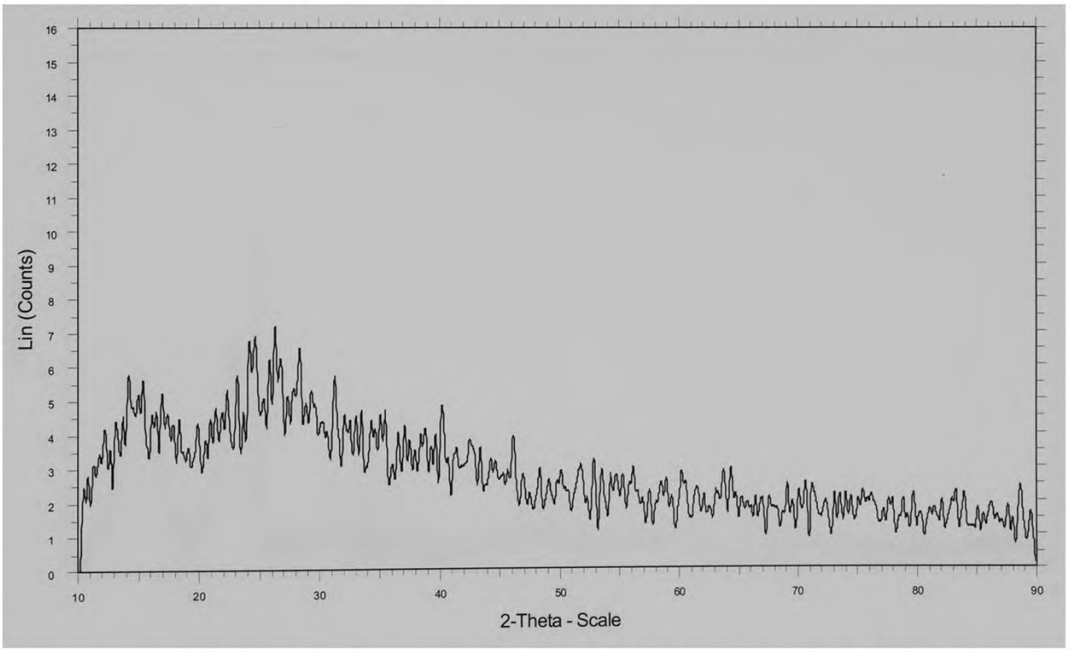

Figure 4.5 X-ray diffraction pattern of LC1380 bulk glass sample after firing

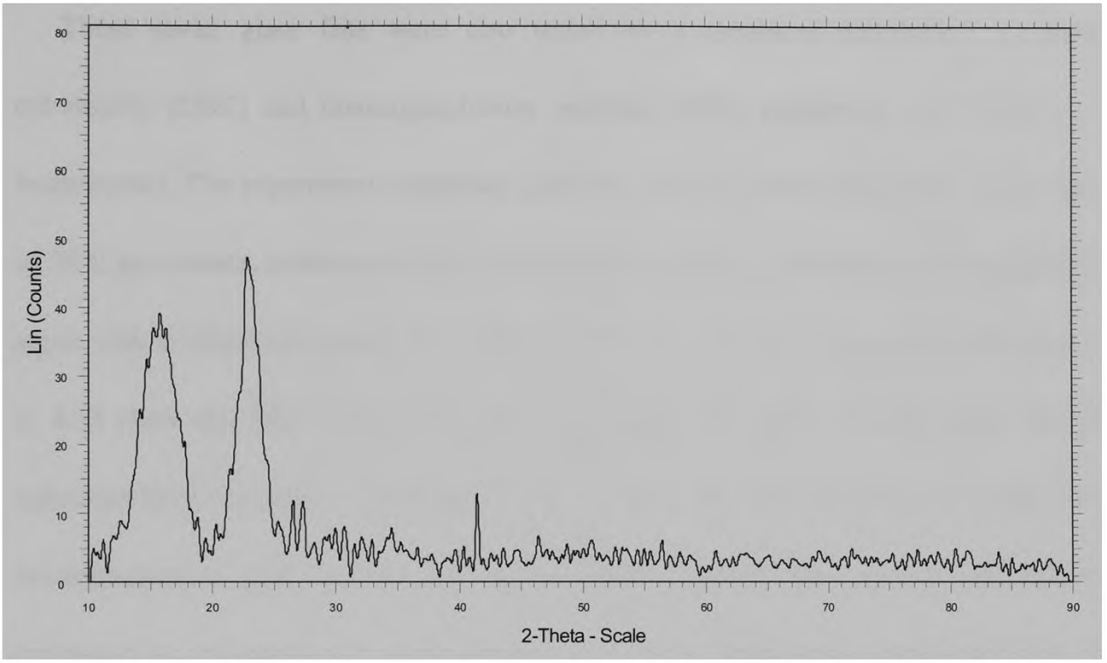

Figure 4.6 X-ray diffraction pattern of LC1428 bulk glass sample after firing

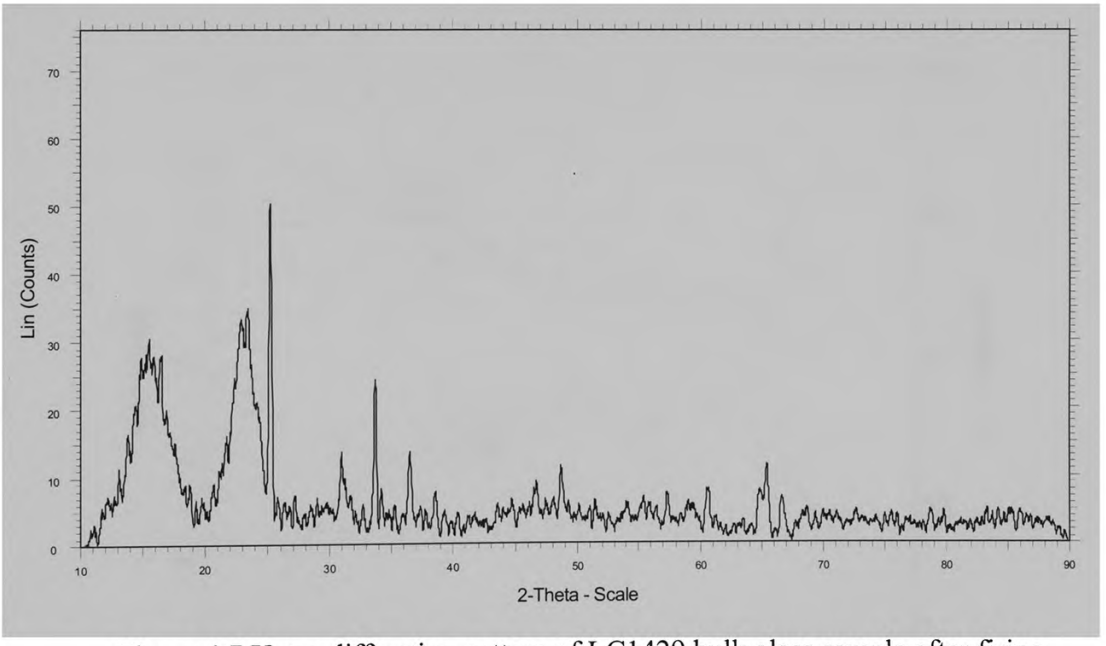

Figure 4.7 X-ray diffraction pattern of LC1429 bulk glass sample after firing

These seven glass frits were also tested by a combined differential scanning calorimetry (DSC) and thermogravimetry analysis (TGA) equipment SDT Q600 (TA Instruments). The experiment conditions used were: heating from 50 to 850°C, ramp rate of 20°C per minute, isothermal hold for 10 minutes at 850°C. The furnace was purged by argon with a 100ml per minute flow rate and air cooled after the experiment. Figures 4.8 to 4.14 show the DSC-TGA curves. The softening temperature of each glass can be estimated from the DSC curve and they fall in the proper range for 850°C firing. The devetrification of glass LC1101, LC1281, LC1366, LC1428 and LC1429 can also be evidenced by the exothermal peaks in the DSC curve. The weight change of most of glasses is within 2%.

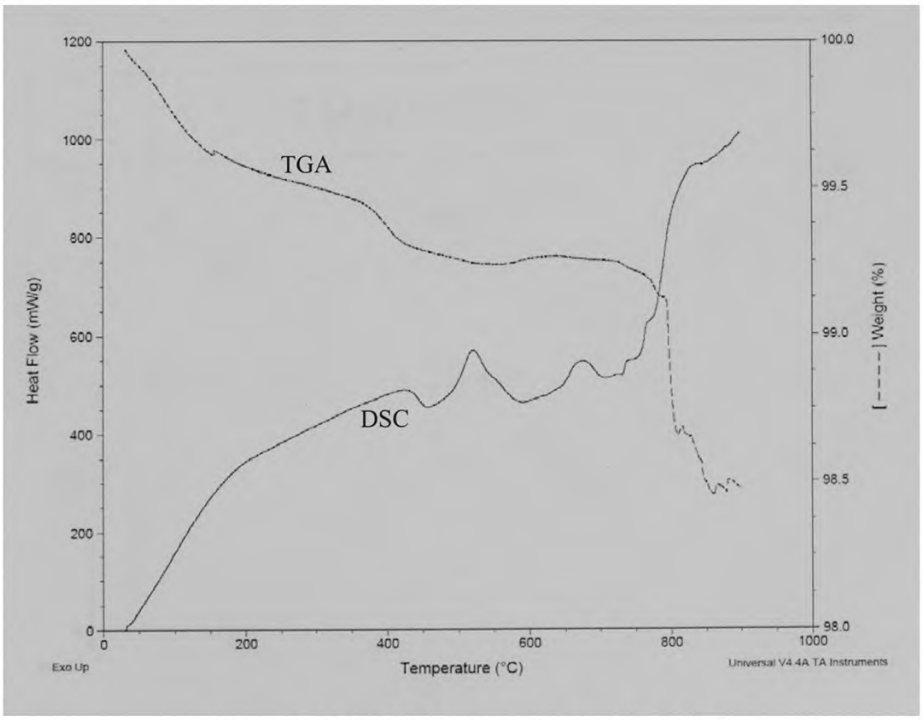

Figure 4.8 DSC-TGA curve of glass LC1101

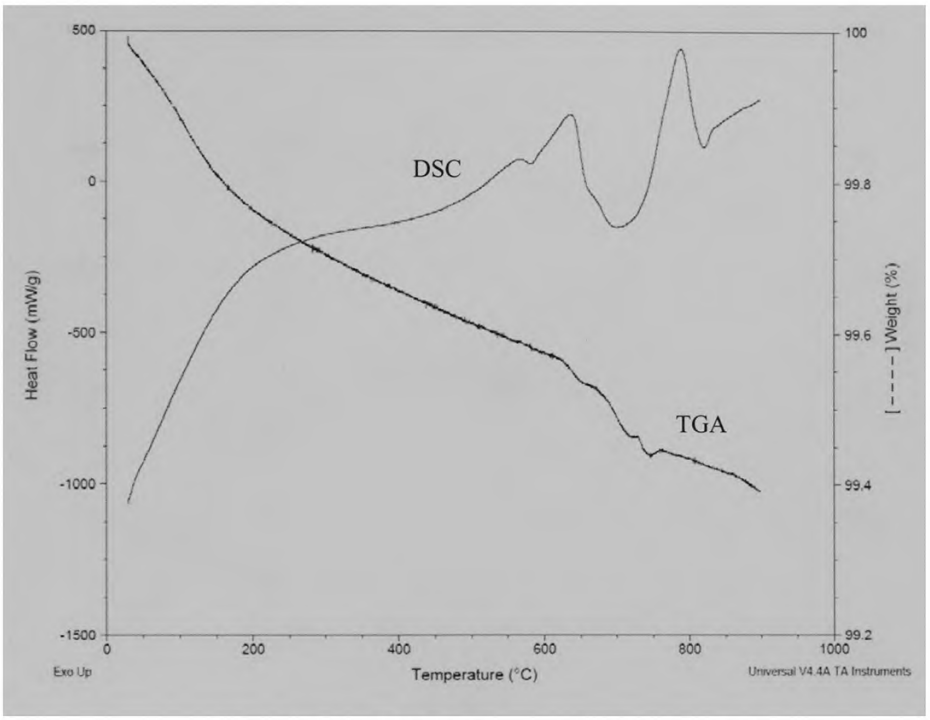

Figure 4.9 DSC-TGA curve of glass LC1281

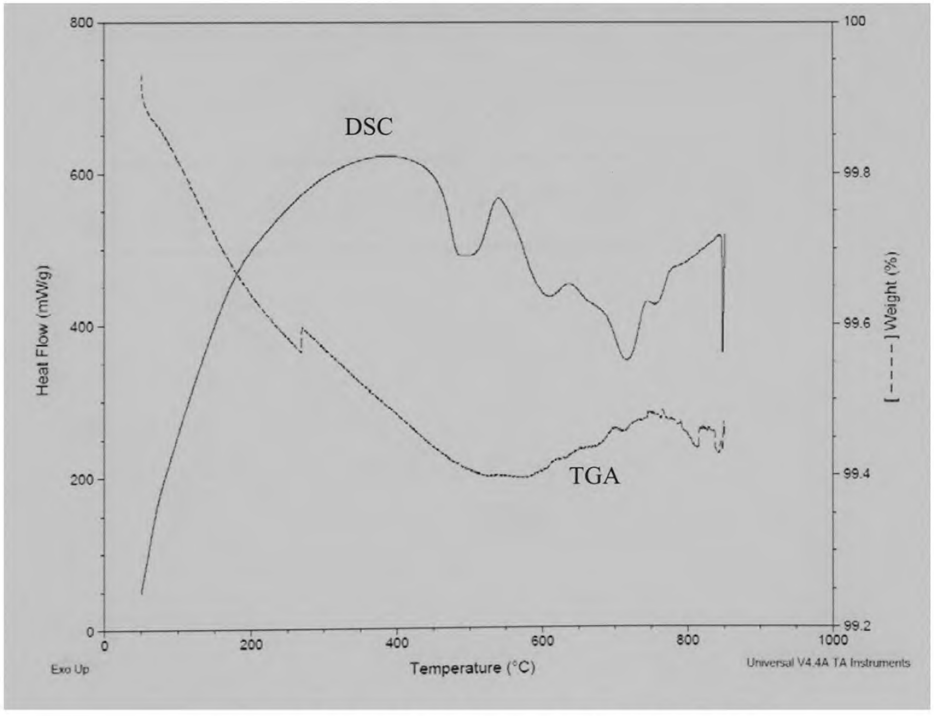

Figure 4.10 DSC-TGA curve of glass LC1309

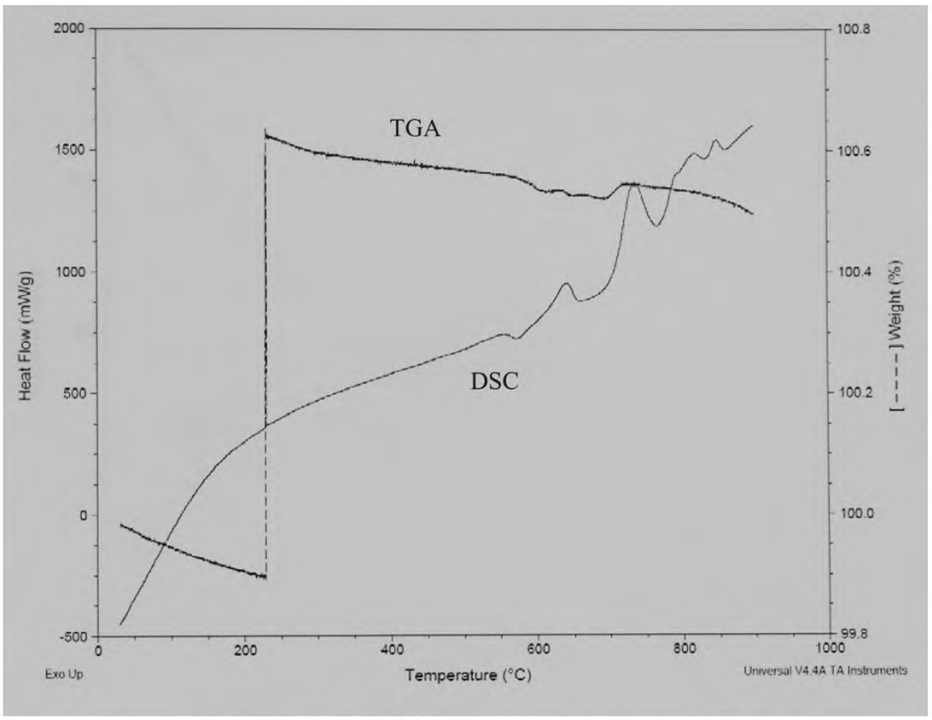

Figure 4.11 DSC-TGA curve of glass LC1366

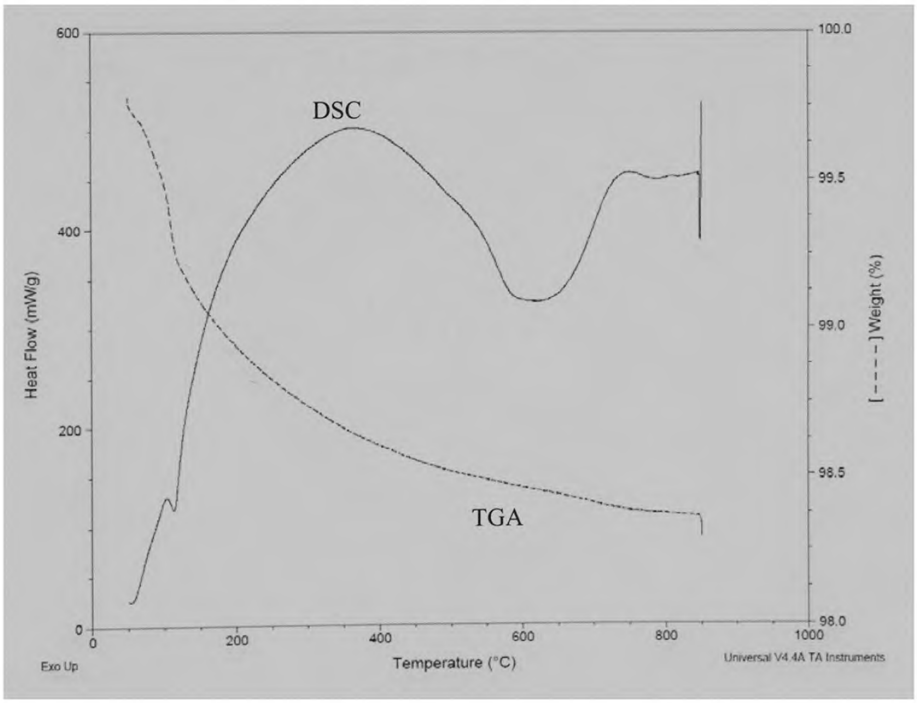

Figure 4.12 DSC-TGA curve of glass LC1380

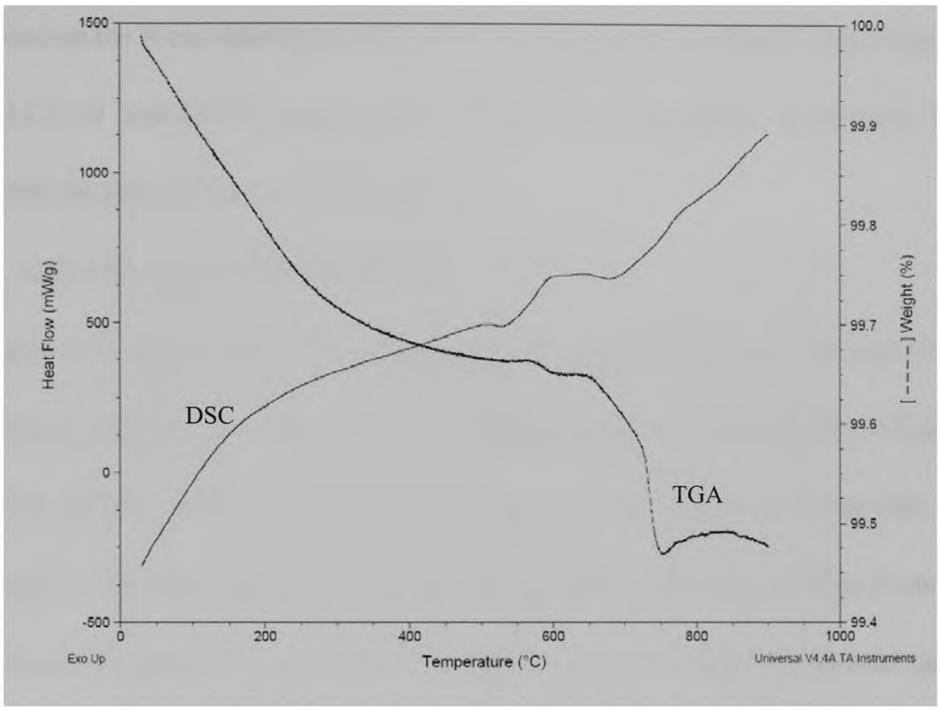

Figure 4.13 DSC-TGA curve of glass LC1428

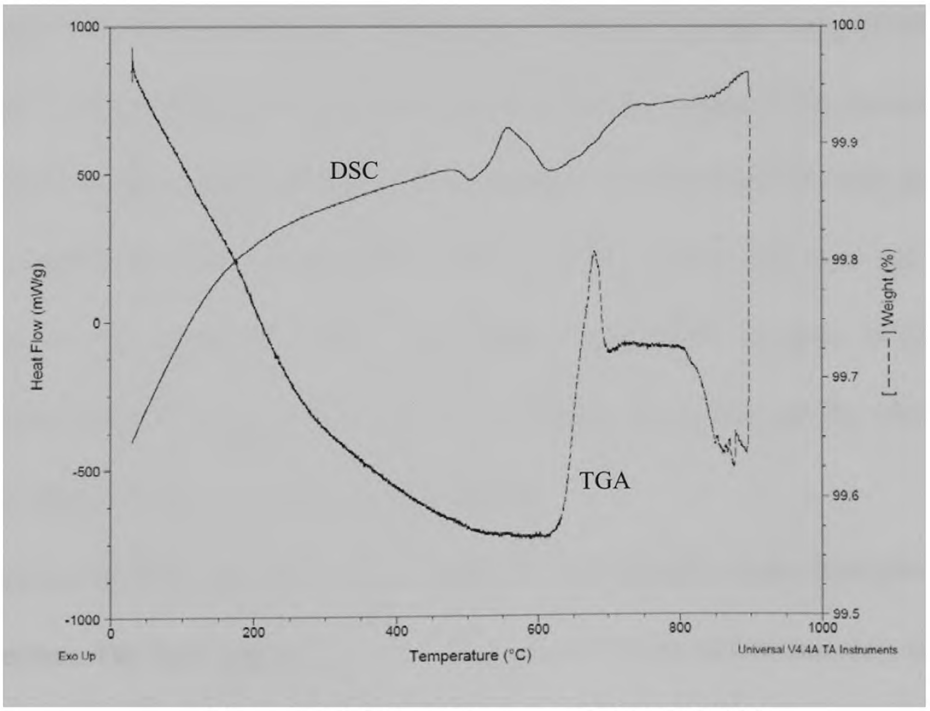

Figure 4.14 DSC-TGA curve of glass LC1429

Based on the X-ray diffraction and DSC-TGA data, the pre-selection is completed and glass LC1309 and LC1380 are selected out from 33 candidates. They were further characterized and prepared into thick film inks.

4.1.2 Characterization of Selected Glass

Figure 4.15 shows the SEM micrographs of the selected glass LC1309 and LC1380. The average particle size of glass LC1309 is around 2μm but large particles (>5μm) also exist. The particle size of LC1380 is much larger, some of them even larger than 10μm. The shape of the glass particles are random and all with sharp edge. Before formulating into pastes, the glass frits were milled to reduce the particle size to a desired range of 2-4μm.

Figures 4.16 and 4.17 shows the EDS spectra of these two glasses. The gold Mα peak at around 2.1keV and Lα peak at around 9.7keV are from the coating on the glass powder during SEM sample preparation. Based on the product description and the EDS data, the major composition of glass LC1309 is B_2O_3-SiO_2-Bi_2O_3-ZnO and there are small fractions of Al, Cr and Sn oxides. The major composition of glass LC1380 is B_2O_3-SiO_2-BaO-$Al_2O_3$with a trace of Ti. The element boron can not be effectively detected using EDS due to its small atomic number.

Figure 4.18 shows the low magnification SEM micrographs of the fired glass pills cross section. The fired glasses all have a flat and smooth top surface and they all have good interface bonding to the alumina substrate. In Figure 4.18(b) the substrate is not

there because it cracked at the bottom during cutting. A dash line bar was put in the micrograph to represent the original position of the substrate. Obviously glass LC1309 has a lower contact angle than glass LC1380.

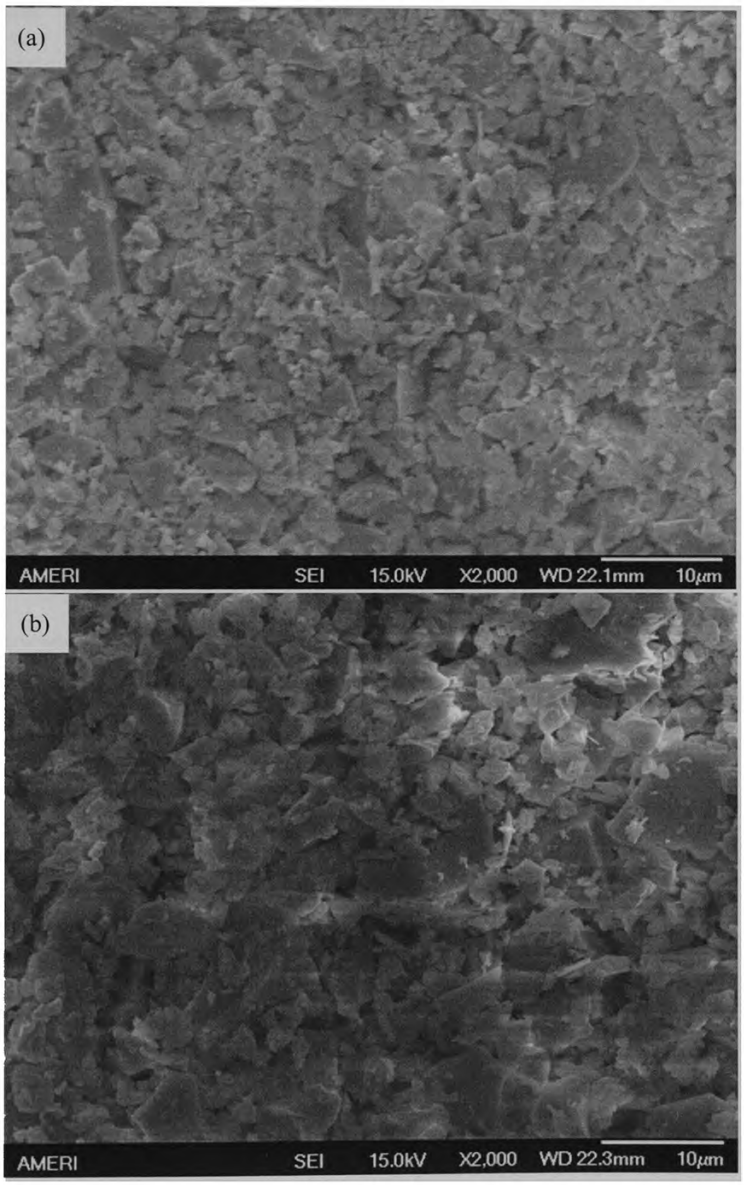

Figure 4.15 SEM micrograph (2000X) of selected glass frits (raw): (a) LC1309, (b) LC1380

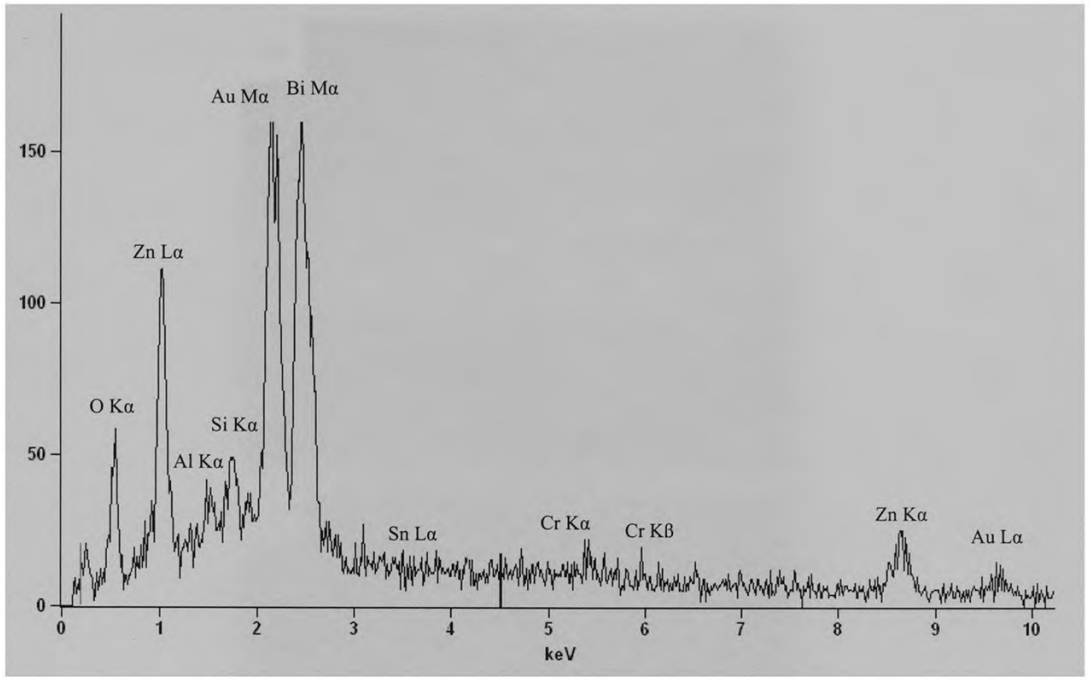

Figure 4.16 EDS spectrum of glass LC1309 powder

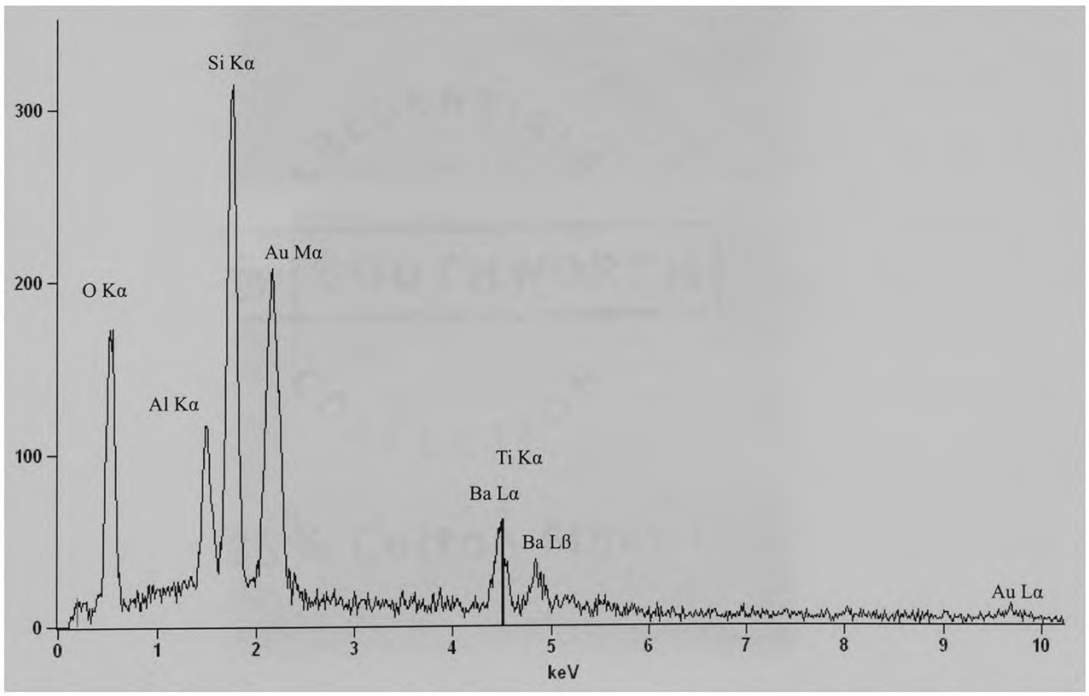

Figure 4.17 EDS spectrum of glass LC1380 powder

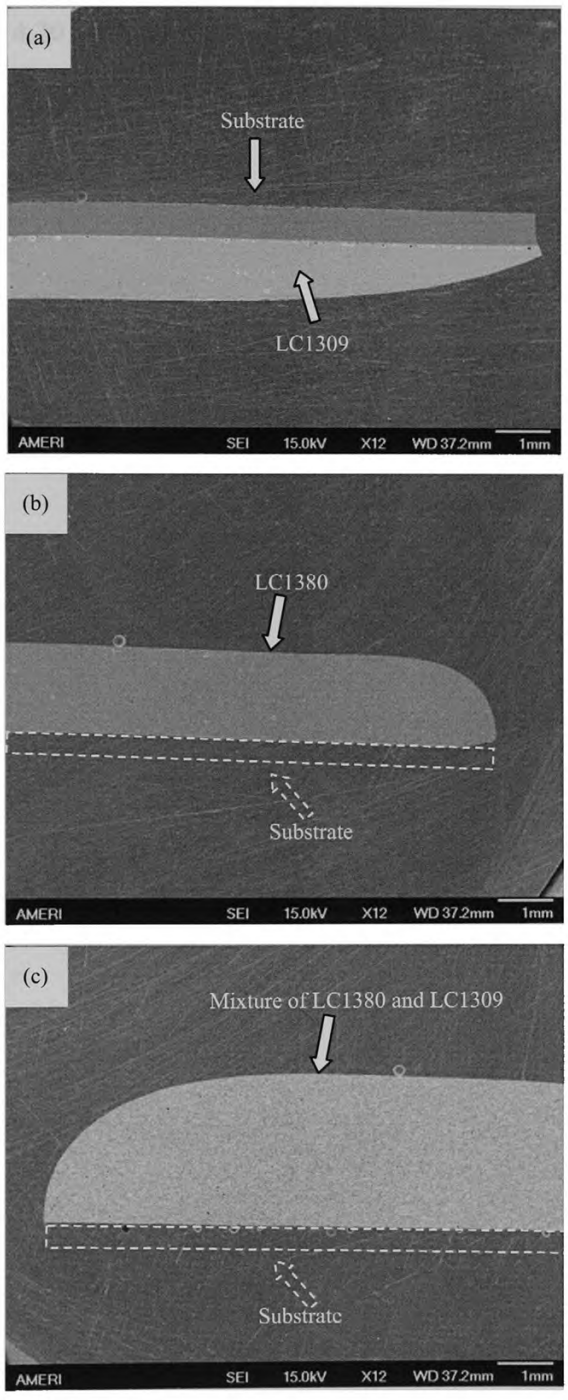

Figure 4.18 SEM micrograph (12X) of fired glass pills cross section (a) LC1309, (b) LC1380, (c) 75wt% LC1380 and 25wt% LC1309

Figures 4.19 and 4.20 are high magnification SEM micrographs of fired LC1309 and LC1380 showing the microstructure of each glass. It can be seen that glass LC1309 completely melted and a relatively uniform microstructure was developed after firing. Since the nominated fire temperature of this glass is only 580°C, the small cracks at the white regions might due to over-firing. But the overall structure is dense and compact. There are no major voids and it can be inferred that glass LC1309 has a lower viscosity during firing. Fired LC1380 exhibited voids and the high magnification micrograph shows some non-melted glass particles around or in these voids. There might be several reasons for this. First of all, the softening point of LC1380 is around 780°C and the 850°C peak temperature for 10 minutes firing might not be sufficient to melt the entire glass particles. Secondly, it is normal that some air might be trapped in the melted glass and can not escape due to the large surface tension of melted glass. It can be inferred that this glass has a high viscosity at 850°C.

The viscosity of glass at peak firing temperature and the wetting-ability of glass to the alumina substrate are key factors that determine the film microstructure. Comparing glass LC1309 and LC1380, it is obvious that LC1309 has a better wetting to the substrate than LC1380 and LC1380 might has a higher viscosity than LC1309. By mixing these two glasses in a proper weight ratio, it is expected to obtain an intermediary viscosity and wetting. Figure 4.18(c) shows the cross section of the fired glass pill containing 75wt% LC1380 and 25wt% LC1309. It can be seen that the wetting condition of the glass

mixture is a little bit better than the pure glass LC1380. Figure 4.21 shows the microstructure of the fired two-glass mixture. Voids and non-melted glass particles still exist but are less than the pure LC1380.

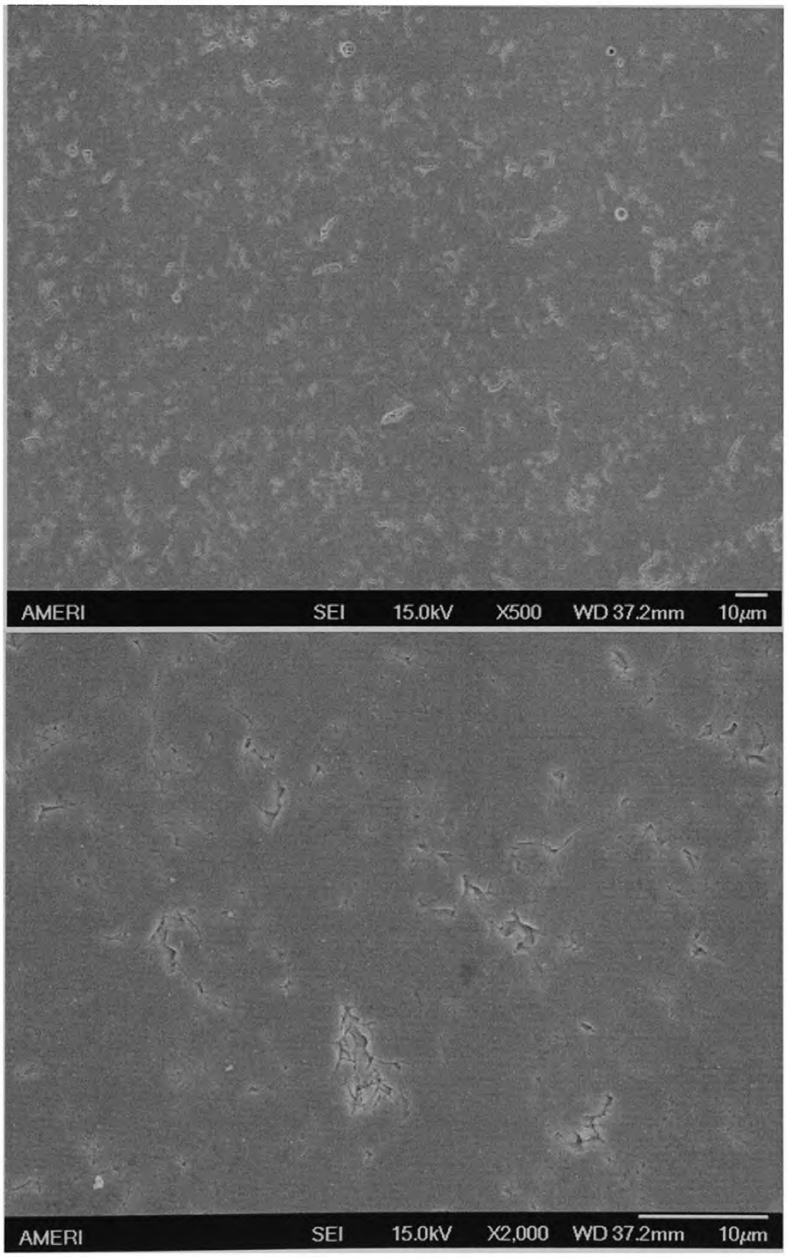

Figure 4.19 SEM micrograph (500X and 2000X) of fired glass LC1309

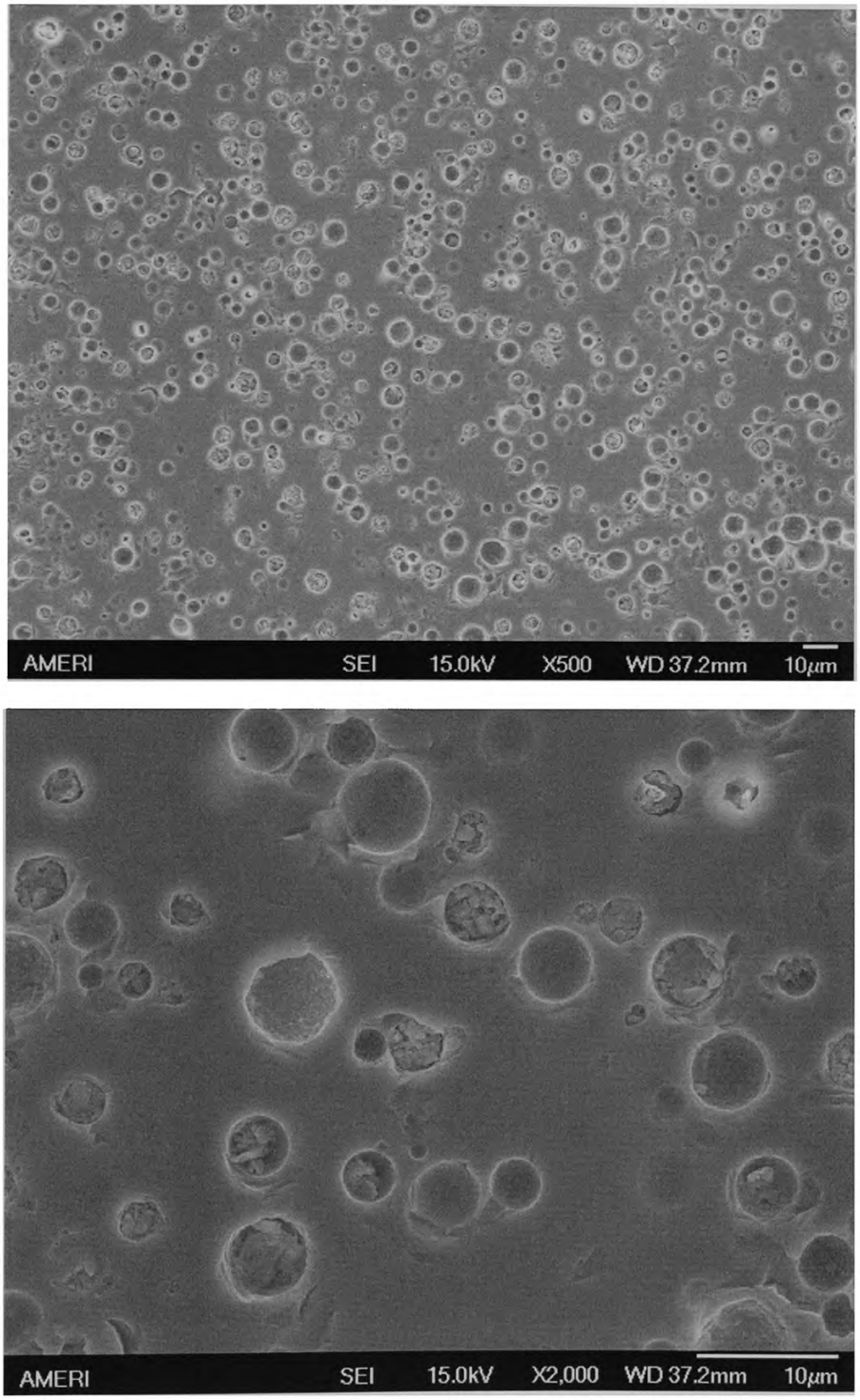

Figure 4.20 SEM micrograph (500X and 2000X) of fired glass LC1380

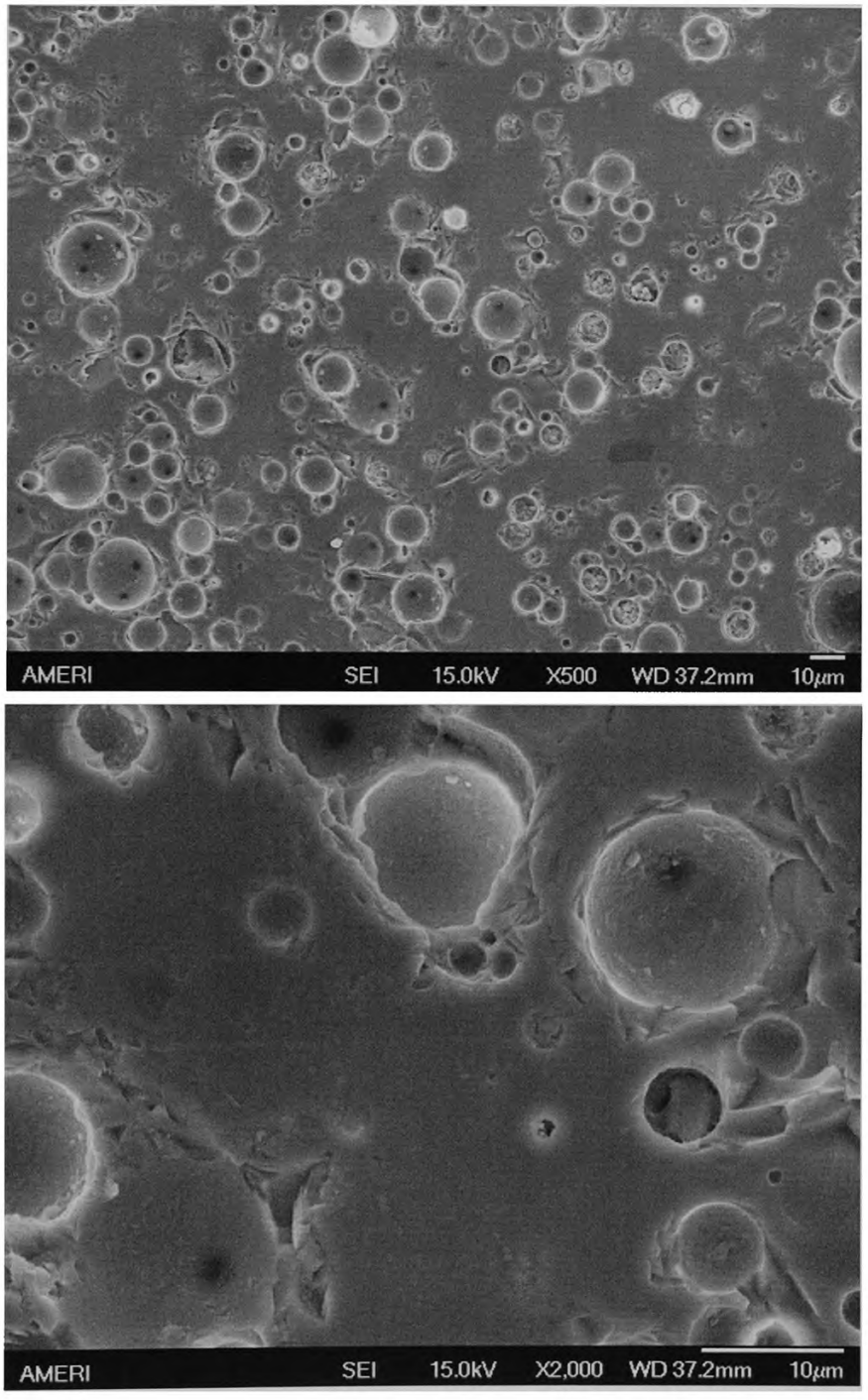

Figure 4.21 SEM micrograph (500X and 2000X) of fired glass with 75wt% LC1380 and 25wt% LC1309

4.1.3 RuO_2

Figure 4.22 shows the SEM micrograph of RuO_2 particles. The actual particles of RuO_2 can not be easily distinguished from the micrograph due to fine particles agglomerate into sub- microns clusters.

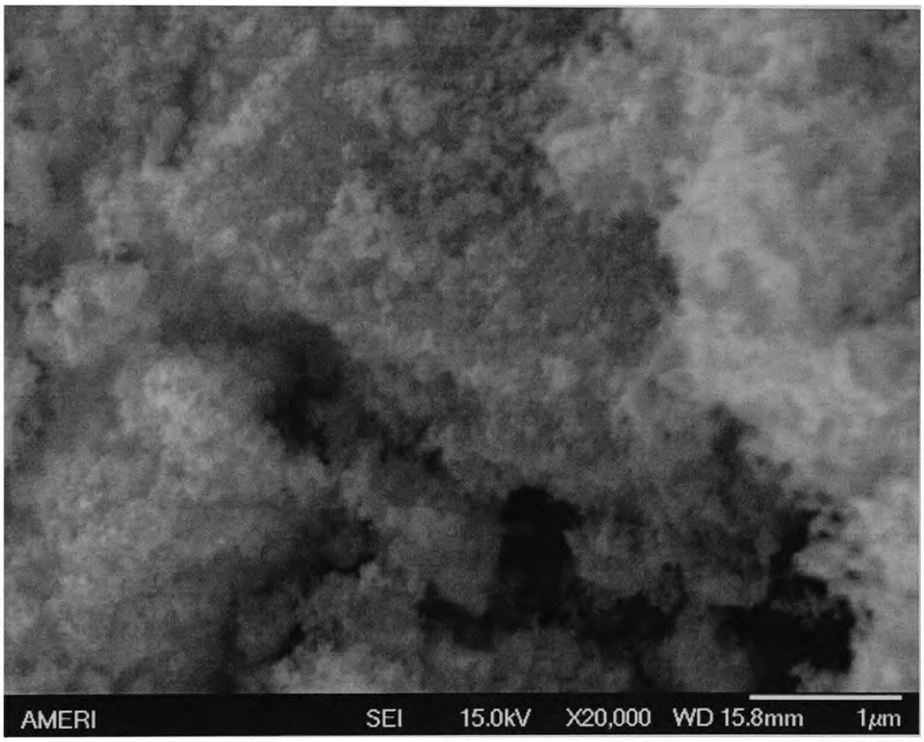

Figure 4.22 SEM micrograph (20000X) of RuO_2 particle

Figure 4.23 shows the TEM micrograph of RuO_2 powders. The RuO_2 grains can be clearly identified and they have an average size of 10-20nm. Most of the particles agglomerate into clusters. This oxide has the rutile (TiO_2) crystal structure and has metallic conductivity like its parent metal.

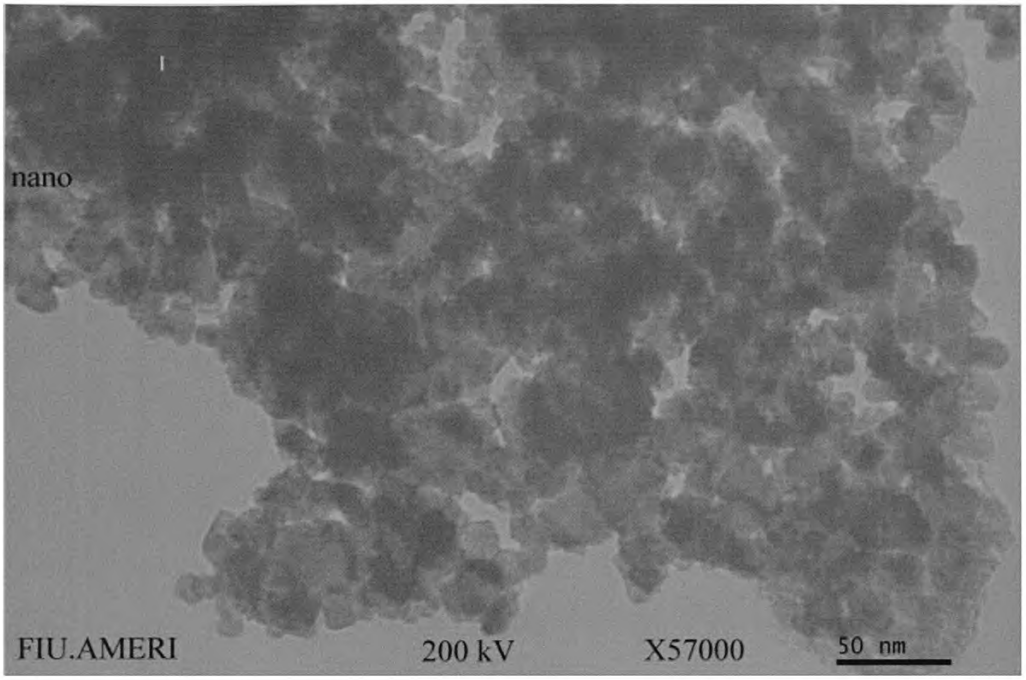

Figure 4.23 TEM micrograph of RuO_2 particle

Figure4.24 shows the X-ray diffraction pattern of RuO_2 particles. The spectra were analyzed with the DIFFAC Plus EVA Version 10.0 software and the incorporated database. The intensity and position of most peaks match with the standard JCPDS (40-1290) file. From the half width broadening, the diameter D of the RuO_2 grains was computed with the Scherrer formula [32]:

$$D=\frac{k\lambda}{\beta\cos\theta}$$

Where k is a constant, typically k=1; β is the corrected line width; θ is the peak position. The average grain size of RuO_2 is around 12 nm based on the calculation.

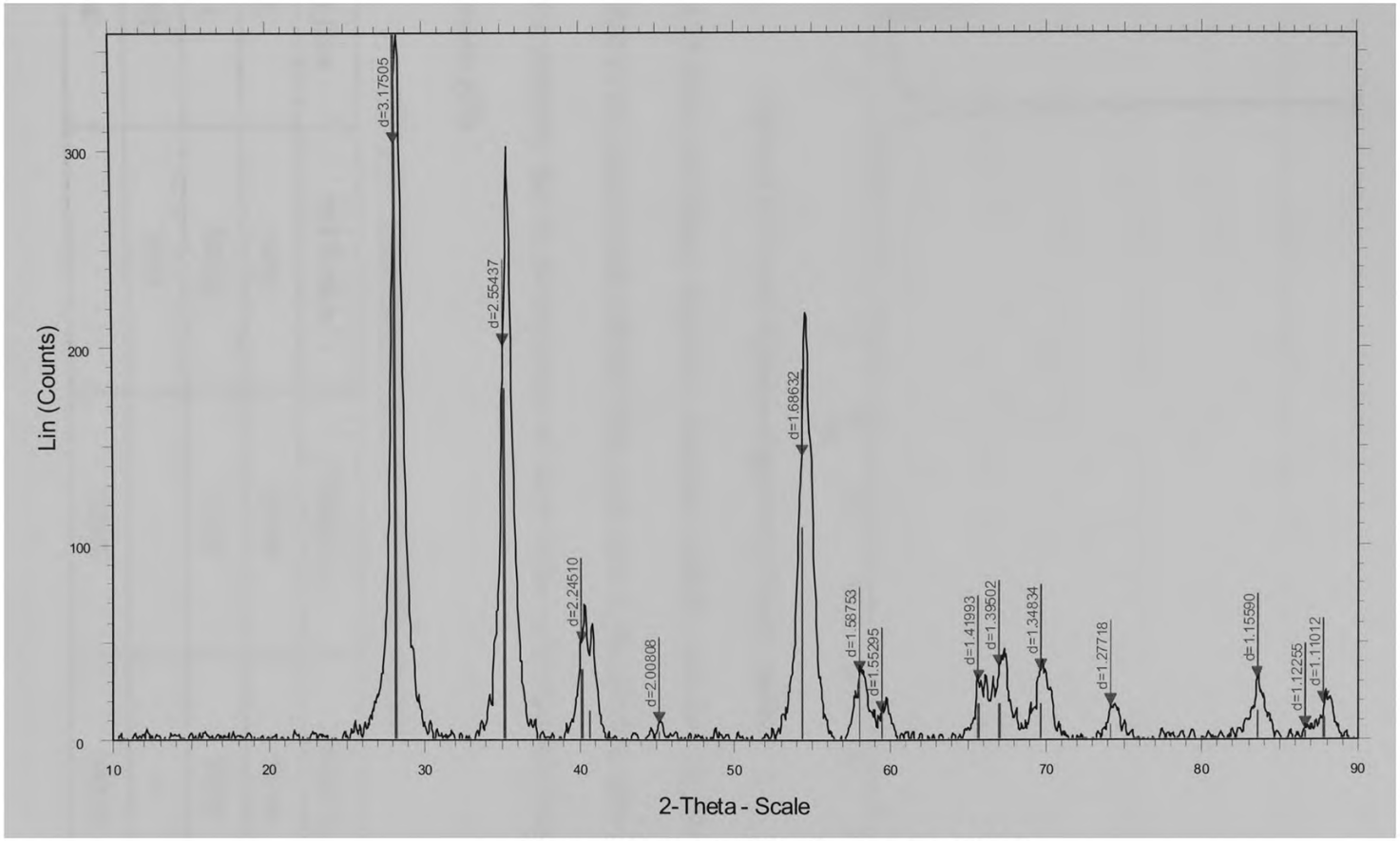

Figure 4.24 X-ray diffraction pattern of RuO_2

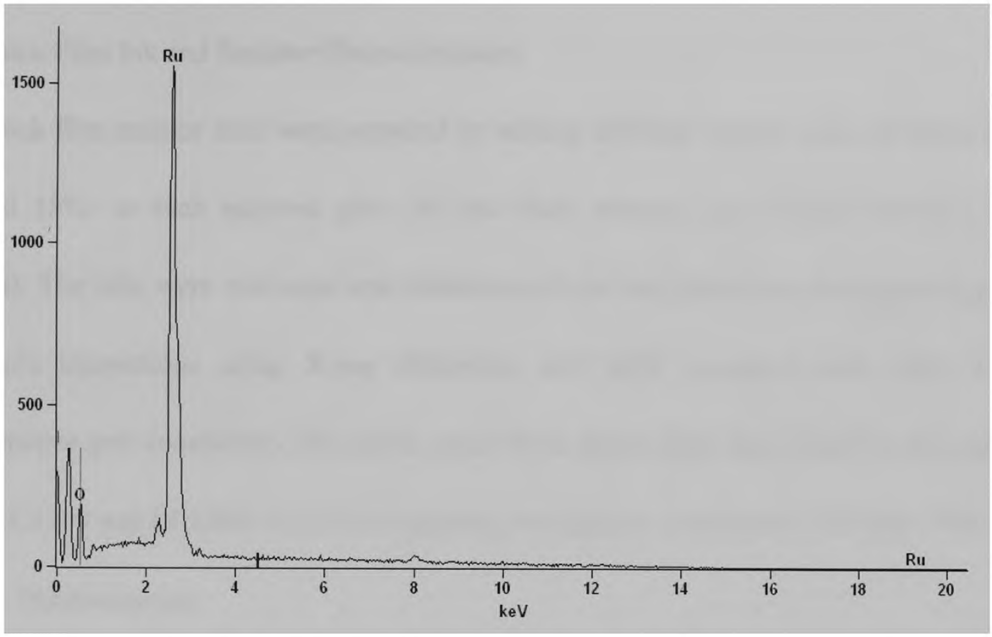

Figure 4.25 Energy dispersive spectrum of RuO_2 particle

Figure 4.25 shows the Energy dispersive spectrum of RuO_2 particles. The elements were identified by the incorporated software. The atom ratio of Ru and O is close to but not exact 1:2 probably due to the existence of other forms of compound during the synthesis process [33].

Table 4-1 Quantitative EDS results of to RuO_2 particles

Element Line	Net Counts	Weight %	Atom %
O K	1640	26.46	69.44
Ru L	30008	73.54	30.56
Ru M	3155	---	---
Total		100.00	100.00

4.2 Thick Film Ink and Resistor Characterization

Thick film resistor inks were prepared by mixing different weight ratios of RuO_2 (5, 10 and 15%) to each selected glass frit and their mixture (LC1380:LC1309=3:1 by weight). The inks were evaluated and characterized for microstructure development and materials interactions using X-ray diffraction and SEM equipped with EDS. For convenience and consistency, the pastes made from single glass are named by the glass code LC1309 and LC1380; the paste containing two glasses is named as LC1309-1380.

4.2.1 Microstructure

The microstructure of TFRs is mainly developed during the firing process and it determines the final electrical properties of TFRs. Generally, there are two models described in the literature. Figure 4.26(a) shows the schematic view of the typical microstructure depicted by M. Prudenziati [4]. It can be drawn from this model that the glass frits, which has much larger particles size than the conductive particles, has relatively large viscosity and does not flow too much after softening and melting. Only the sharp edges of the glass particles deform and the glass particles basically remain their original shape and position and are sounded through the conductive particles. The conduction path is obviously formed by the conductive particle chain by particle to particle contact.

Another one is still under debating due to the unclear conduction mechanism based on it [29, 34]. In this model, the glass has relatively low viscosity at high temperature and

deforms significantly. The conductive particles are uniformly embedded in the glass matrix as shown in Figure 4.26(b).

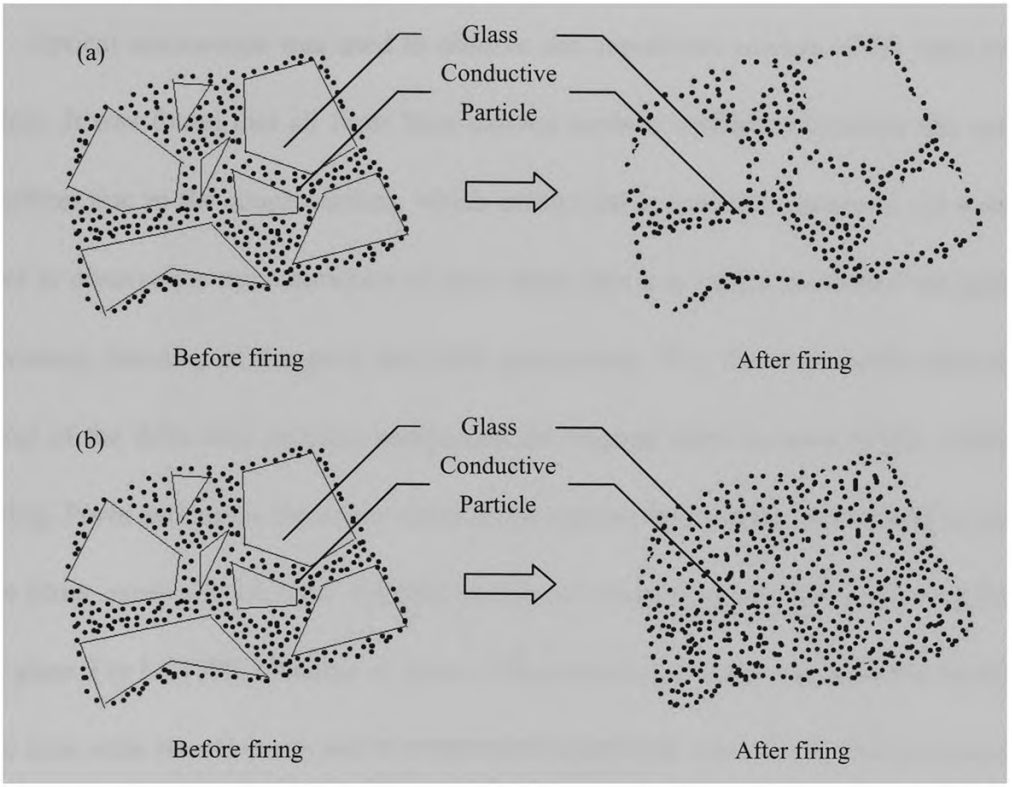

Figure 4.26 A schematic view of the microstructure of TFR before and after firing

Figure 4.27 shows the SEM micrographs of the surface of dried but not unfired (green) thick films with 15wt% RuO_2. Generally, after drying the solvent has been completely removed and inorganic particles are held together by the remaining polymeric material. The glass particle size of both LC1309 and LC1380 was effectively reduced to only a few micrometers by ball milling. No large agglomeration of RuO_2 particles was found and the fine particles are unable to be distinguished under the scale in these graphs. The particles size of LC1309 is smaller than LC1380, which makes the space between particles smaller

and results in a denser film. Besides, the ink making and printing process might also affect the quality of the green films.

Optical microscope was used to observe the unpolished surface of the fired resistor films. It was found that all films have uneven surfaces and microstructure did not look uniform due to the rough surface, which makes the optical microscope is not a reliable tool to observe the microstructure of thick films. But it is useful to monitor the geometry accuracy, bleeding of the glass and other phenomena. The observed results showed that most of the thick film resistors maintained the original shape in term of line width after firing. Pores and voids, the major cause of the uneven film surface were found on most of the films, especially LC1780. And the number of voids increases with increasing fraction of glass. For LC1309, bleeding of glass on the alumina substrate was found at the edge of the lines with 10wt% RuO_2 and it turned more significant when RuO_2 fraction goes down to 5wt%. The surface of LC1309-1380 is smoother than LC1380 probably because the addition of LC1309 lowers the viscosity at high temperature. Also, no bleeding of glass was found from LC1309-1380 resistor films.

Figures 4.28 to 4.30 show the SEM micrograph of polished resistor film LC1309, LC1380 and LC1309-1380 fired at 850°C in air. It can be seen from the micrographs that almost most glass particles of resistor film LC1309 melted after firing, which enabled a relatively more uniform microstructure than LC1380. The latter one still has a certain amount of glass particles that were not completely melted, which resulted in a non-fully

developed microstructure. Most resistor films exhibited voids and pores. Some researchers [19] compared the number of voids and pores in the same resistor film fired at the same profile in different furnaces.

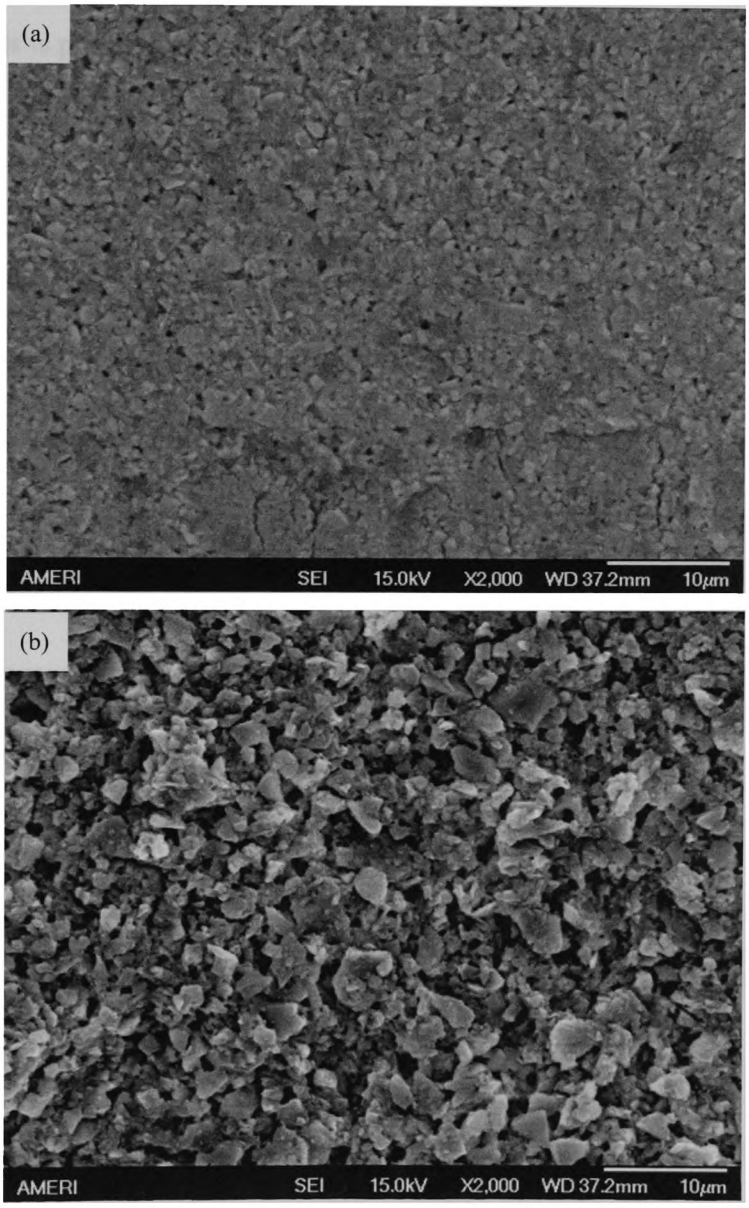

Figure 4.27 SEM micrograph (2000X) of dried green films with 15wt% RuO_2
(a) LC1309, (b) LC1380

It was evidenced that the films fired in a belt furnace exhibited less voids and pores, appeared more smooth and uniform than the ones fired in a tube furnace. Under the condition of no enough air flow in the box furnace used in this work, the existence of voids and pores is possibly due to the trapped air or gas generated from decomposition of the polymeric materials can not escape from the melted glass with a high viscosity. The spherical shaped voids with a smaller average size raging from 1-2μm appeared in the films are possibly due to reactions occurring between the glass compositions, organic vehicle and RuO_2. Once the temperature reaches to the softening point, inorganic particles start to coalesce towards each other for densification. It is normal that some gas product formed primarily at the interface to diffuse towards the free surface through the dense matrix [35].

The SEM micrographs also showed that the number of pores and voids increases with increasing glass fraction for most of the films. The possibility that reactions between RuO_2 and the glass composition resulted in voids can be excluded. According to Figures 4.20 and 4.21, the fired glass LC1380 and the glass mixture of LC1309-1380 exhibited quite a number of pores and voids, which are obviously inevitable when they were mixed with RuO_2. Figure 4.19 shows that he pure glass LC1309 did not exhibit spherical pores and voids after firing. A few of them were found in resistor film LC1309, which might resulted from the air or gas generated from decomposition of the polymeric materials during firing.

It can be seen from Figure 4.30 that the number of pores and voids in the two-glass formulation LC1309-1380 is less than LC1380. A smoother surface and a relatively uniform microstructure were obtained by mixing glass LC1309 with glass LC1380 in a certain ratio. Therefore, it is possible to reduce or even eliminate pores and voids by using a glass with better wetting and lower viscosity as an additive to adjust the wetting and viscosity of a glass with high viscosity and less wetting provided that there is no significant reaction between the two glasses.

The microstructure of film LC1309 can be categorized as the model described in Figure 4.26(b). A complete sintering of the glass LC1309 matrix was obtained at a peak temperature 850°C. The fine RuO_2 particles are possibly surrounded by the melted glass and can not be easily distinguished in the micrograph. For film LC1380, the microstructure was not fully developed because some glass particles remain non-melted. From the successive background free of pores and voids, a common feature was found that the black areas (glass) were surrounded by the bright net-like area (RuO_2). And the bright area increases with the increasing weight fraction of RuO_2. Therefore, the microstructure of this formulation might fall into the model described in Figure 4.26(a). Regarding film LC1309-1380, it is much easier to see the distribution of different phases from the micrographs due to less pores and voids. The conductive particles constructed a bright network, which is embedded in the glass matrix. Some large glass particles more or less maintained their shape though melted. Generally, the microstructure of this

formulation matches with the second model. But it should be noted that the size of the conductive path is around 1μm, which might be formed by either the agglomeration of RuO_2 fine particles, or a local microstructure as the first model due to the addition of glass LC1309. Figure 4.31 shows the cross section of resistor films with 15% RuO_2. The films are mechanically and chemically bonded well to the substrate. Pores and voids can also be observed in resistor films LC1309 and LC1380.

4.2.2 Materials Interaction

The interactions between each ingredient material are always considered to be complicated in thick film resistors. X-ray diffraction is one of the best techniques to study material interactions. Energy dispersive X-ray Spectroscopy was also used to observe possible interaction between the glass composition, RuO_2 and substrate.

4.2.2.1 X-ray diffraction

Single crystal sapphire rather than alumina was used as the substrate in the X-ray diffraction experiment. Figures 4.32 and 4.33 show the diffraction pattern of alumina and sapphire substrate respectively. For comparison, the RuO_2 pattern is also superimposed in the graph. Obviously the diffraction pattern of alumina substrate has multiple peaks and some of them are at same position as RuO_2 peaks. However, single crystal sapphire only has one major peak while the same composition is maintained; therefore it is easier for analysis. Thick film resistor inks were printed on sapphire substrate into 10 by 10mm square samples and fired at peak temperature 850° for 10 minutes in air.

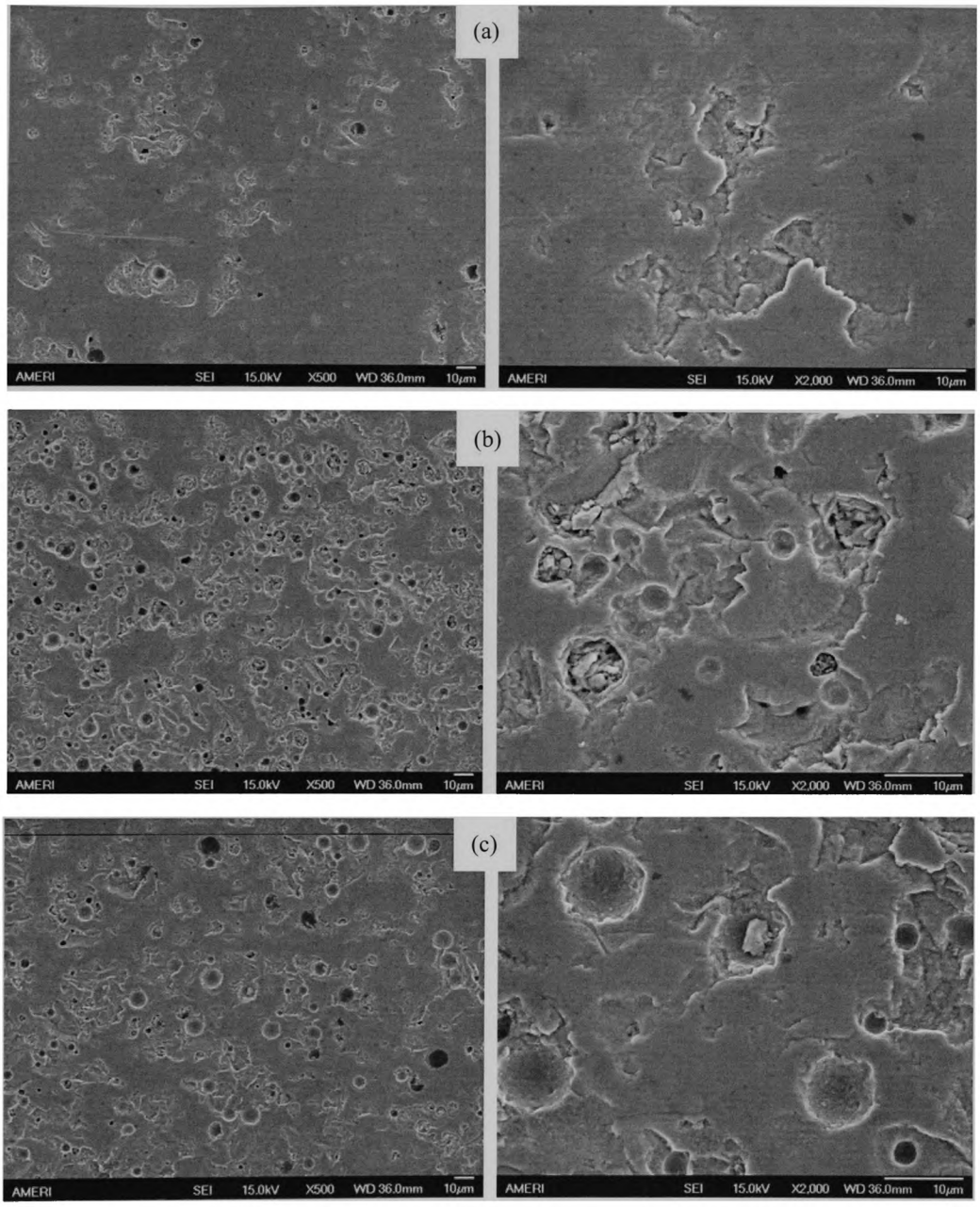

Figure 4.28 SEM micrograph (500X and 2000X) of resistor film LC1309 with 15% (a), 10% (b), and 5% (c) RuO_2

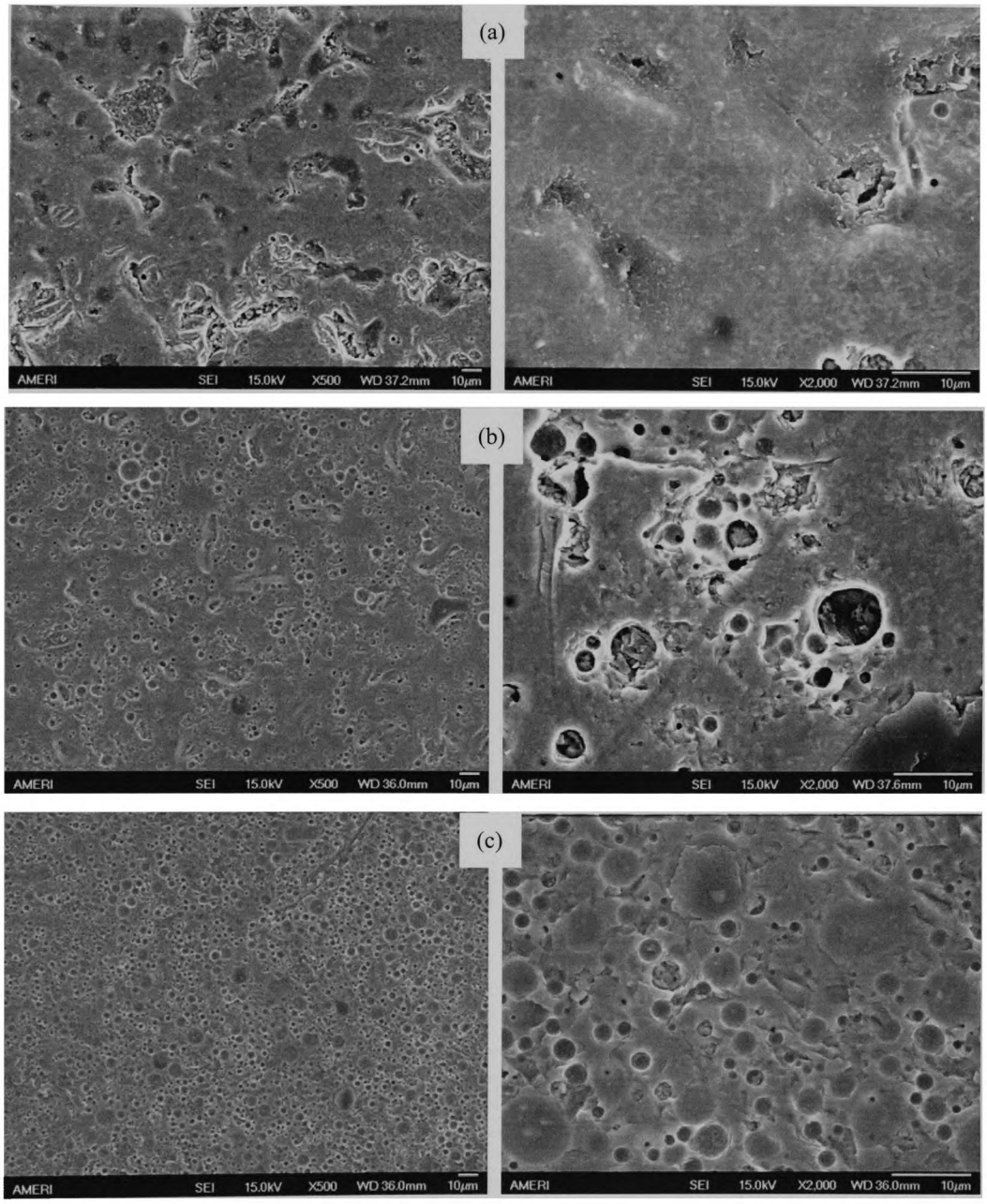

Figure 4.29 SEM micrograph (500X and 2000X) of resistor film LC1380 with 15% (a), 10% (b), and 5% (c) RuO_2

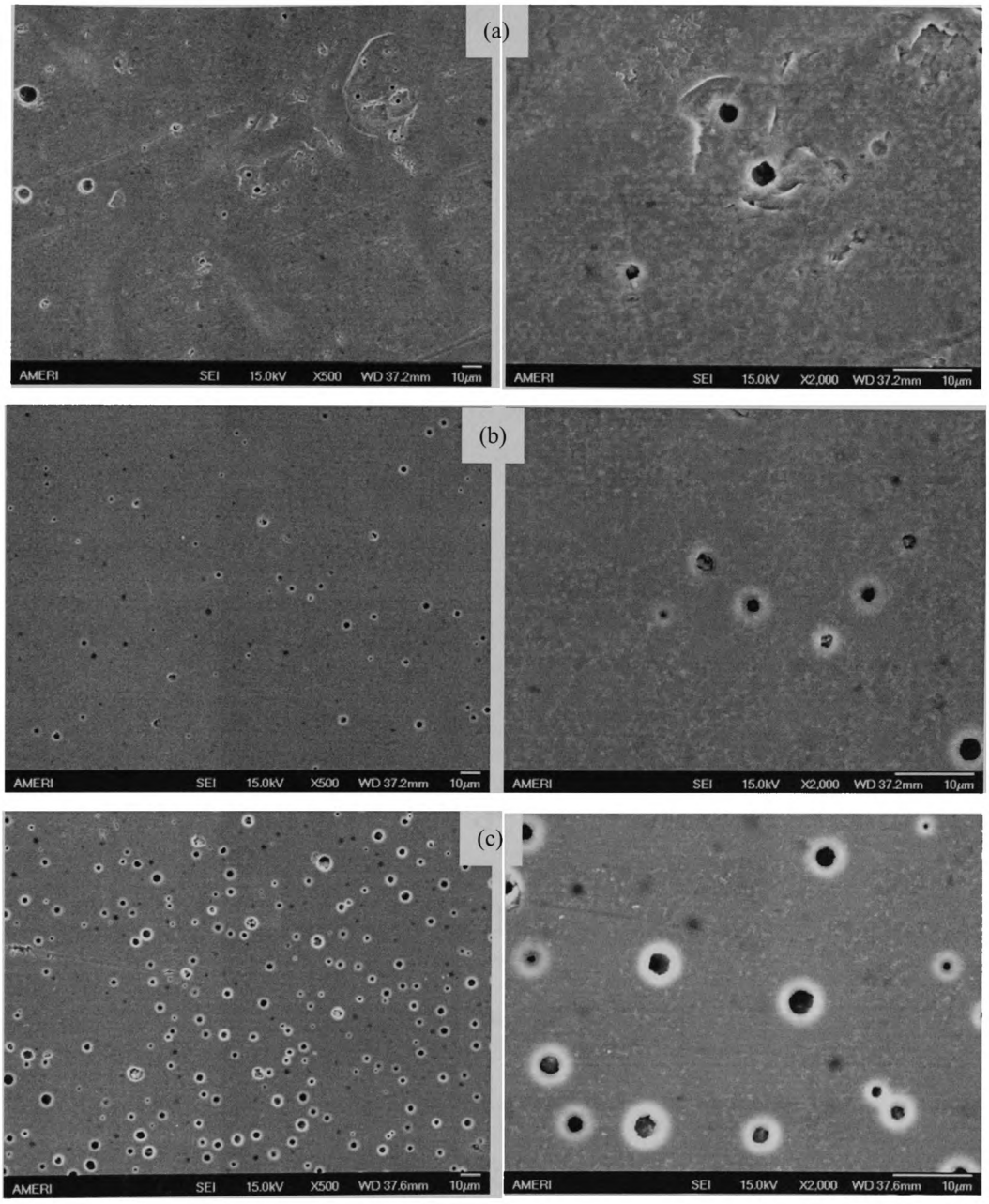

Figure 4.30 SEM micrograph (500X and 2000X) of resistor film LC1309-1380 with 15% (a), 10% (b), and 5% (c) RuO_2

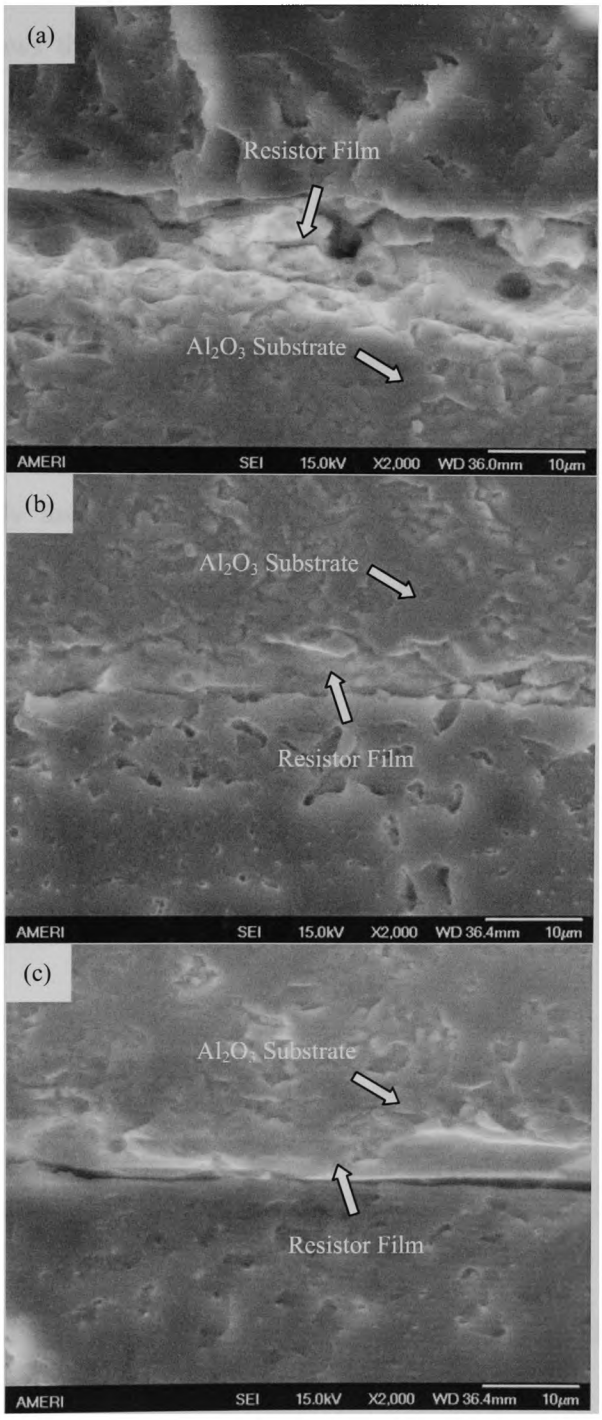

Figure 4.31 SEM micrograph (2000X) of resistor film cross section with 15% RuO_2: (a) LC1309 (b) LC1380 (c) LC1309-1380

Figure 4.34 shows the diffraction patterns of resistor film LC1309 with different RuO_2 weight fraction. For better comparison, the patterns of sapphire substrate and pure RuO_2 are also superimposed in the graph. The peaks found from the films include two parts. Since the film is only 10 to 20 microns thick, the peaks of single crystal sapphire substrate were still captured at around 20, 37.5, and 80°. The peaks at around 28 and 35° are RuO_2 with a tiny shift comparing to the pure RuO_2 powder diffraction pattern. Several peaks with relatively low intensity between 58 and 65° are also RuO_2. There is no significant difference between the films with different RuO_2 weight fractions.

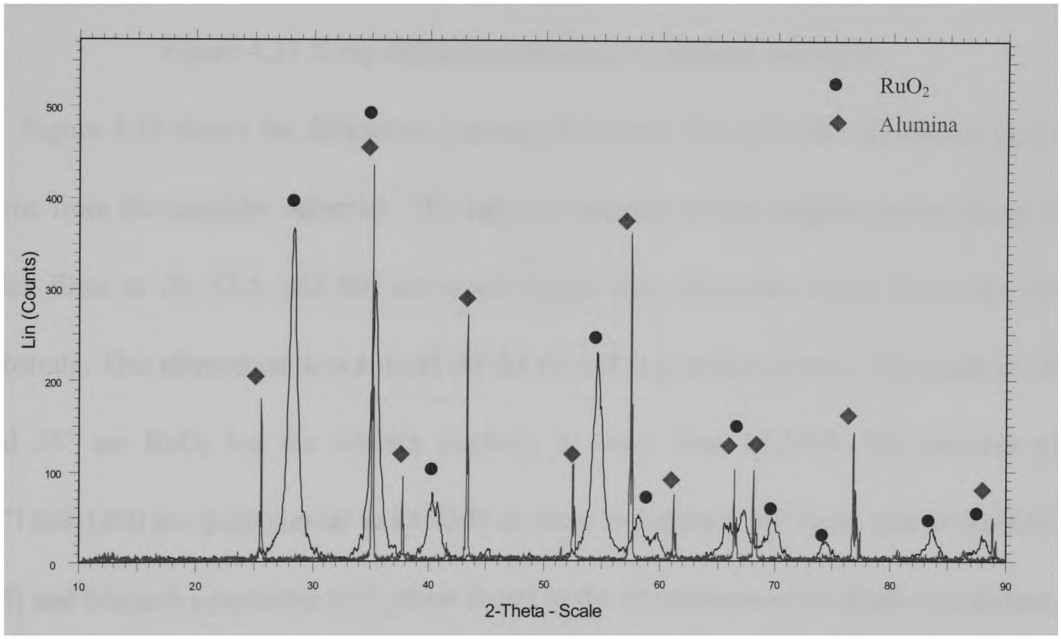

Figure 4.32 X-ray diffraction patterns of Alumina and RuO_2

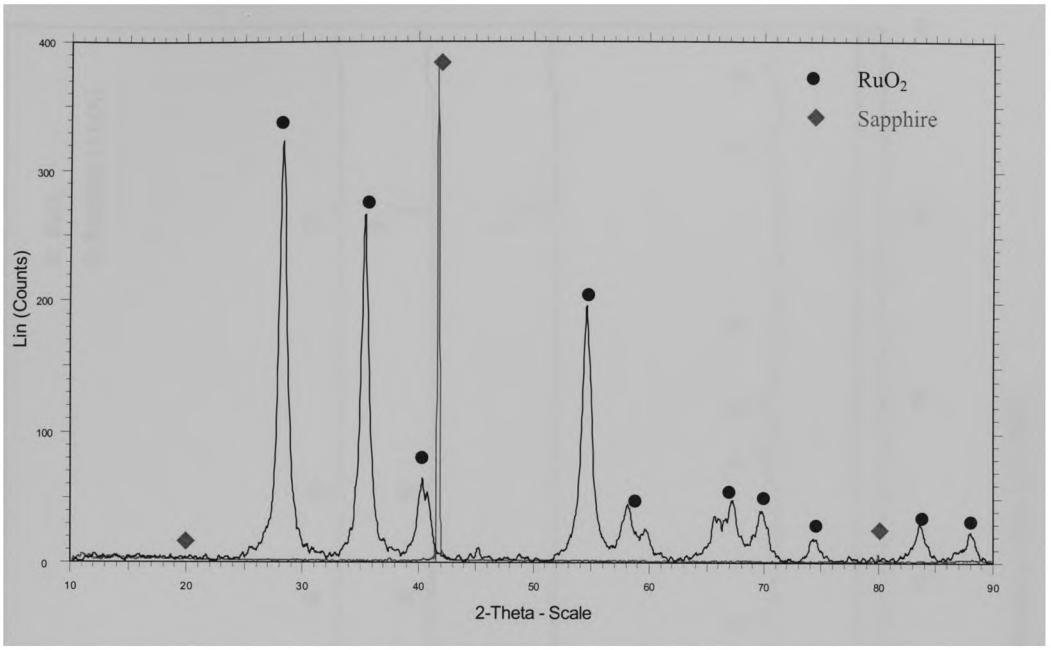

Figure 4.33 X-ray diffraction patterns of sapphire and RuO_2

Figure 4.35 shows the diffraction patterns of resistor film LC1380. Almost all peaks came from the sapphire substrate. The relative intensity of the sapphire peaks found in thick films at 20, 37.5, and 80° are much higher than the peaks found from only the substrate. This phenomenon is normal for the cut off axis single crystals. The peaks at 28 and 35° are RuO_2 but the relative intensity is lower than LC1309. The patterns of LC1309-1380 are quite similar to LC1380 as show in Figure 4.36. There was no ZnB_4O_7 [15] and bismuth pyrochlore [16] phase found in the films prepared by these two glasses, which have similar major composition to the ones used in the literature.

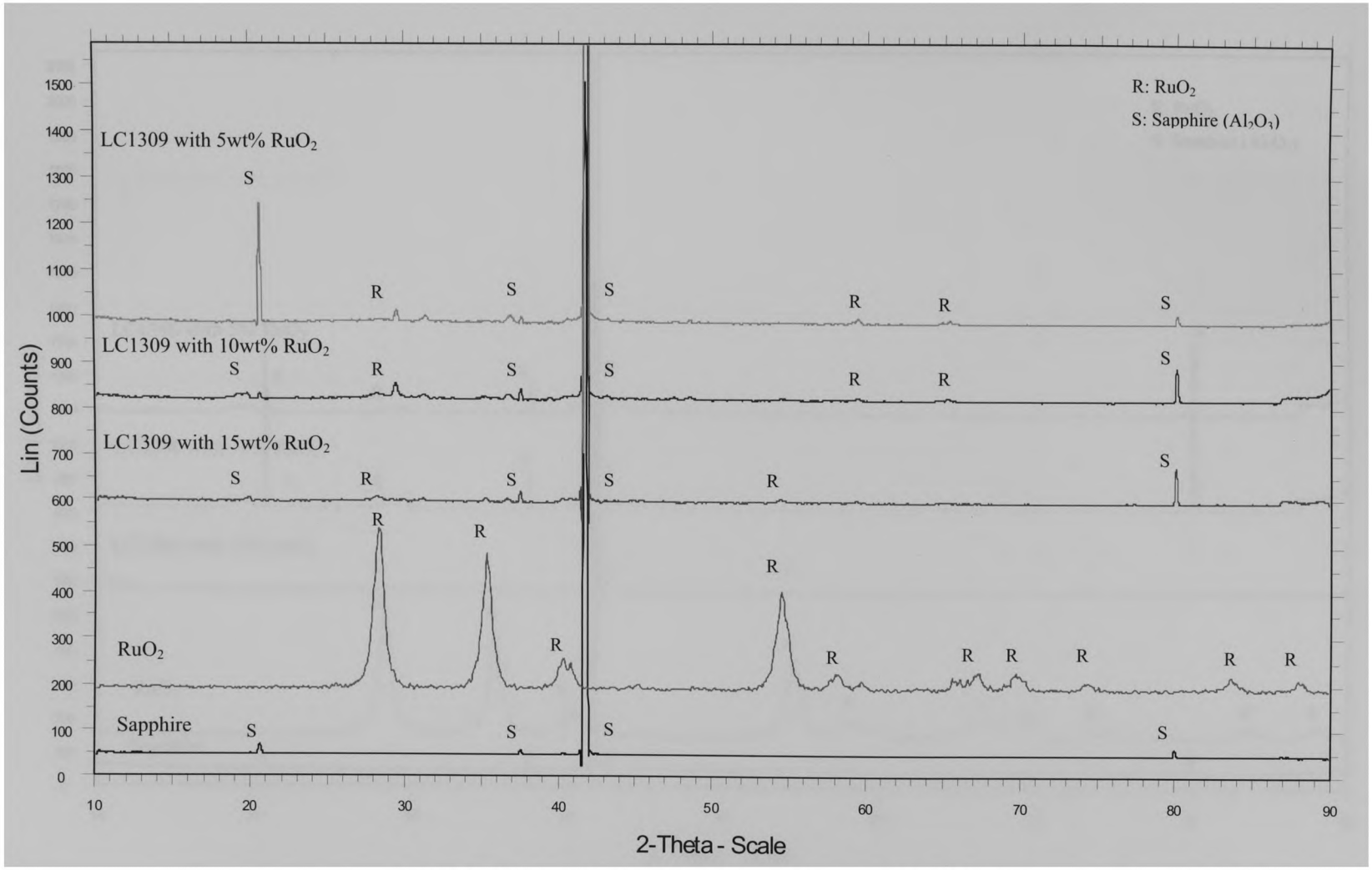

Figure 4.34 X-ray diffraction pattern of resistor film LC1309

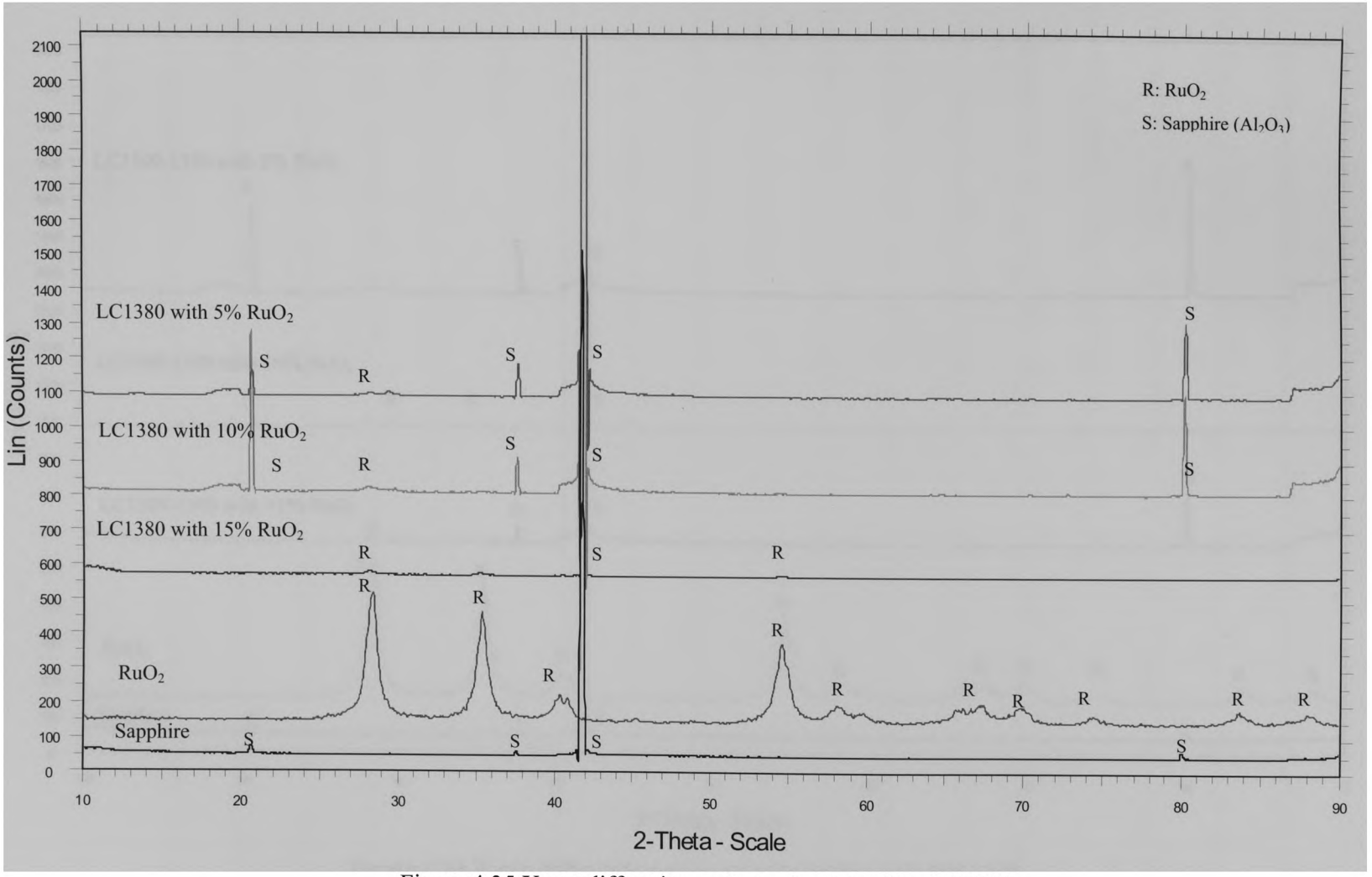

Figure 4.35 X-ray diffraction pattern of resistor film LC1380

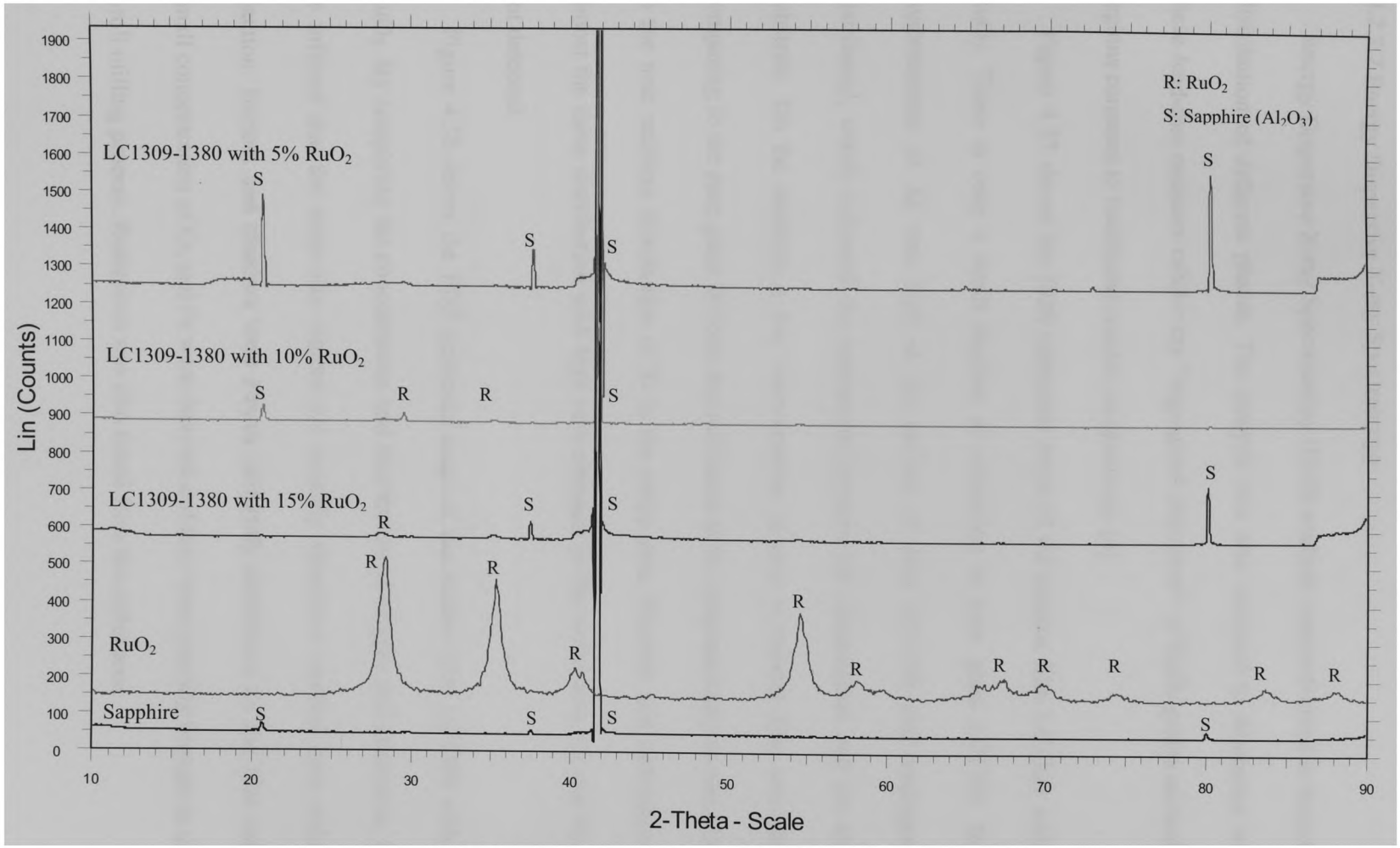

Figure 4.36 X-ray diffraction pattern of resistor film LC1309-1380

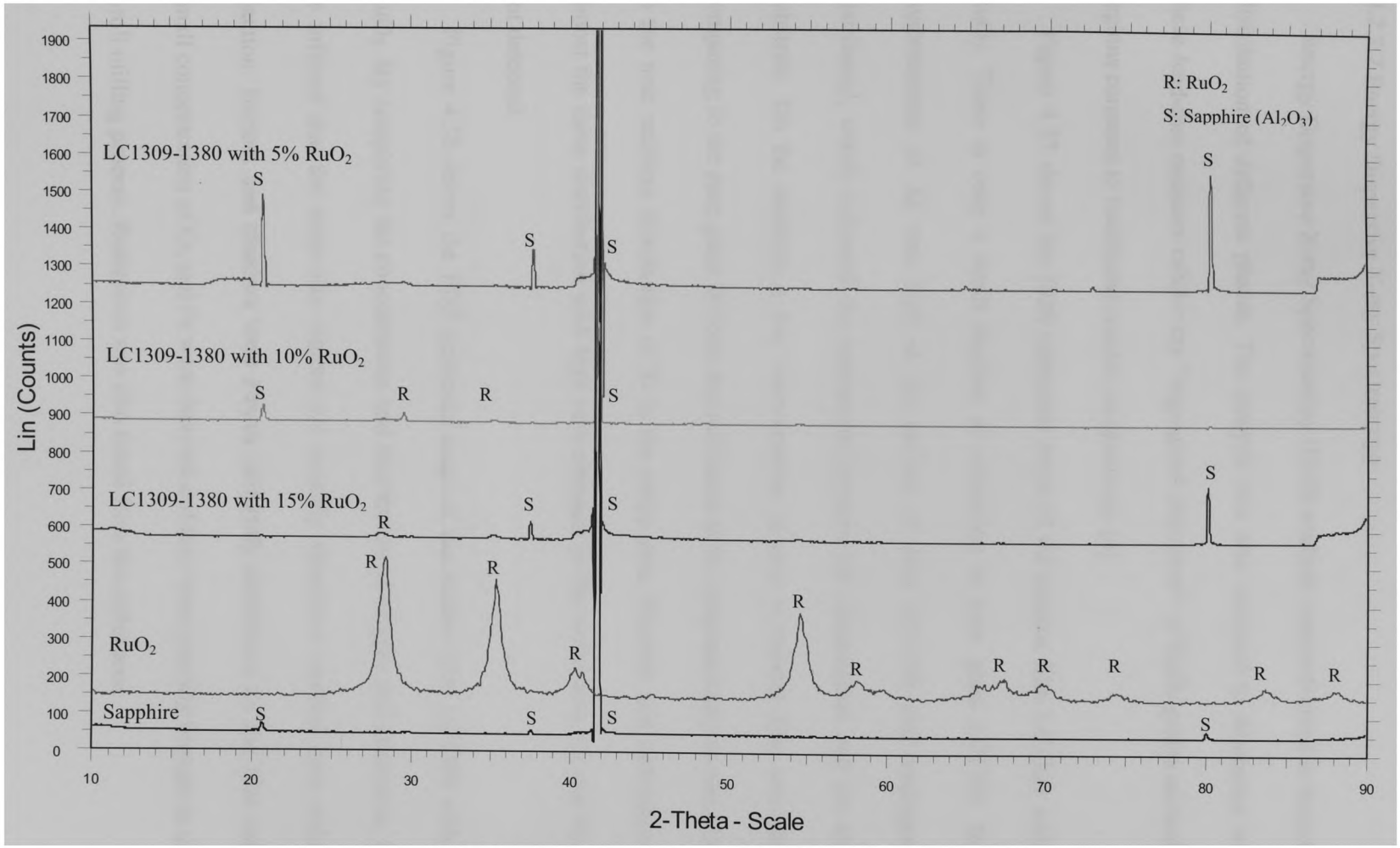

Figure 4.36 X-ray diffraction pattern of resistor film LC1309-1380

4.2.2.2 Energy Dispersive X-ray Spectroscopy

Energy Dispersive X-ray Spectroscopy (EDS) analysis was performed to evaluate the distribution of different phases. The analysis was also intended to determine whether these lead-free resistors exhibit the "segregated structures" of RuO_2 grains around glass regions common to traditional resistor compositions [4].

Figure 4.37 shows the EDS elemental maps of the resistor film LC1309 with 15% RuO_2. There is only a small fraction of aluminum in pure glass LC1309. But the concentration of Al was high at the surface of film LC1309 and homogenously distributed, which indicated the interaction between ink composition and the alumina substrate. On the contrary, a low concentration of zinc in resistor film was detected comparing to the pure glass. Silicon was not found to be complementary to zinc [16] due to the near uniform distribution of Si in the entire area. Bismuth and ruthenium have almost the same distribution with high concentration in the entire area. Cr and Sn were not detected.

Figure 4.38 shows the EDS elemental maps of the resistor film LC1380 with 15% RuO_2. By comparing the concentration and distribution of oxygen and aluminum, it can be inferred that the stripe-like regions are possibly aluminum resulted from reduction reaction. Barium and titanium were almost uniformly distributed on the film surface. Small concentration of Cr, and Fe were detected and they were possibly brought in during 3-roll milling process. Ruthenium was also found from the entire area.

Generally, it is difficult to clearly picture the phase distribution from the obtained results. Information on the local composition of the intergranular materials was hardly obtained. High resolution Transmission Electron Microscope (TEM) and more sophisticated techniques are required to have a better understanding of microstructure development.

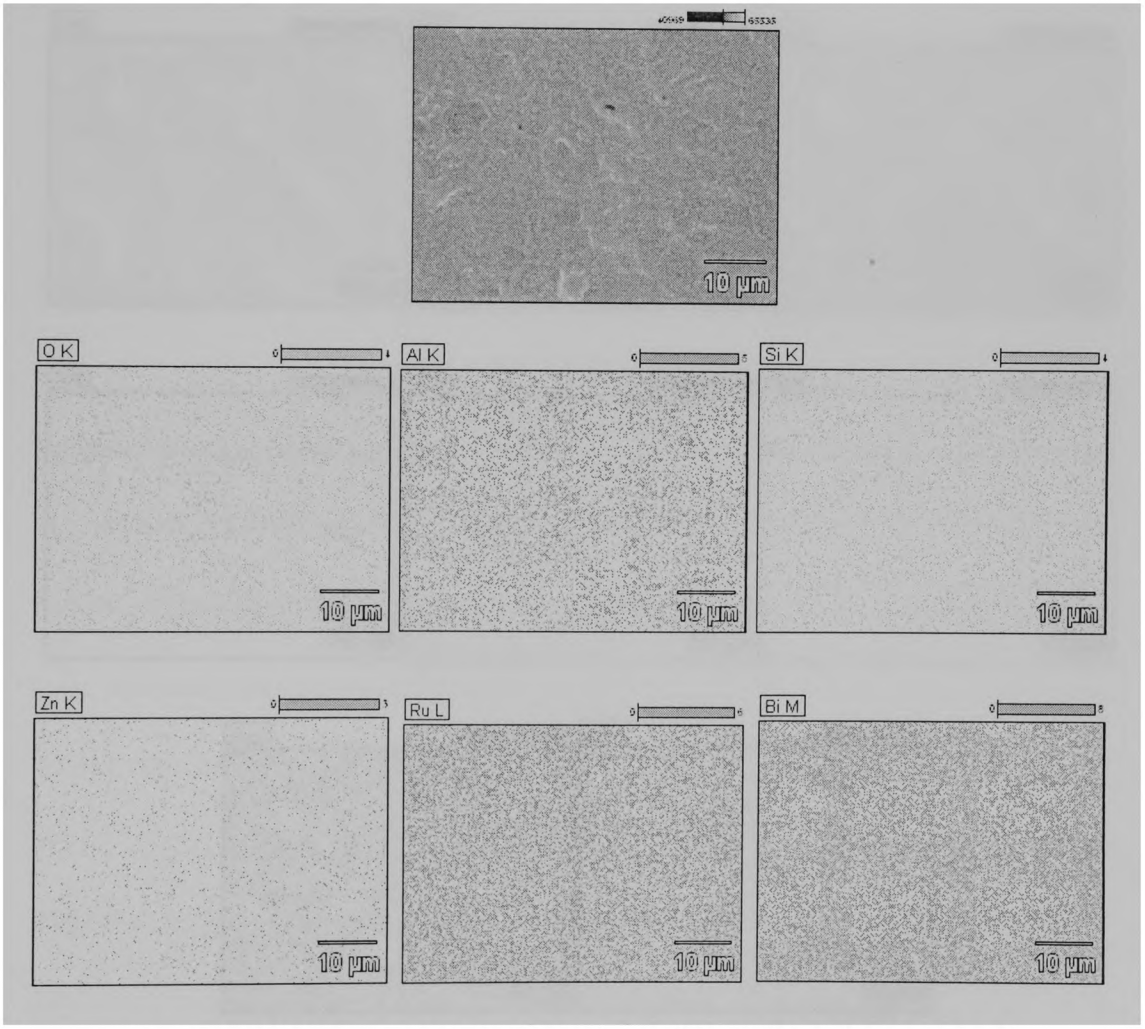

Figure 4.37 EDS elemental maps of resistor film LC1309 with 15% RuO_2

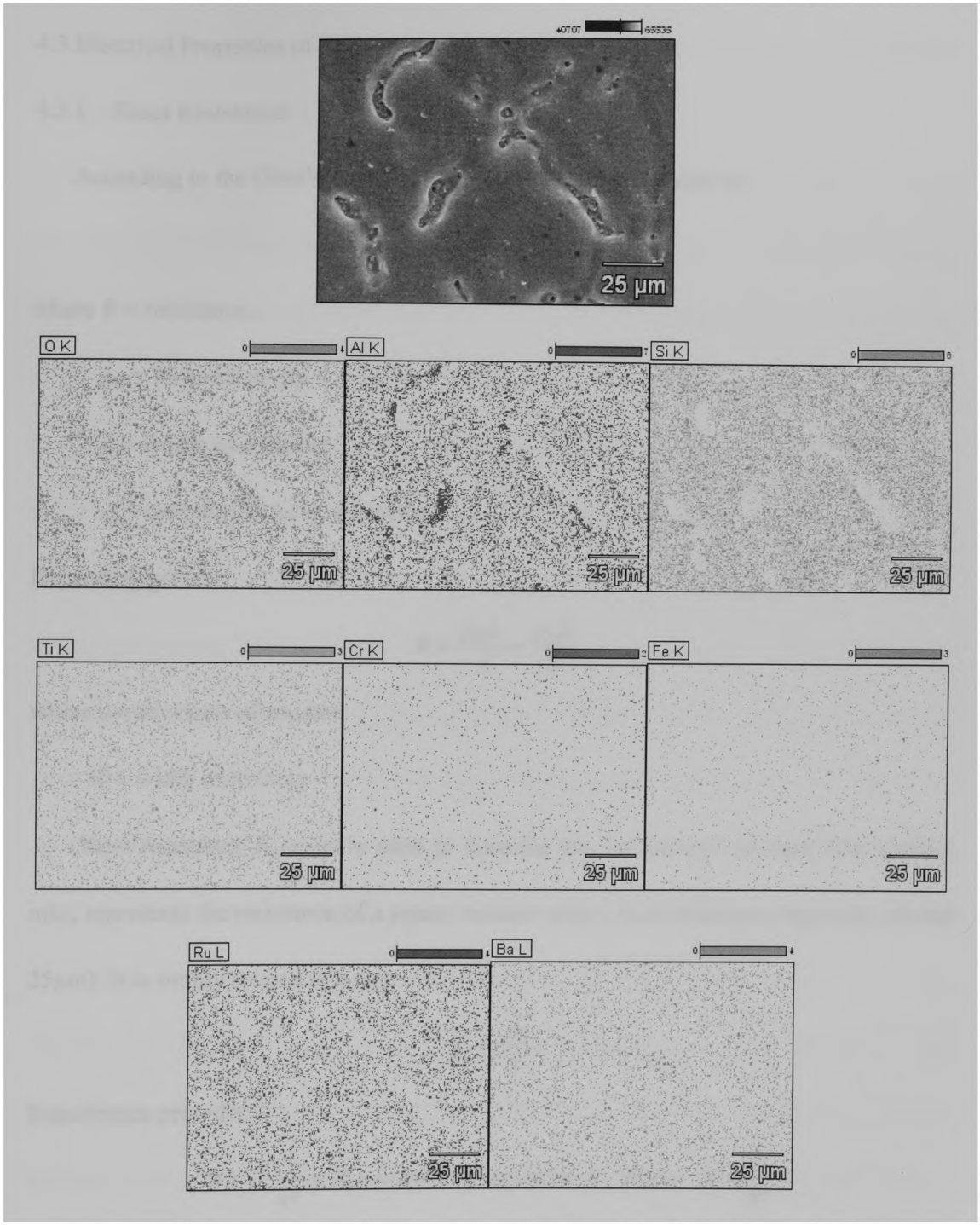

Figure 4.38 EDS elemental maps of resistor film LC1380 with 15% RuO_2

4.3 Electrical Properties of TFRs

4.3.1 Sheet Resistance

According to the Ohm's Law, the basic equation for resistance is:

$$R = \frac{\rho_B L}{A}$$

where R = resistance,

ρ_B = bulk resistivity

L = length of resistor

A = area of resistor cross section

Expanding gives:

$$R = \frac{\rho_B L}{A} = \frac{\rho_B L}{tW}$$

where t = thickness of resistor

W = width of resistor

Sheet resistance R_s, usually used to describe the "resistivity" of thick film resistor inks, represents the resistance of a square resistor with a fixed thickness (typically around 25μm). It is simply related to ρ_B as:

$$R_s = \frac{\rho_B}{t}$$

Substitution provides:

$$R = R_s \frac{L}{W} = R_s \times number\ of\ squares\ \ N, \text{ where } \ N = \frac{L}{W}$$

In this work, resistors with the same width but different length except half-square ones were prepared for testing. The pattern is shown in Figure 3.1. The resistance R of

each thick film resistor was measured using two-probe method on a HP 34401A multimeter at 25°C and the R_s value was calculated.

Compared to LC1309 and LC1309-1380, resistor LC1380 has less repeatability in term of sheet resistance value, probably due to the non-uniform microstructure. Tables 4-2 to 4-4 show the average sheet resistance of LC1309, LC1380, and LC1309-1380 fired at peak temperature 850°C. Resistor LC1309 covers a range from several hundred ohms to around 0.4 mega-ohms per square with RuO_2 weight fraction from 15% to 5%. By adjusting the RuO_2 fraction, this formulation has the potential to go up to 10 mega-ohms per square or go down to tens of ohms per square to cover a resistance range comparable to the lead bearing TFRs. Resistor LC1380 has a relatively shorter resistance range. The resistance of resistors with 5% RuO_2 is larger than 100MΩ, which is generally considered as an insulator. Resistor LC1309-1380 has a similar resistance range as LC1309 and it is also a good candidate to be tailored to the desired resistance from 10Ω/□ to 10M Ω/□.

Previous studies have shown that a decrease of resistance was often observed [36] near the contacts of resistor film and conductor termination. This so called "direct size effect" may be ascribed to the conductor element diffusion from the termination to the film. Conductor Ag diffusion from the termination to resistor film was found to happen although the conductor film is pre-fired [4]. For the resistors less than one square, typically the overlapped area of resistor film and conductor film is larger, which might results in more Ag diffusion. In this case, these resistors usually have a lower sheet

resistance value due to the diffusion. On the other hand, an increase of resistance near the contacts may also occur [37], which is called "inverse size effect". This phenomenon may be ascribed to the onset of contact resistance [16]. Figure 4.39 gives the relationship between the sheet resistance and the geometry of the resistors containing 15wt% RuO_2. It is clear that resistor LC1380 and LC1309-1380 have an inverse size effect. Resistor LC1309 exhibited a slight size effect comparing to the others. The research on size effect and the interaction between the resistor film and conductor termination is beyond the scope of this study. Further investigations are required to support these hypotheses.

The plot in Figure 2.1 is also know as "blending curve", i.e. a wide sheet resistance range is obtained simply by changing the relative fraction of the conductive phase in respect to the glass fraction. The plots in Figures 4.41 to 4.43 give a general view of how the blending curves might look like for the formulations prepared in this work based on the limited data. More experiment work on resistors with different RuO_2 fraction is required to complete the curves. It should be noted that consideration of the blending curve should take into account that this behavior depends not only on the nature of the conductive phase but also on the relative particle size of conductive phase and glass frit, glass composition and the firing condition [4]. Percolation theory [38, 39] was one of the simplest theoretical approaches for analyzing this curve. However a sound basis for the interpretation of this curve is not available, especially for the prediction of the behavior of new systems.

Several electrical transport mechanisms in TFRs have been suggested. In the case that conductive particles contact each other and form a uniform network in the glass matrix, the electrical charge transport is done by the conductive path constructed by conductive particles [3, 9]. In the case that there is no conductive chain formed by contacting particles, electron tunneling [3, 9, 10, 40] was considered to be the dominant mechanism for electrical charge transport while the conductive grains or their clusters are separated by very thin layer of glass. Hopping of charge carriers [42] over deep localized states in the energy gap of glass was another model. All of these developed models are just able to describe some specific electrical properties of TFRs but fail to give a satisfactory explanation of the whole behavior of these complex composites. For the new resistor material systems in this work, a good understanding of conduction mechanism can only be supported by a systematic experimental program to relate the electrical properties of the thick films to the material properties and processing conditions through microstructure.

Table 4-2 Sheet resistance of LC1309 resistor fired at 850°C

RuO_2 weight fraction	Number of Squares N	Sheet Resistance
15%	1	279 Ω/□
	1/2	333 Ω/□
	2	278 Ω/□
	3	278 Ω/□
	5	284 Ω/□
	10	229 Ω/□
Average	282 Ω/□	
10%	1	1.739 KΩ/□
	1/2	2.285 KΩ/□
	2	1.750 KΩ/□
	3	1.692 KΩ/□
	5	1.630 KΩ/□
	10	1.385 KΩ/□
Average	1.763 KΩ/□	
5%	1	464.5 KΩ/□
	1/2	378.7 KΩ/□
	2	380.0 KΩ/□
	3	427.8 KΩ/□
	5	392.3 KΩ/□
	10	382.1 KΩ/□
Average	426.3 KΩ/□	

Table 4-3 Sheet resistance of LC1380 resistor fired at 850°C

RuO_2 weight fraction	Number of Squares N	Sheet Resistance
15%	1	1.078 KΩ/□
	1/2	1.339 KΩ/□
	2	1.122 KΩ/□
	3	1.270 KΩ/□
	5	1.481 KΩ/□
	10	0.961 KΩ/□
Average	1.169 KΩ/□	
10%	1	67.4 KΩ/□
	1/2	18.7 KΩ/□
	2	71.9 KΩ/□
	3	47.4 KΩ/□
	5	44.9 KΩ/□
	10	36.1 KΩ/□
Average	74.6 KΩ/□	
5%	1	>100 MΩ/□
	1/2	
	2	
	3	
	5	
	10	
Average	>100 MΩ/□	

Table 4-4 Sheet resistance of LC1309-1380 resistor fired at 850°C

RuO_2 weight fraction	Number of Squares N	Sheet Resistance
15%	1	457 Ω/□
	1/2	647 Ω/□
	2	484 Ω/□
	3	518 Ω/□
	5	555 Ω/□
	10	473 Ω/□
Average	499 Ω/□	
10%	1	2.120 KΩ/□
	1/2	2.857 KΩ/□
	2	1.972 KΩ/□
	3	1.748 KΩ/□
	5	1.731 KΩ/□
	10	1.571 KΩ/□
Average	2.066 KΩ/□	
5%	1	347.9 KΩ/□
	1/2	429.4 KΩ/□
	2	324.5 KΩ/□
	3	346.5 KΩ/□
	5	427.2 KΩ/□
	10	196.0 KΩ/□
Average	353.0 KΩ/□	

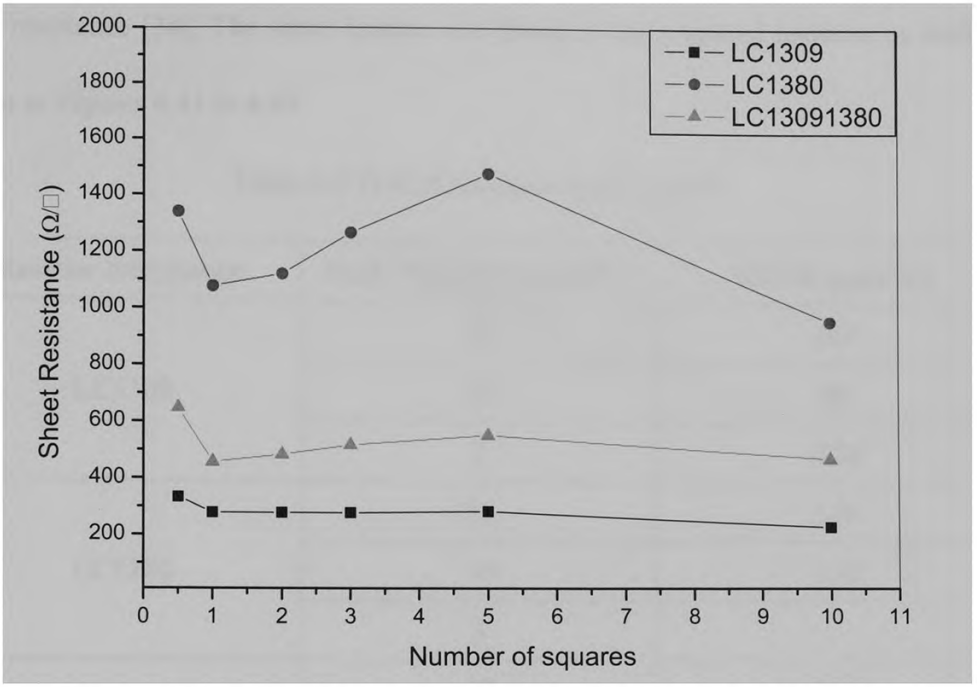

Figure 4.39 Relationship between number of squares and sheet resistance for 15wt% RuO_2 resistors fired at 850°C

4.3.2 Temperature Coefficient of Resistance

By measuring the resistance value at both 25 and 125°C, hot temperature coefficient of resistance (HTCR) of TFRs prepared in this work was calculated by the following formula:

$$HTCR = \frac{R_{125} - R_{25}}{R_{25}(125-25)} \times 10^6$$

Table 4-5 shows the average HTCR values of prepared resistors. The negative TCR value indicates a semiconductor-like electrical conduction and the positive TCR indicates a metal-like electrical conduction [42-44]. In addition, as shown in Figure 4.40, for RuO_2-based TFRs, the TCR changes from positive to negative with the increasing of

sheet resistance [34]. The same feature was found in the prepared resistors as well, as shown in Figures 4.41 to 4.43.

Table 4-5 TCR of resistors fired at 850°C

Resistor formulation	RuO_2 Weight Fraction(%)	HTCR (ppm/°C)
LC1309	15	165
	10	89
	5	-224
LC1380	15	119
	10	-152
	5	-
LC1309-1380	15	356
	10	53
	5	-259

Typically, commercial leaded TFRs have a HTCR range of ±50ppm/°C. To obtain a low TCR value, the usual approach to adjust it is to change the chemistry of the ink, namely to include in the ink small amounts of additives. For example, MnO_2, CdO, Rh_2O_3, V_2O_5 are added as negative TCR drivers while conversely Cu and precious metals are used as positive TCR drivers [4]. Generally, type and amount of TCR modifiers as well as the characteristic of conductive and glassy phases are selected on the basis of experience or trail and error approach since no predictive model is available yet. Without any additives, the HTCR of resistors prepared in this work spanned from -250ppm/°C to +350ppm/°C, which can be adjusted to a desired range by adding TCR drivers.

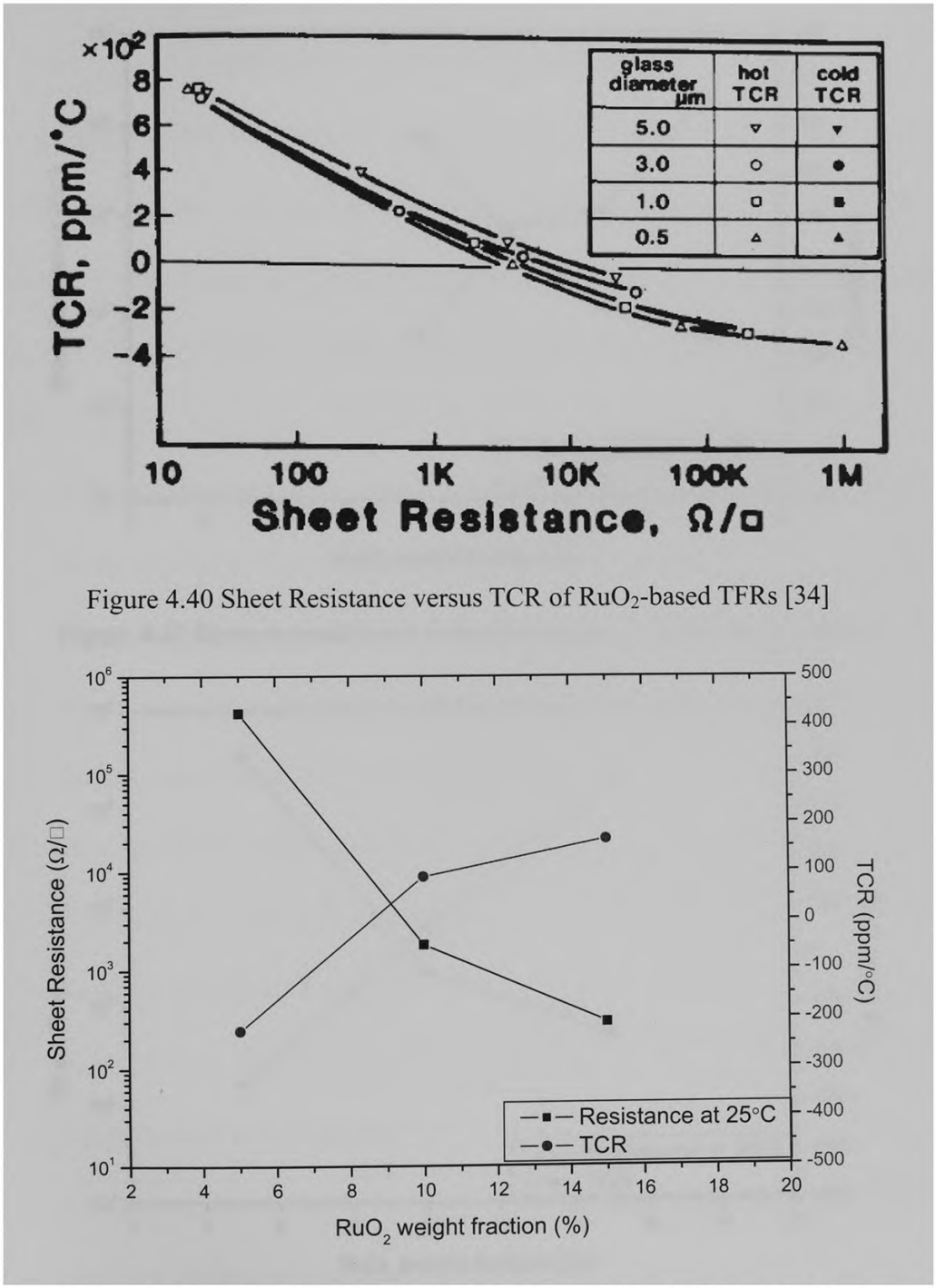

Figure 4.40 Sheet Resistance versus TCR of RuO_2-based TFRs [34]

Figure 4.41 Sheet resistance and TCR of resistors LC1309 fired at 850°C

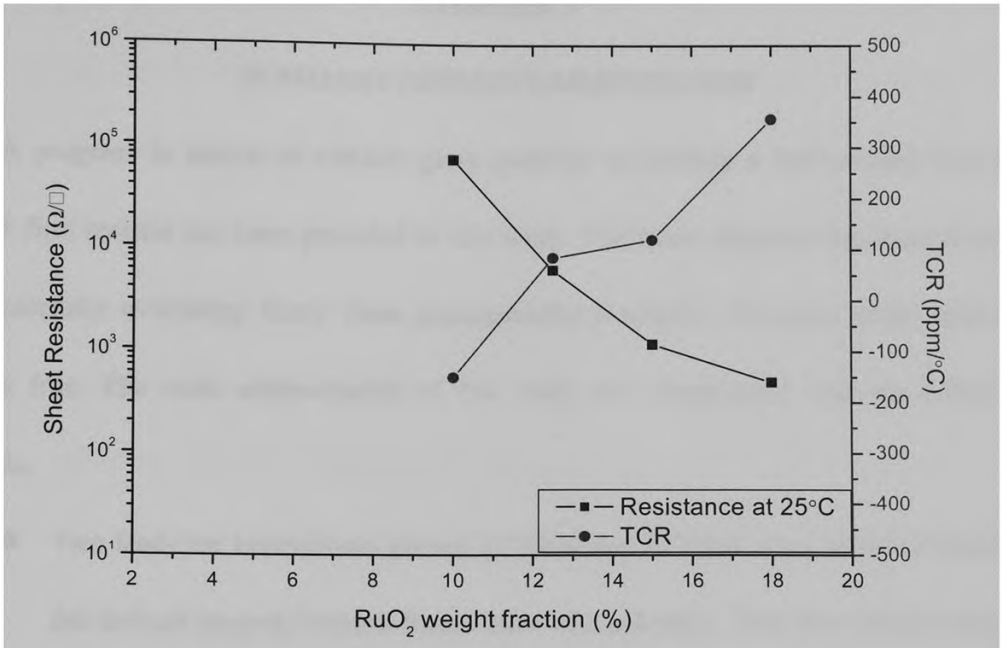

Figure 4.42 Sheet resistance and TCR of resistors LC1380 fired at 850°C

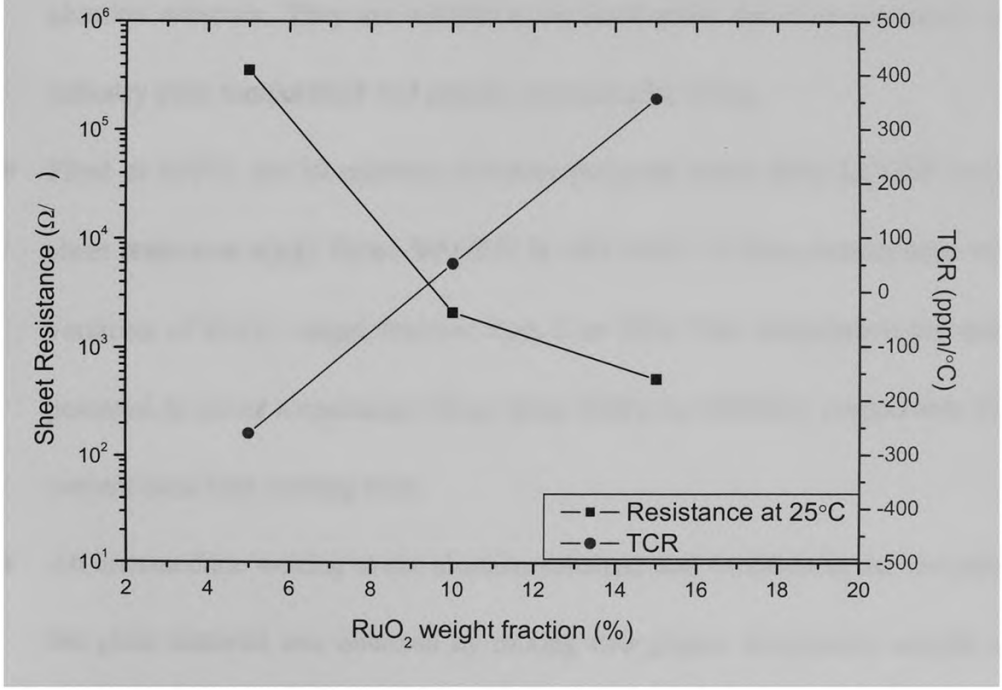

Figure 4.43 Sheet resistance and TCR of resistors LC1309-1380 fired at 850°C

CHAPTER 5

SUMMARY AND RECOMMENDATION

A progress in search of suitable glass material to develop a RuO_2-based lead-free thick film resistor has been provided in this work. The main objective has been fulfilled by carefully evaluating thirty three commercially available electronic grade lead-free glass frits. The main achievements of this work are summarized with the following points:

- Two lead-free borosilicate glasses LC1309 and LC1380 were selected based on the defined property criteria from a pool of candidates. They have proper wetting and good bonding to the 96% alumina substrate, and a CTE that matches with the alumina substrate. They are suitable to be fired under the most commonly used industry peak temperature and remain vitreous after firing.
- Fired at 850°C for 10 minutes, resistors prepared using glass LC1309 cover a sheet resistance range from ~300 Ω/□ to ~0.4 MΩ/□ at room temperature with a variation of RuO_2 weight fraction from 5 to 15%. This formulation the quite a potential to cover a resistance range from 10Ω/□ to 10MΩ/□, comparable to the current used lead bearing ones.
- An intermediate wetting to the alumina substrate and variation in the viscosity of the glass material was obtained by mixing two glasses in a certain weight ratio (LC1309:LC1380=1:3). Resistors prepared using this mixture exhibited a

relatively more stable sheet resistances than resistors prepared using only LC1380. In addition, this two-glass resistor system overcame the phenomenon of glass bleeding onto conductor terminations in the formulation of LC1309 with low RuO_2 weight fraction (≤5%). The sheet resistance of LC1309-1380 spans from ~500Ω/□ to 0.35MΩ/□ at room temperature with a variation of RuO_2 weight fraction from 5 to 15%.

- All of the resistors prepared using each glass and their mixture exhibit relatively low (in the range of -250 to 350ppm/°C) HTCR values, even without the additions of any TCR drivers.

Generally, the prepared RuO_2-based resistors in this work exhibit superior electrical property than the work reported previously. It can be concluded that a RuO_2-based lead-free thick film resistor that can cover a wide sheet resistance range could be developed by selecting a suitable glass material and well controlled process. The resistor performances including stability, noise, compatibility with conductor terminations etc. still need to be evaluated by standard industry test procedures. It is expected that improvements can be achieved by further work on these RuO_2-based lead-free TFRs. More extensive studies are required to collect data on glass viscosity temperature dependence, resistor film microstructure development and ingredient material interactions, from which a better understanding of reaction kinetics and conduction mechanism of these lead-free TFRs might be obtained.

In addition, as part of the preliminary study of this project, IrO_2, $CaRuO_3$, $Bi_2Ru_2O_7$ and $BaRuO_3$ were found to be good conductive phase candidates as well. Future experimental work on TFRs based on these conductive phases and the selected glasses is recommended.

REFERENCES

[1] D. W. Hamer, J. V. Biggers. Thick Film Hybrid Microcircuit Technology. John Wiley & Sons Inc., New York, 1972.

[2] Morton L. Topfer. Thick Film Microelectronics: Fabrication, Design and Applications. Van Nostrand Reinhol Company, New York, 1971.

[3] R. W. Vest. Conduction Mechanisms in Thick Film Microelectronics. Ph.D Dissertation, College of Engineering, Purdue University. West Lafayette, 1980.

[4] M. Prudenziati. Thick Film Sensors. Elsevier Science, 1994.

[5] Tapan K. Gupta. Handbook of Thick- and Thin-Film Hybrid Microelectronics. John Wiley & Sons Inc., Hoboken, New Jersey, 2003.

[6] R. W. Vest. Materials Science of Thick Film Technology. Ceramic Bulletin, Vol. 65 No. 4, 1986.

[7] Charles A. Haper, Ronald M. Sampson. Electronic Materials and Process Handbook. 2nd ed. McGraw-Hill, Inc. New York, 1994.

[8] B. Li, P. A. Clark, K. H. Church. Robust Direct-Write Dispensing Tool And Solutions For Micro/Meso-Scale Manufacturing And Packaging. Proceedings of the 2007 International Manufacturing Science And Engineering Conference, MSEC2007, October 15-17, 2007, Atlanta, Georgia, USA.

[9] M. Prudenziati. Conduction mechanisms in thick film resistors. Proc. Of European Hybrid Microelectronics Conf. 1981, Avignon, France, 1-10.

[10] R. W. Vest. A Model for Sheet Resistivity of RuO_2 Thick Film Resistors. IEEE Transactions on Components, Hybrids, and Manufacturing Technology, Vol. 14, No.2, june 1991, 396-406.

[11] Yu-Hung Hsieh, Shen-Li Fu. A Conduction Model for $BaPbO_3$-Based Thick Film Resistors. IEEE Transactions on Components, Packaging, and Manufacturing Technology-Part A. Vol.17, No.2, June (1994), 316-319

[12] Yiwu Ma, Jianqun Chen, Minqiang Li. $B_{i2}Ru_2O_7$ Conductive Phase and its Effects on the Gauge Factor of Ru-based Thick-film Resistors. Proceedings of the 2006 IEEE International Conference on Information Acquisition. August 2006, Weihai, Shandong, China, 245-248.

[13] B. S. Chiou and R. W. Vest. High-temperature thick-film dielectrics. American Ceramic Society Bulletin, 63 (6), 1984, 811-815.

[14] B. Morten, G. Ruffi, F. Sirotti, A. Tombesi, L. Moro. Lead-free ruthenium-based thick-film resistors: a study of model systems. Journal of Materials Science: Materials in Electronics, 2 (1991) 46-53.

[15] M. Prudenziati, F. Zanardi, B. Morten. Lead-free thick film resistors: an explorative investigation. Journal of Materials Science: Materials in Electronics 13 (2002), 31-37

[16] M. G. Busana, M. Prudenziati, J. Hormadaly. Microstructure development and electrical properties of RuO_2-based lead-free thick film resistors. Journal of Materials Science: Materials in Electronics, 17 (2006), 951-962.

[17] S. Rane, M. Prudenziati, B. Morten, L. Golonka, A. Dziedzic. Structural and electrincal properties of perovskite ruthenate-based lead-free thick film resistors on alumina and LTCC. Journal of Materials Science: Materials in Electronics, 16 (2005) 687-691.

[18] S. Rune, M. Prudenziati, B. Morton. Environment friendly perovskite ruthenate based thick film resistors. Materials Letters, 61 (2007) 595-599.

[19] A. Kshirsagar, S. Rane, U. Mulik, D. Amalnerkar. Microstructure and electrical performance of eco-friendly thick film resistor compositions fired at different firing conditions. Materials Chemistry and Physics, 101 (2007) 492-498.

[20] Dziedzic Andrzej. Iridium dioxide-based thick film resistors: manufacturing conditions and percolation. Materials Science, (1987), 13(3-4), 199-204.

[21] Dziedzic Andrzej. Thick film resistors with iridium dioxide and calcium iridium titanate ($CaIr_xTi_{1-x}O_3$)-examples of chemically reactive and unreactive systems. Microelectronics Journal, (1988), 19(6), 24-42.

[22] Dziedzic Andrzej, Golonka, L. Electrical properties of conductive materials used in thick-film resistors. Journal of Materials Science (1988), 23(9), 3151-5.

[23] Tankiewicz S., Morten B., Prudenziati M., Golonka L. J. IrO_2-based thick-film resistors. Journal of Applied Physics (2002), 91(7), 4261-4266.

[24] J. Setina, V. Akishin, J. Vaivads. Glass composition for the thick-film resistors. Materials Science Forum, Vol. 502, Dec 2005, 231-236.

[25] R. Klein, W. Jones. Evaluation of new $CaRuO_3$ thick film resistor formulations compatible with LTCC co-firing. Proceesding of International Symposium on Microelectronics, Denver, September 2002, 57-60.

[26] S. Rane, M. Prudenziati, B. Morten. $CaRuO_3$-based 'Green' thick film resistors. Journal of Active and Passive Electronic Devices, Vol.1 2005, 123-135.

[27] J. Hormadaly. Cadmium-free and lead-free thick-film paste compositions. US Patent 5,491,118 (Feb 13, 1996).

[28] J. Hormadaly. Cadmium-free and lead-free glass compositions, thick film formulations containing them and uses thereof. US Patent 6,171,987 B1 (Jan 9, 2001).

[29] Osamu Abe, Yoshiaki Taketa and Miyoshi Haradome. Microstructure and electrical conduction in RuO_2 Thick film resistors. Electrical Engineering in Japan, Vol. 110, No. 1, 1990, 21-30.

[30] M. Prudenziati, B. Morten, B. Forti, A.F. Gualtieri, G. Mihai Dilliway. Devitrification kinetics of high lead glass for hybrid microelectronics. International Journal of Inorganic Materials, 3 (2001), 667–674.

[31] Kenji Adachi, Hiroko Kuno. Effect of glass composition on the electrical properties of thick film resistors. J. of American Ceramic Society, 83 (10), 2000, 2441-2448.

[32] Abraham Taylor. X-Ray Metallopraphy. John Wiley, New York, 1961.

[33] S. Music, S. Popovic, M. Maljkovic, A. Saric. Synthesis and characterization of nanocrystalline RuO_2 powders. Materials Letters, 58 (2004) 1431– 1436.

[34] Toshio Inokuma, Yoshiaki Taketa, Miyoshi Haradome. The microstructure of RuO_2 thick film resistors and the influence of glass particle size on their electrical properties. IEEE Transactions on Components, Hybrids, and Manufacturing Technology, Vol. CHMT-7, No. 2, June 1984, 166-175.

[35] Wenjea J. Tseng, Chir-JangTsai, Shen-Li Fu. Porosity development of RuO_2 filled glass thick films on aluminum nitride substrates at elevated temperatures. Journal of Materials Science: Materials in Electronics, Vol. 11 (2000), 411-417.

[36] M. Prudenziati, B. Morton, L. Moro, L. Olumekor, A. Tombesi. Interactions between thick-film resistors and terminations: the role of bismuth. Journal of Physics D: Applied Physics, 19 (1986), 275-282.

[37] M. Prudenziati, F. Sirotti, M. Sacchi, B. Morten, A. Tombesi, T. Akomolafe. Size Effects in Ruthenium-Based Thick-Film Resistors: Rutile VS. Pyrochlore-Based Resistors. Active and Passive Electronic Components, Vol.14 (1991), 163-173.

[38] Scott Kirkpatrick. Percolation and conduction. Review of Modern Physics, Vol. 45, No. 4, 1973, 574-588.

[39] Andrzej Szpytma, Andrzej Kusy. On the segregation of the conductive phase in RuO_2-based thick resistive films. Thin Solid Films, 121(1984), 263-270.

[40] P. K. Khanna, S. K. Bhatnagar, M. L. Sisodia. Inter-diffusion phenomena and electrical conduction in thick-film segemented-resistor structures. Journal of Physics D: Applied Physics, 21 (1988), 1796-1801.

[41] K. M. Anisur, Susan C. Schneider, Martin A. Seitz. Hopping and ionic conduction in tin oxide-based thick-film resisto rcompostions. Journal of American Ceramic Society, 80 [5], 1997, 1198-1202.

[42] Osamu Abe, Yoshiaki Taketa. Electrical conduction in thick film resistors. Journal of Physics D: Applied Physics, 24 (1991), 1163-1171.

[43] Kenji Adachi, Hiroko Kumo. Decomposition of ruthenium oxides in lead borosilicate glass. Journal of American Ceramic Society, 80 [5], 1997, 1055-1064.

[44] Joon Lee, R. W. Vest. Firing studies with a model thick film resistor system. IEEE Transactions on Components, Hybrids, and Manufacturing Technology, Vol. CHMT-6, No. 4, Dec 1983, 430-435.

APPENDIX 1 GLASS CATALOG

Code	Glass Type	Coefficient of Thermal Expansion, $\times 10^{-7}$/°C, 25°C ~300°C	Specific Gravity, g/cm^3	Softening Point, °C	Particle Size (D_{50}), μm	Color (Powder)	Color (After Firing)	Photograph of glass pill after firing
LC1101	ZnO-Ti_2O_3 -SiO_2	106	3.4	525	~7	white	light yellow	
LC1102	B_2O_3-ZnO-SiO_2-CaO-TiO_2 -Sb_2O_3	-	-	504	~5	white	white	
LC1246	Zinc compound	-	4.4-4.5	300-500	~5.5	white	white	

Code	Glass Type	Coefficient of Thermal Expansion, $\times 10^{-7}$/°C, 25°C ~300°C	Specific Gravity, g/cm^3	Softening Point, °C	Particle Size (D_{50}), μm	Color (Powder)	Color (After Firing)	Photograph of glass pill after firing
LC1247	Zinc compound (Bi-Zn-B)	63.5-72	4.6-4.8	550	~4	white	light yellow	
LC1248	Zinc compound (Bi-Zn-B)	77-88.5	5.9-6.0	505	~5	white	white	
LC1260	B_2O_3-Al_2O_3 -CaO-SiO_2	32	2.2	930	~2.5	white	white	

Code	Glass Type	Coefficient of Thermal Expansion, $\times 10^{-7}$/°C, 25°C ~300°C	Specific Gravity, g/cm^3	Softening Point, °C	Particle Size (D_{50}), μm	Color (Powder)	Color (After Firing)	Photograph of glass pill after firing
LC1264	BO_3-ZnO-Al_2O_3-SiO_2-Bi_2O_3	54	5.5	520	4.5-5	white	light yellow	
LC1269	SiO_2-Ti_2O_3-Na_2O-K_2O	-	2.8	660	~6	white	white	
LC1276	ZnO-Ti_2O_3-SiO_2	-	2.8	570	~4.5	white	white	

Code	Glass Type	Coefficient of Thermal Expansion, $\times 10^{-7}$/°C, 25°C ~300°C	Specific Gravity, g/cm^3	Softening Point, °C	Particle Size (D_{50}), μm	Color (Powder)	Color (After Firing)	Photograph of glass pill after firing
LC1281	BO_3-ZnO-SiO_2	-	3.7	660	3.5-4	white	light gray	
LC1288	BO_3-ZnO-Al_2O_3-TiO_2-SiO_2-ZrO_2-SnO_2-BaO	-	3.4	660	2-2.5	white	dark gray	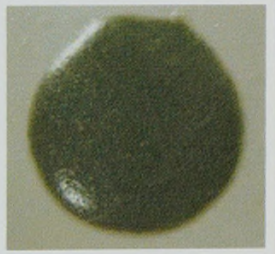
LC1309	B_2O_3-ZnO-Bi_2O_3	65	5.1	540	2.8	green	brown	

Code	Glass Type	Coefficient of Thermal Expansion, $\times 10^{-7}$/°C, 25°C ~300°C	Specific Gravity, g/cm^3	Softening Point, °C	Particle Size (D_{50}), μm	Color (Powder)	Color (After Firing)	Photograph of glass pill after firing
LC1281	BO_3-ZnO-SiO_2	-	3.7	660	3.5-4	white	light gray	
LC1288	BO_3-ZnO-Al_2O_3-TiO_2-SiO_2-ZrO_2-SnO_2-BaO	-	3.4	660	2-2.5	white	dark gray	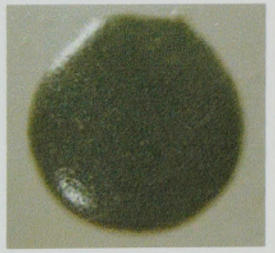
LC1309	B_2O_3-ZnO-Bi_2O_3	65	5.1	540	2.8	green	brown	

Code	Glass Type	Coefficient of Thermal Expansion, $\times 10^{-7}$/°C, 25°C ~300°C	Specific Gravity, g/cm^3	Softening Point, °C	Particle Size (D_{50}), μm	Color (Powder)	Color (After Firing)	Photograph of glass pill after firing
LC1361	Zinc compound (Zn-B-Si)	34-44	3.6-3.8	644	~7	white	light gray	
LC1362	Zinc compound (Si-Ba, Alkali)	124-146	2.6	580	~5.5	white	white	
LC1364	Zinc compound	-	4.8	>568	~5	white	white	

Code	Glass Type	Coefficient of Thermal Expansion, $\times 10^{-7}$/°C, 25°C ~300°C	Specific Gravity, g/cm^3	Softening Point, °C	Particle Size (D_{50}), μm	Color (Powder)	Color (After Firing)	Photograph of glass pill after firing
LC1365	Zinc compound	-	5.6-5.7	300-500	~5	white	light yellow	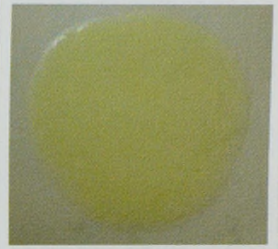
LC1366	Zinc compound (Zn-B-Si)	49	3.7-3.9	654	~4.5	white	white	
LC1367	Zinc compound	-	4.0	>625	~4	light yellow	yellow	

Code	Glass Type	Coefficient of Thermal Expansion, $\times 10^{-7}$/°C, 25°C ~300°C	Specific Gravity, g/cm^3	Softening Point, °C	Particle Size (D_{50}), μm	Color (Powder)	Color (After Firing)	Photograph of glass pill after firing
LC1365	Zinc compound	-	5.6-5.7	300-500	~5	white	light yellow	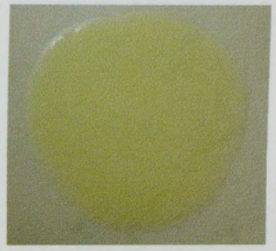
LC1366	Zinc compound (Zn-B-Si)	49	3.7-3.9	654	~4.5	white	white	
LC1367	Zinc compound	-	4.0	>625	~4	light yellow	yellow	

Code	Glass Type	Coefficient of Thermal Expansion, $\times 10^{-7}$/°C, 25°C ~300°C	Specific Gravity, g/cm^3	Softening Point, °C	Particle Size (D_{50}), μm	Color (Powder)	Color (After Firing)	Photograph of glass pill after firing
LC1380	SiO_2-B_2O_3-RO (R can be Mg, Ca, Sr or Ba)	52	2.5	780	3.8	white	gray	
LC1391	Sb_2O_3-BO_3-ZnO-CaO-Al_2O_3-Ti_2O_3-SiO_2	-	2.8	505	~7	white	white	
LC1394	Zinc compound	-	5.3	>500	~5	light yellow	light yellow	

Code	Glass Type	Coefficient of Thermal Expansion, $\times 10^{-7}$/°C, 25°C ~300°C	Specific Gravity, g/cm^3	Softening Point, °C	Particle Size (D_{50}), μm	Color (Powder)	Color (After Firing)	Photograph of glass pill after firing
LC1428	B_2O_3-SiO_2-ZnO-Bi_2O_3-BaO-Al_2O_3	67.5	4.5	619	3.5-4	white	light yellow	
LC1429	ZnO-B_2O_3-SiO_2	67	4.9	571	~3	white	white	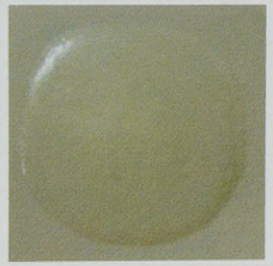
LC1430	Ba(compound)-B_2O_3-SiO_2	49	2.5	688	~4	white	light gray	

Code	Glass Type	Coefficient of Thermal Expansion, $\times 10^{-7}$/°C, 25°C ~300°C	Specific Gravity, g/cm^3	Softening Point, °C	Particle Size (D_{50}), μm	Color (Powder)	Color (After Firing)	Photograph of glass pill after firing
LC1431	ZnO-B_2O_3-SiO_2	65	3.3	570	~5	white	gray	
LC1432	Ba(compound)-B_2O_3-SiO_2-ZnO	80	3.3	575	3-3.5	white	white	
LC1433	ZnO-B_2O_3-SiO_2	97	6.8	463	~6	light yellow	yellow	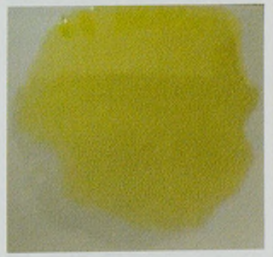

Code	Glass Type	Coefficient of Thermal Expansion, $\times 10^{-7}$/°C, 25°C ~300°C	Specific Gravity, g/cm^3	Softening Point, °C	Particle Size (D_{50}), μm	Color (Powder)	Color (After Firing)	Photograph of glass pill after firing
LC1434	Al_2O_3-B_2O_3-SiO_2-SrO-Bi_2O_3	95.4	5.3	582	7-8	light gray	yellow	
LC1435	Ba(compound)-B_2O_3-SiO_2-ZnO	94	5.3	544	6.5-7	white	light yellow	
LC1440	SiO_2-BO_3-ZnO-Al_2O_3-TiO_2-Bi_2O_3	-	5.3	520	~3.5	gray	white	

Code	Glass Type	Coefficient of Thermal Expansion, $\times 10^{-7}$/°C, 25°C ~300°C	Specific Gravity, g/cm^3	Softening Point, °C	Particle Size (D_{50}), μm	Color (Powder)	Color (After Firing)	Photograph of glass pill after firing
LC1452	SiO_2-B_2O_3-RO (R can be Mg Ca, Sr or Ba)	90	3.76803.5	582	7-8	white	white	
LC1588	SiO_2-BO_3-ZnO-Al_2O_3-TiO_2-Bi_2O_3	-	6.8	400-440	~4	yellow	amber	
RF110	B_2O_3-Bi_2O_3	113.5	6.4	441	5.2	yellow	yellow